EFFECTS OF DNA GEOMETRY AND TOPOISOMERASE II POISONS ON HUMAN AND BACTERIAL TYPE II TOPOISOMERASES

By

Rachel Erin Ashley

Dissertation

Submitted to the Faculty of the

Graduate School of Vanderbilt University

in partial fulfillment of the requirements

for the degree of

DOCTOR OF PHILOSOPHY

in

Biochemistry

May, 2017

Nashville, Tennessee

Approved:

Neil Osheroff, Ph.D.

John D. York, Ph.D.

Charles R. Sanders, Ph.D.

Eric P. Skaar, Ph.D., M.P.H.

Timothy R. Sterling, M.D.

.

To Him who always does immeasurably more

Ephesians 3:20

ACKNOWLEDGEMENTS

I would first like to thank my advisor, Dr. Neil Osheroff, for allowing me to work in his laboratory. Thank you for providing a positive work environment, for being committed to educating graduate students, and overall for being a great mentor from the start of my rotation all the way through graduate school. I learned a lot from you and I am definitely a better scientist now than I was when I came here. Thank you, as well, for allowing and encouraging me to pursue opportunities to develop teaching skills in addition to research skills while I was in graduate school. Finally, thank you for your constant and exceptional generosity with your time and with the treats you provided for lab!

To my dissertation committee, Dr. John York, Dr. Chuck Sanders, Dr. Eric Skaar, and Dr. Tim Sterling: Thank you for your support and encouragement over the past few years. I appreciate your willingness to devote your time to helping graduate students progress, and I benefitted from your questions and expertise in areas I would not have otherwise considered.

I also want to thank our collaborators. To Dr. Chuck Turnbough and Sylvia McPherson at the University of Alabama: Thank you for your endless help in making the *B. anthracis* enzymes and in troubleshooting the purification protocol so I could learn to make the enzymes as well. To Dr. Rob Kerns at the University of Iowa: Thank you for all of the compounds you provided our lab with so we could fully investigate quinolone-enzyme interactions. I especially want to thank Dr. Keir Neuman and Dr. Andrew Dittmore at the National Institutes of Health – thank you for welcoming me into your lab and teaching me the magnetic tweezers system for examining topoisomerases at the single molecule level,

and thank you for your extensive work on the single molecule experiments with *B. anthracis* gyrase. Your contributions added a completely new dimension to our studies with the enzyme, and I am incredibly grateful for all of your work.

To Jo Ann Byl: I think all of us in lab realize that the lab would not be functioning without you. Thank you for everything you do to make sure we all have everything we need for our projects, and thank you for the endless amount of time you put in to training each student. I know this often means that your own projects get set aside for you to help everyone else. It is greatly appreciated!

To former lab members Dr. Adam Ketron, Dr. Hunter Lindsey, Dr. Katie Aldred, MaryJean Pendleton, and Dr. Kendra Vann: Thank you for making the lab a fun place to work! I enjoyed getting to know each of you, and I appreciate how willing you all were to train other students. Each of you taught me at least one type of experiment that was crucial to my work. Furthermore, you taught me the essential life skills of doing crossword and KenKen puzzles!

To the current lab members, Lorena Infante Lara and Elizabeth Gibson: I have really enjoyed being in lab with both of you over the past couple of years! Thank you for troubleshooting experiments and preps with me, proofreading things for me, and overall keeping the lab fun. I will miss you both!

I owe a lot to the support I have from my entire family, my friends, and my church family at Hermitage Church of Christ. I cannot thank each of you individually, but thank you all for your constant love, for really being my family, and for being there for me!

To my dad and mom, Dr. Jim and Laura Hoffmann: I can never thank you enough for what you have done for me. Thank you for teaching me to value the things that are truly

important. Thank you for training me to think critically and make my own decisions. Thank you for instilling curiosity and a love of learning in me from the beginning, no matter how many questions that meant you had to put up with from me. Thank you for constantly supporting me and encouraging me in each phase of my life. I definitely would not be where I am without you.

To my second set of parents, Pat and RuthAnn Ashley: I do not know how I ended up being blessed with a *second* great set of parents. Thank you for welcoming me into your family and for treating me like a daughter. Thank you for your love and all of your encouragement as I have gone through graduate school. And thank you for supporting Nathan and me as we have started our life together.

To my husband, Nathan: I really think you deserve a degree for helping me get through graduate school. You have seen me through the entire process, and I do not know how I would have made it without you. Thank you for uprooting your life to move here to be with me while I worked on this degree. Thank you for your unending love and patience. Thank you for encouraging me when I have been struggling or frustrated and for celebrating with me when things have worked out. Thank you for making me a better person. The past five years of being with you and three-and-a-half years of being married to you have been the best part of my life, and I hope this is still just the beginning. I love you so much, and I am excited about our next adventure of being parents together!

Finally, and above everyone else, I thank God for what he has done for me. Lord, you really are the one who always does immeasurably more than I ask or can even imagine. Your world is marvelous, and I am in constant awe of you as I study it. I pray that I can honor you with this degree and with my life. I owe it all to you.

TABLE OF CONTENTS

LIST OF TABLES

LIST OF FIGURES

LIST OF ABBREVIATIONS

(-)SC	negatively supercoiled
(+)SC	positively supercoiled
3'-(AM)P	3'-(aminomethyl)pyrrolidinyl
A	alanine
Ala	alanine
Asp	aspartic acid
ATP	adenosine triphosphate
bp	base pair
BSA	bovine serum albumin
C	cysteine
Cys	cysteine
DTT	dithiothreitol
E	glutamic acid
EDTA	ethylenediaminetetraacetic acid
F	pheynlalanine
Glu	glutamic acid
His	histidine
IPTG	isopropyl β-D-1-thiogalactopyranoside
K	lysine
kb	kilobase
L	leucine

Lk	linking number
MDR-TB	multidrug-resistant tuberculosis
PCB	polychlorinated biphenyl
PCR	polymerase chain reaction
Rel	relaxed
S	serine
SDS	sodium dodecyl sulfate
Ser	serine
TB	tuberculosis
Tw	twist
Wr	writhe
WT	wild-type
Y	tyrosine
ΔLk	change in linking number

CHAPTER I

INTRODUCTION

DNA Topology

The topological state of DNA has a dramatic effect on nucleic acid processes in cells.[1-5] DNA topology can be defined mathematically by three straightforward concepts: twist (Tw), writhe (Wr), and linking number (Lk).[2,6-10] Twist is the number of double helical turns in a defined DNA segment. Conventionally, positive twist is defined as the right-handed twist observed in the Watson-Crick structure. Writhe is defined as the number of times the double helix crosses itself if the DNA segment is projected in two dimensions. The crossovers are assigned a positive or negative value based on their handedness; left-handed crossings are counted as positive, and right-handed crossings are counted as negative (Figure 1). The linking number is the sum of twist and writhe in the molecule:

$$Lk = Tw + Wr$$

Relaxed DNA is defined as DNA that is not under torsional stress, as observed in the canonical Watson-Crick structure. In this form, the double helix makes one helical turn for every 10.5 bp. Therefore, a relaxed DNA molecule of 1050 bp would have an Lk = 100 (1050 ÷ 10.5 bp/turn). An important point is that Lk for a right-handed plectonemically coiled double helix is always positive; Lk = 0 would mean that the DNA was completely melted with no crossings between the two strands of the helix (yielding a paranemic structure). Therefore, DNA topology is often expressed as the change in Lk, ΔLk, which is defined as the difference between the actual Lk of a DNA molecule and the Lk if the

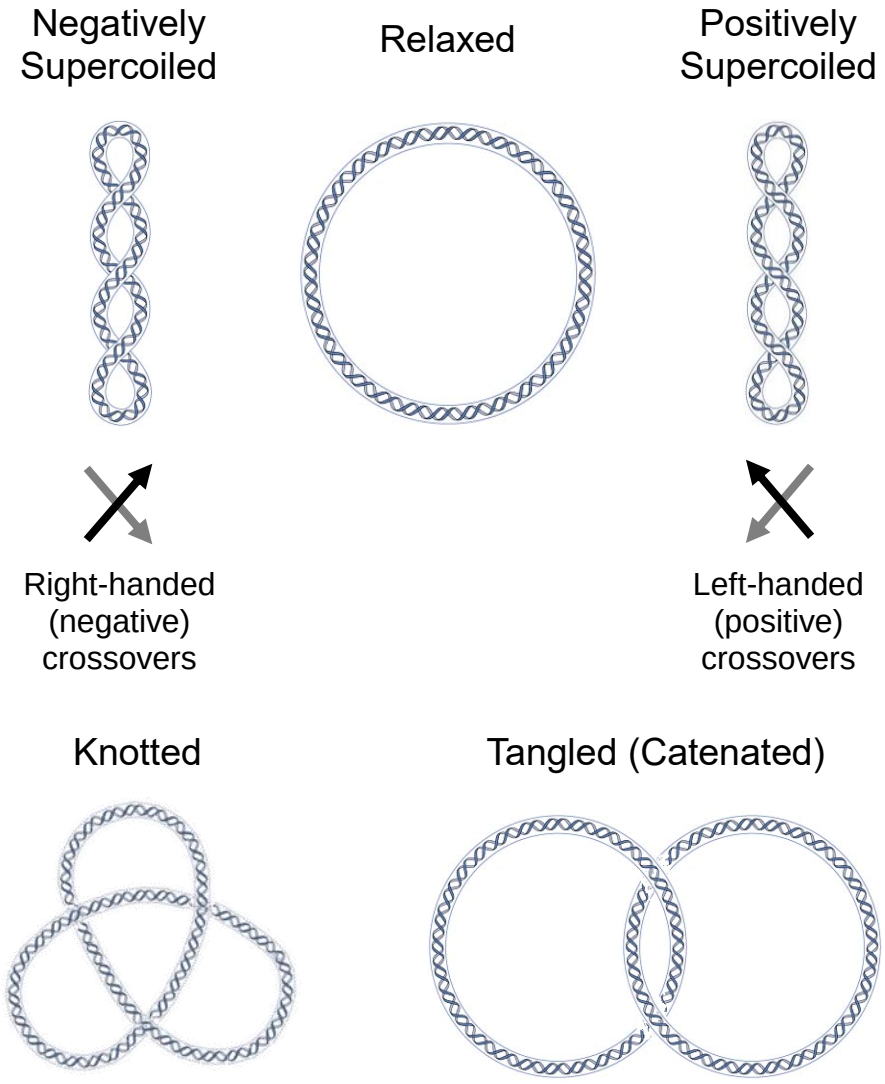

Figure 1. Topological relationships in DNA. Top: DNA that is not under torsional stress is referred to as "relaxed" (middle). Underwinding or overwinding the DNA results in negatively supercoiled (left) or positively supercoiled (right) DNA. Supercoiling is depicted here as Wr (DNA crossovers) for visual clarity, but it should be noted that Tw and Wr are interconvertible within these molecules. Bottom: Intramolecular knots (left) and intermolecular tangles (catenanes, right) can also form in DNA. In these cases, Tw and Wr are not interconvertible.

molecule were completely relaxed. For example, if the 1050-bp molecule above had an actual Lk of 94, then $\Delta Lk = 94 - 100 = -6$, which would mean that the molecule would have 6% fewer links in it than relaxed DNA. A DNA molecule with a $\Delta Lk \neq 0$ is under torsional stress, which can be distributed over the molecule and converted to axial stress, resulting in the superhelical twists depicted as crossovers in Figure 1. DNA under torsional stress is therefore referred to as being supercoiled. DNA with a *positive* ΔLk is referred to as *overwound* or *positively supercoiled* [(+)SC]. Likewise, DNA with a *negative* ΔLk is referred to as *underwound* or *negatively supercoiled* [(-)SC]. Note that throughout the dissertation, "overwound" and "(+)SC" will be used interchangeably, as will "underwound" and "(-)SC." Also note that "(+)SC" and "(-)SC" will be used exclusively as adjectives describing the state of DNA, while the actual positive or negative supercoils within the molecule will be referred to as "(+) supercoils" or "(-) supercoils," respectively.

Although DNA is typically drawn as a relaxed molecule, this form does not exist in nature. Organisms typically maintain their genome in an ~6% underwound state,[2,6-8] which enhances the opening of the double helix and facilitates replication and transcription. Sections of (+)SC DNA are generated ahead of replication and transcription machinery, because these tracking systems move through the DNA without rotating, thereby pushing extra twists ahead of the replication or transcription bubble (Figure 2). This overwinding makes it increasingly difficult to open the double helix and, if unresolved, can block the progression of the tracking systems.[1,2,11-13] Meanwhile, other topological issues occur behind the fork. Replication creates tangles between the two daughter chromosomes (catenanes) that must be removed in order for chromosome segregation to occur during cell division, and transcription generates regions of (-)SC DNA behind the moving machinery.

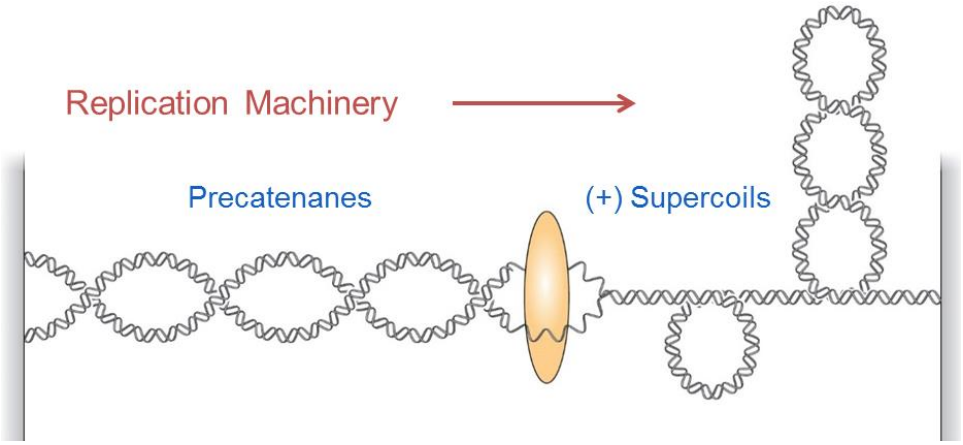

Figure 2. Moving DNA tracking machinery creates topological problems. As tracking systems move through the DNA, twists are pushed ahead of the fork, resulting in the accumulation of (+) supercoils. In the case of replication, precatenanes (links between newly synthesized daughter chromosomes) form behind the fork; during transcription, (-) supercoils arise behind the moving machinery. Artwork by Ethan Tyler, NIH Medical Arts.

Furthermore, other fundamental cellular processes such as recombination introduce intramolecular links (knots) within chromosomes, which impede DNA tracking systems.[1,2,12,14]

Topoisomerases

All organisms encode multiple enzymes to regulate the topological state of their genome.[1,14-17] Collectively, these enzymes are known as "topoisomerases," because they can interconvert DNA topoisomers. Topoisomerases function by creating transient breaks in the DNA backbone and are divided into two classes based on how many strands they cleave: type I enzymes create single-strand breaks, and type II enzymes create double-strand breaks.[1,14-17] These different cleavage activities give the enzyme classes different abilities to function on Tw and Wr within the DNA (Figure 3). By cutting a single strand of the DNA backbone, type I enzymes work solely on Tw. Therefore, these enzymes can relax supercoiled DNA, because Tw and Wr are interconvertible.[16,18,19] In the case of catenanes and knots, however, Tw and Wr are not interchangeable. The resolution of these structures requires the removal of Wr, which type II topoisomerases are able to do as a result of their double-strand break mechanism.[1,3,5,16,20-22] Thus, type II topoisomerases can remove supercoils as well as resolve knots and tangles. This dissertation will focus exclusively on type II enzymes.

Type II topoisomerases function by creating a transient double-strand break in one double helix and passing a separate intact DNA segment through the opening.[5,16,20-22] All type II enzymes utilize fundamentally the same catalytic cycle to carry out their functions, and complete catalytic activity requires a divalent metal ion and ATP.[14,23-26] One round of the catalytic cycle is shown in Figure 4. The two DNA segments that participate in the

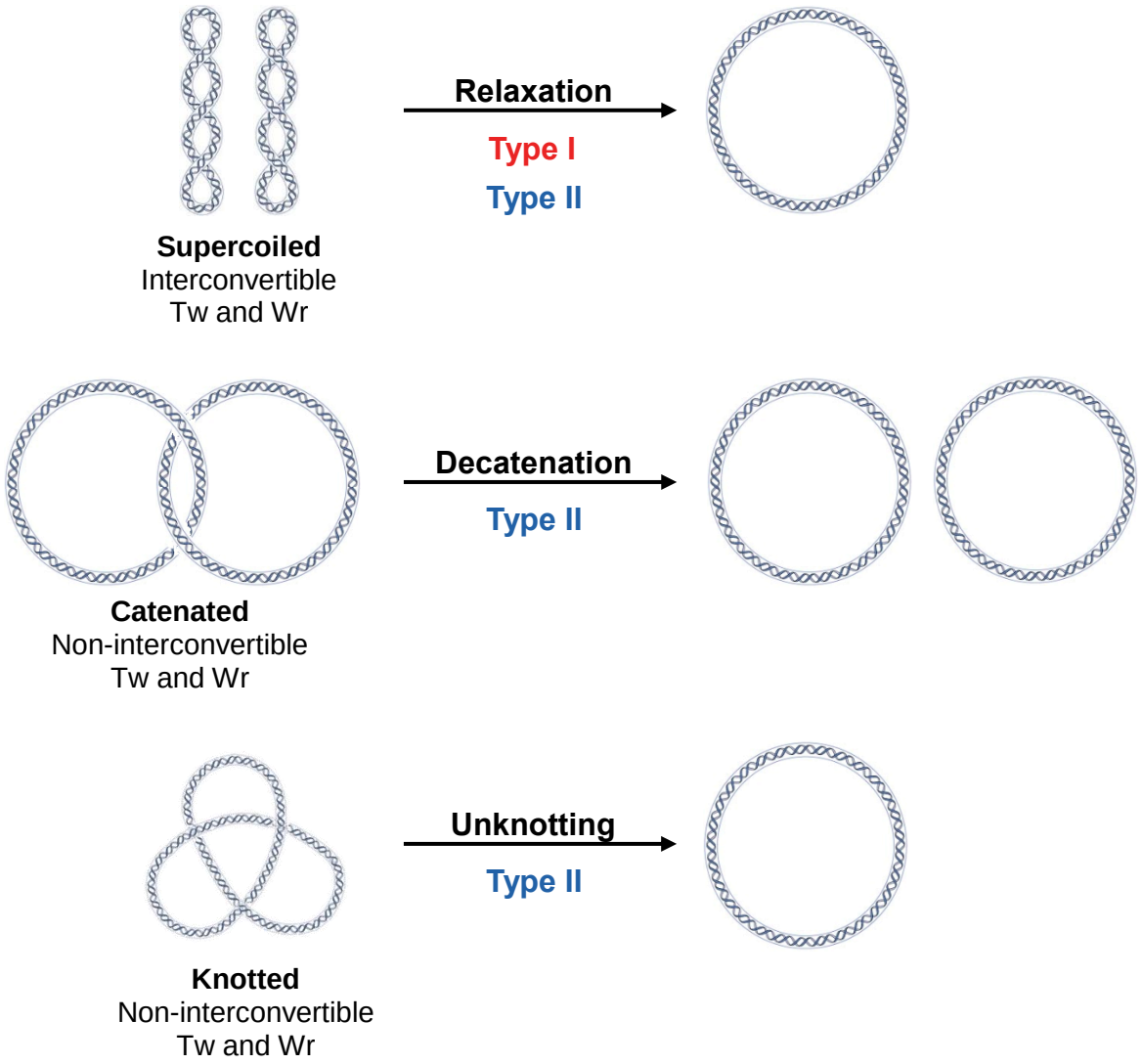

Figure 3. Actions of type I and type II topoisomerases. The different cleavage activities of type I and type II topoisomerases allow them to work on different DNA topologies. Because type I enzymes only cut one strand of the DNA, they are restricted to working on Tw. Because type II enzymes cut both strands of the DNA, they are able to work on Wr.

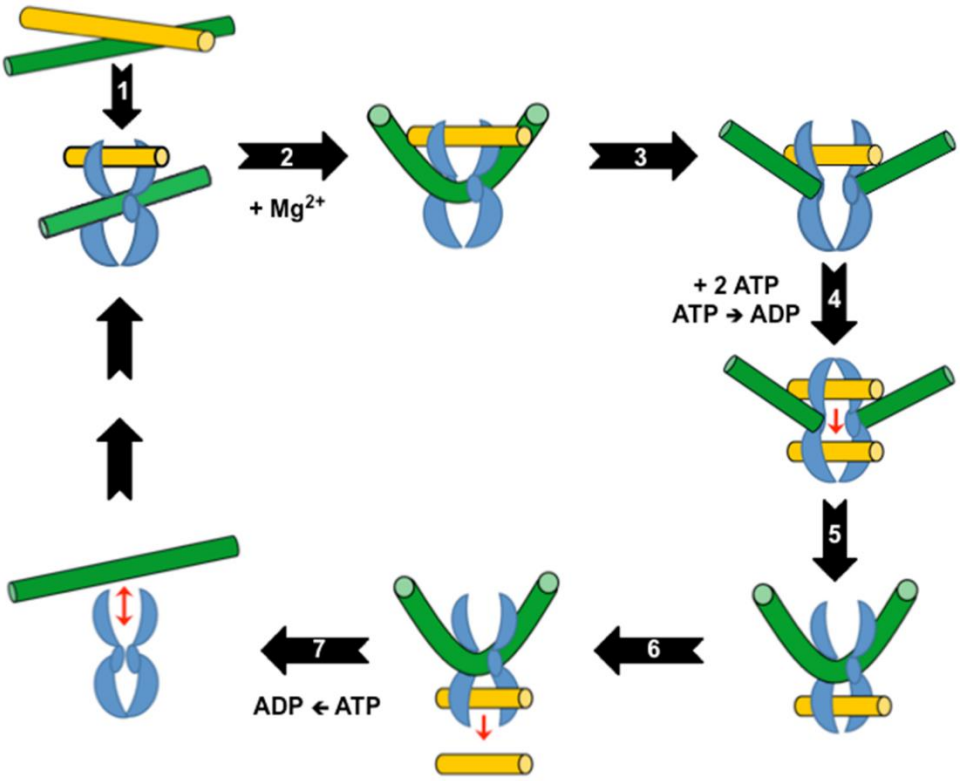

Figure 4. Catalytic cycle of type II topoisomerases. The enzyme is shown in blue, the DNA segment that is cleaved (G-segment) is in green, and the DNA segment that is transported through the DNA break (T-segment) is in yellow. The catalytic cycle has seven steps: (1) DNA binding; (2) DNA bending; (3) DNA cleavage; (4) Helix transport; (5) Religation; (6) Release of the T-segment; (7) Release of the G-segment and enzyme recycling. Figure adapted from Ketron and Osheroff.[10]

cycle are the gate-segment (G-segment), which is cleaved by the enzyme, and the transport-segment (T-segment), which is transported through the gate created in the G-segment. Briefly, the steps of the catalytic cycle are 1) DNA binding; 2) DNA bending; 3) DNA cleavage; 4) helix transport; 5) religation of the G-segment; 6) release of the T-segment; and 7) release of the G-segment and enzyme recycling.[23-31] During the DNA cleavage-religation process, the enzymes remain covalently attached to the DNA backbone in order to maintain the integrity of the genome. A hallmark of the catalytic cycle is the formation of the covalent enzyme-cleaved DNA complex, known as the cleavage complex.[5,16,20-22]

Human type II topoisomerases

Humans and other vertebrates encode two closely related type II topoisomerases: topoisomerase IIα and topoisomerase IIβ.[1,14,16,26,32-39] These enzymes function as homodimers. Although they share ~70% of their amino acid sequence, they are encoded by separate genes and have different protomer molecular weights (170 and 180 kDa, respectively). While topoisomerase IIα and topoisomerase IIβ are enzymatically similar, they differ in their patterns of expression and their cellular functions.[3,5,14,20,21,36,40] Topoisomerase IIα is essential in proliferating cells, and its expression increases over the cell cycle, peaking in G2/M.[41-43] This isoform is associated with replication complexes and remains bound to chromosomes throughout mitosis, suggesting that it has important functions in growth-related processes such as replication and chromosome segregration.[1,44]

Topoisomerase IIβ is required for neural development in mammals, but is otherwise dispensable at the cellular level.[3,5,21,36,40,42,45] Unlike topoisomerase IIα, topoisomerase IIβ is expressed at high concentrations in most cell types independent of proliferation status. The physiological functions of the β isoform are not yet fully defined. However, it

dissociates from chromatin during mitosis and seems to have an important role in the transcription of developmentally and hormonally regulated genes.[5,45-47]

Bacterial type II topoisomerases

Most bacteria encode two type II topoisomerases, gyrase and topoisomerase IV.[48-50] Gyrase was discovered in 1976 and was the first type II topoisomerase to be described.[51] It is composed of two subunits, GyrA and GyrB, and functions as an A_2B_2 heterotetramer.[5,16,40,52] The A subunit contains the active site tyrosine that covalently bonds with the DNA backbone during cleavage, and the B subunit forms the N-terminal gate of the enzyme and contains ATP binding and hydrolysis sites.

Gyrase is the only known topoisomerase that is able to introduce (-) supercoils into DNA.[5,16,40,52,53] To accomplish this task, gyrase wraps the DNA around the C-terminal domain of GyrA in a right-handed fashion, thereby generating a constrained (+) supercoil on the enzyme. Because wrapping the DNA cannot change the Lk of the molecule, a compensatory, unconstrained (-) supercoil is also introduced into the unbound portion of the DNA. When strand passage occurs, the (+) supercoil is converted to a (-) supercoil, causing a net introduction of two (-) supercoils per catalytic cycle.[2,9,40,53] Another important implication of this wrapping mechanism is that the G- and T-segments are on the same DNA molecule and are only ~140 bp apart.[54] Consequently, gyrase is much more efficient at relaxing (+) supercoils and introducing (-) supercoils than it is at decatenating or unknotting DNA, because these latter reactions require the use of G- and T-segments that are on different DNA molecules (or are distal to each other on the same DNA molecule).[5,16,40,52,53]

The major cellular roles of gyrase stem from its ability to carry out intramolecular reactions and to actively underwind DNA. Gyrase functions ahead of replication forks and transcription complexes to alleviate torsional stress induced by DNA overwinding. Additionally, acting in conjunction with the bacterial type I topoisomerase (the ω protein), gyrase modulates the overall level of DNA supercoiling in the bacterial genome by introducing (-) supercoils to maintain the genetic material in an underwound state.[4,5]

Topoisomerase IV was discovered in 1990 and also functions as an A_2B_2 heterotetramer.[5,16,40,52,53] The subunits of topoisomerase IV were first identified in Gram-negative species as being required for chromosome partitioning and were named ParC and ParE. Sequence analysis revealed that these proteins were homologous to GyrA and GyrB, respectively, and later functional studies showed that the ParC/ParE complex was a distinct type II topoisomerase. In Gram-positive species, the subunits were named as gyrase-like proteins, GrlA and GrlB.

Although gyrase and topoisomerase IV display sequence homology, they have distinct properties and functions.[5,16,40,48,52,53,55] The C-terminal domain of ParC/GrlA does not wrap DNA, so topoisomerase IV is unable to introduce (-) supercoils into relaxed DNA. Instead, the enzyme is able to relax both (+) and (-) supercoils and can also carry out the intermolecular strand passage reactions required for decatenation and unknotting. While topoisomerase IV may be involved in regulating DNA over- and underwinding,[56-58] its primary function is to remove knots and tangles formed by recombination and replication.[48,59-61]

Topoisomerase II Poisons

Beyond their essential cellular functions, type II topoisomerases are targets for a number of anticancer and antibacterial drugs known as topoisomerase poisons that act by stabilizing cleavage complexes.[5,16,20,22,50,62-76] These necessary, but dangerous, complexes are usually maintained in a critical balance in the cell (Figure 5).[14,25] Under normal conditions, topoisomerases generate enough cleavage complexes to allow DNA topology to be regulated appropriately, thereby promoting normal cell growth. If levels of cleavage complexes fall, slow growth rates or mitotic failure can ultimately lead to cell death. If levels of cleavage complexes rise too high, accumulated cleavage intermediates can be converted to non-ligatable strand breaks if replication forks or other DNA tracking systems encounter these "roadblocks" in the DNA.[14,25,77,78] These permanent breaks must then be repaired by DNA damage response pathways, which can trigger mutations, translocations, or other genetic anomalies. Topoisomerase II poisons exert their cytotoxic effects by overwhelming cells with DNA strand breaks that exhaust DNA repair systems and lead to cell death.[14,25,73,77-81]

Targeting human type II topoisomerases: anticancer drugs and natural products

A number of well-characterized chemotherapeutic drugs, such as etoposide and doxorubicin, as well as several natural products with anticancer or chemopreventive effects are topoisomerase II poisons with activity against human topoisomerase IIα and topoisomerase IIβ (together, these enzymes are referred to as "topoisomerase II").[5,16,20,22,62-67,69-72,74,75] Topoisomerase II poisons can be categorized as interfacial or covalent (Table 1).[20,74,82,83] Interfacial poisons, including several anticancer drugs and dietary compounds (Figure 6), interact non-covalently with both the enzyme and the DNA

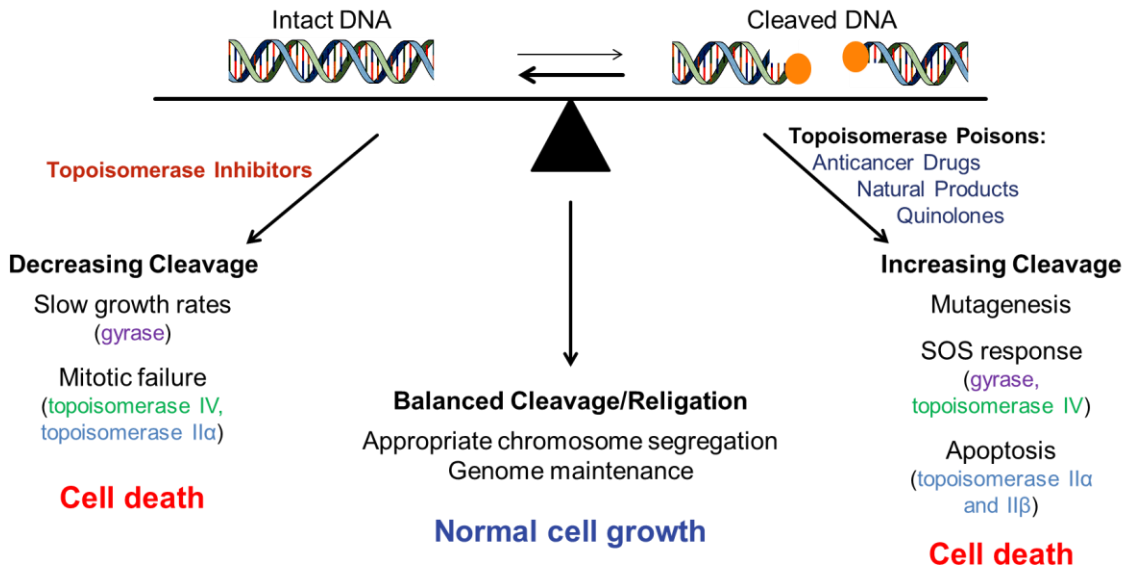

Figure 5. The critical balance of DNA cleavage and religation. The activity of type II topoisomerases must be tightly controlled in the cell. When an appropriate level of cleavage complexes is maintained, topological problems are resolved and the cell can grow normally. If the levels of cleavage complexes decrease, slow growth rates and mitotic failure can cause cell death. Conversely, if the levels of cleavage complexes are too high, DNA damage can overwhelm the cell and also lead to cell death. Figure adapted from Pendleton *et al*.[39]

Interfacial Poisons	Covalent Poisons
• Act non-covalently at the cleavage/religation active site	• Covalently adduct to the enzyme at sites distal to the active site
• Unaffected by reducing agents	• Abrogated by reducing agents
• Enhance enzyme-mediated DNA cleavage when added to the enzyme-DNA complex	• Enhance enzyme-mediated DNA cleavage when added to the enzyme-DNA complex
• Enhance DNA cleavage when incubated with the enzyme prior to the addition of DNA	• Inhibit DNA cleavage when incubated with the enzyme prior to the addition of DNA
• Enhance DNA cleavage by intercalating into the cleaved bond and physically blocking religation	• Enhance DNA cleavage possibly by a mechanism related to the ability to close the N-terminal protein gate

Table 1. Properties of interfacial and covalent topoisomerase II poisons.

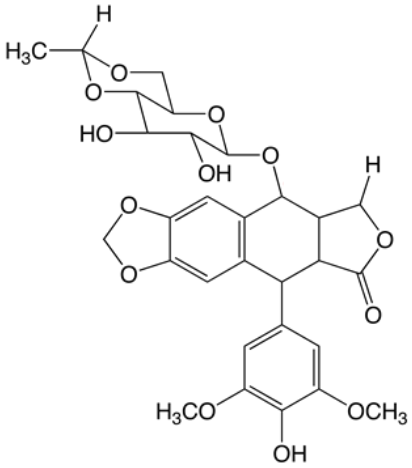

Etoposide

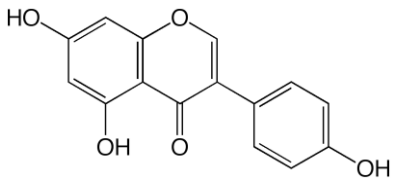

Genistein

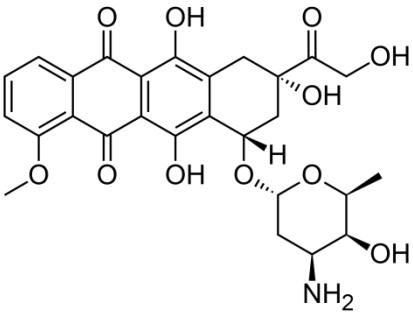

Doxorubicin

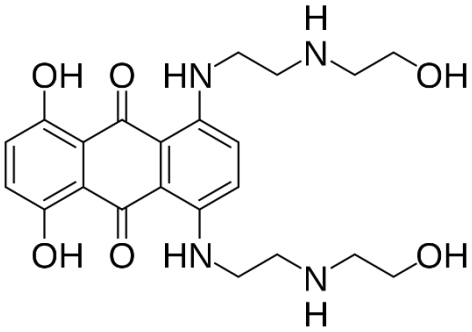

Mitoxantrone

Figure 6. Examples of interfacial topoisomerase II poisons. Etoposide, doxorubicin, and mitoxantrone are anticancer drugs. Genistein is a bioflavonoid found in soy products.

near the cleavage site.[20,82,83] After cleavage occurs, these compounds intercalate into the DNA at the scissile bond and prevent religation.[20,82,83]

Covalent topoisomerase II poisons contain protein-reactive groups such as quinones, isothiocyanates, and maleimides (Figure 7).[20,70,84-87] Unlike interfacial poisons, covalent poisons form adducts with the type II enzyme.[70,85,88] A number of modified cysteine residues have been identified, all of which are distal to the DNA cleavage-religation active site.[70,85,86] It is believed that covalent poisons enhance topoisomerase II-mediated DNA cleavage, at least in part, by closing the N-terminal gate of the protein.[89,90]

Because the oxidation state of covalent poisons is critical for the adduction chemistry, reducing agents, such as DTT, prevent their activity against topoisomerase II.[84,87,88] Additionally, although covalent poisons increase DNA cleavage when added to the enzyme-DNA complex, they inhibit topoisomerase II activity when incubated with the enzyme prior to the addition of DNA.[87,88] This inhibition is a hallmark of covalent poisons.

Targeting bacterial type II topoisomerases: quinolone antibacterials

Quinolones are among the most commonly prescribed antibacterials worldwide and are used to treat infections caused by a broad spectrum of Gram-negative and Gram-positive bacteria in humans and animals (Figure 8).[22,68,91-94] Quinolones are topoisomerase poisons that target both gyrase and topoisomerase IV.[50,68,92,95,96] Like the interfacial poisons discussed above, quinolones bind non-covalently at the enzyme-DNA interface within the cleavage-religation active site.[97-100] After DNA scission, quinolones insert into the DNA at the cleaved bonds and physically block religation, thereby increasing the steady-state concentrations of cleavage complexes.

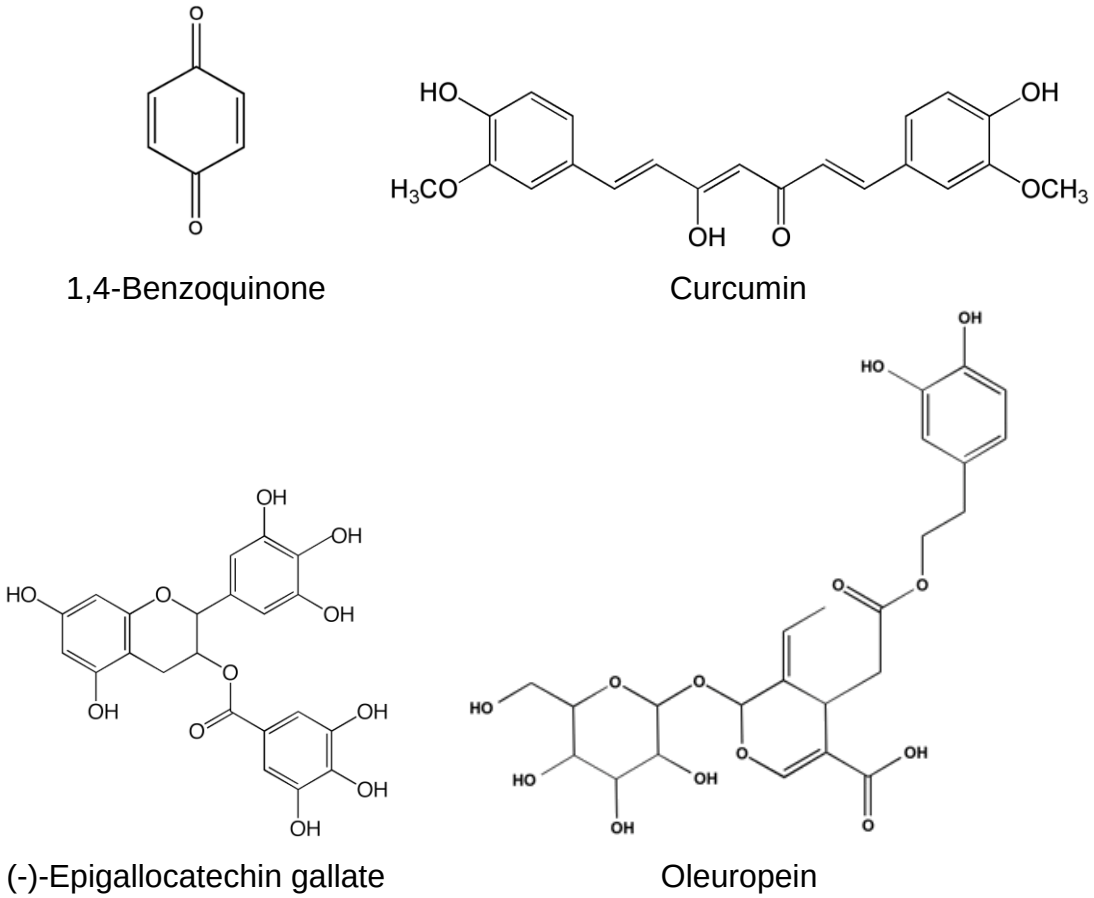

Figure 7. Examples of covalent topoisomerase II poisons. 1,4-benzoquinone is a benzene metabolite. Curcumin is the principal flavor compound of turmeric, (-)-epigallocatechin gallate is the most abundant polyphenol in green tea, and oleuropein is one of the major polyphenols in olive tree species.

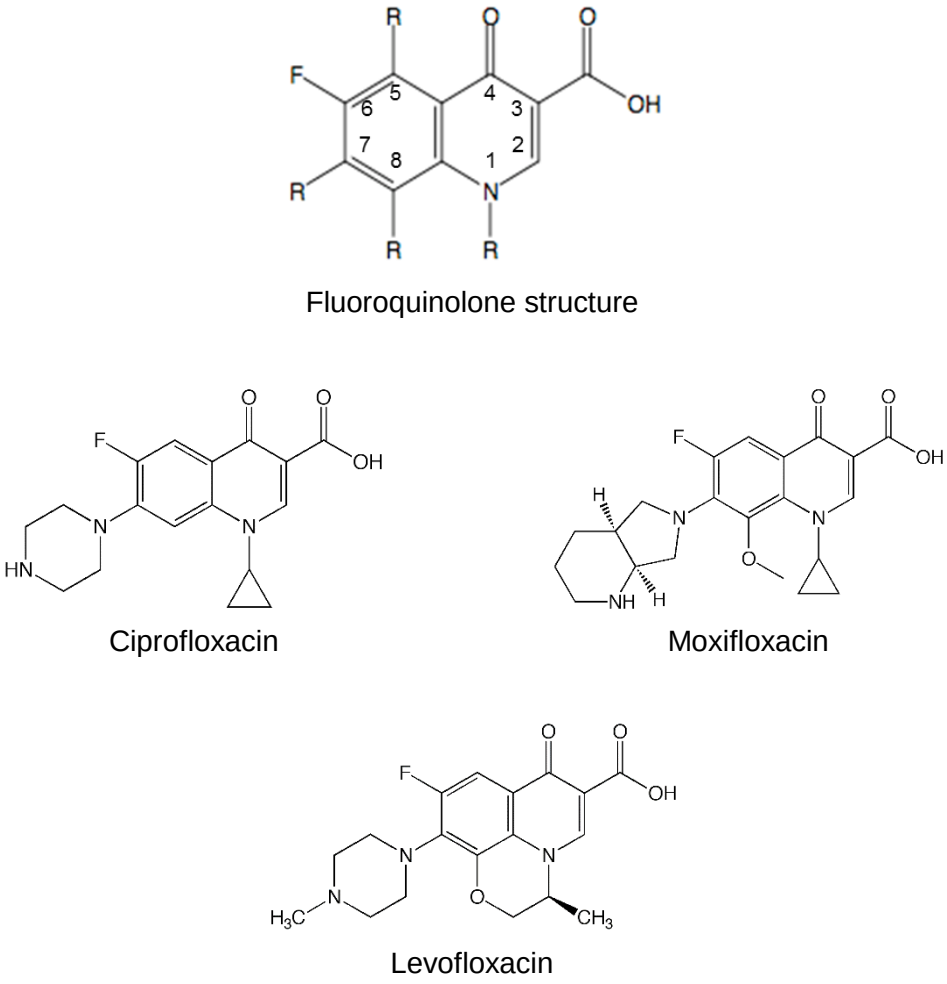

Figure 8. Examples of quinolone antibacterials. A general fluoroquinolone structure is shown at the top.

Although quinolones target both gyrase and topoisomerase IV, the relative importance of each enzyme appears to be both species- and drug-dependent.[73,101-106] As a generalization, gyrase is the primary cellular target for most quinolones in Gram-negative species, whereas topoisomerase IV plays a more important role in many Gram-positive bacteria. This trend notwithstanding, gyrase appears to be the primary target for clinically relevant quinolones in *Bacillus anthracis*, a Gram-positive organism that is the causative agent of anthrax.[107-109]

Unfortunately, the continued clinical efficacy of quinolones is threatened by the rising prevalence of resistance, which has been seen in nearly every infection treated with these drugs.[68,94] Quinolone resistance is usually associated with mutations in gyrase and/or topoisomerase IV.[22,50,68,92,95,106,108-111] For both enzymes, the most common resistance-conferring mutations occur at a highly conserved serine residue in the A subunit and, to a lesser extent, an acidic residue four amino acids downstream (originally described as Ser83 and Glu87 in *Escherichia coli* gyrase).[68,110,112-115] Despite the prevalence of these mutations across a broad spectrum of quinolone-resistant isolates, the mechanistic basis by which they led to resistance remained an enigma for decades.

The first report proposing a mechanism for the serine and acidic residues in mediating quinolone action and resistance described a structure of a cleavage complex formed by *Acinetobacter baumannii* topoisomerase IV in the presence of the quinolone moxifloxacin.[100] The structure showed that the C3/C4 keto acid of moxifloxacin chelated a non-catalytic magnesium ion that was coordinated to four water molecules. Two of these water molecules appeared to form hydrogen bonds with the serine and acidic residues. Biochemical evidence that confirmed the existence and role of this "water-metal ion

bridge" in mediating quinolone-enzyme interactions came from a series of reports on *B. anthracis* and *E. coli* topoisomerase IV.[116-118] These studies provided strong evidence that the serine and acidic residues anchored the quinolone to the enzyme through the water-metal ion bridge (Figure 9) and that mutations at either residue caused quinolone resistance by disrupting the function of the bridge. Recent biochemical and structural studies also extended the work to *Mycobacterium tuberculosis* gyrase.[119,120] However, as further discussed in Chapter VII, each of these enzymes has a unique way of interacting with quinolones through the water-metal ion bridge.

Scope of the Dissertation

Although human and bacterial type II topoisomerases are useful targets for anticancer and antibacterial drugs, much about the interactions between the enzymes, drugs that target them, and their DNA substrates remains unknown. The goals of this dissertation are to further investigate the mechanism of action of covalent poisons with human topoisomerase IIα, to determine how bacterial type II topoisomerases interact with overwound DNA, and to define the interactions between quinolone antibacterials and *B. anthracis* gyrase.

Chapter I provides an introduction to DNA topology, topoisomerases, and topoisomerase-targeting drugs. Materials and methods used in this dissertation are described in Chapter II.

Chapter III describes the effects of thymoquinone, a natural product, on DNA cleavage mediated by human topoisomerase IIα. Thymoquinone acts as a covalent poison, even in its more complex herbal form, suggesting that medicinal herbs and natural products with chemopreventive properties may partially exert their effects through topoisomerases. The results presented in this chapter have been published.[121] Additional studies on the actions

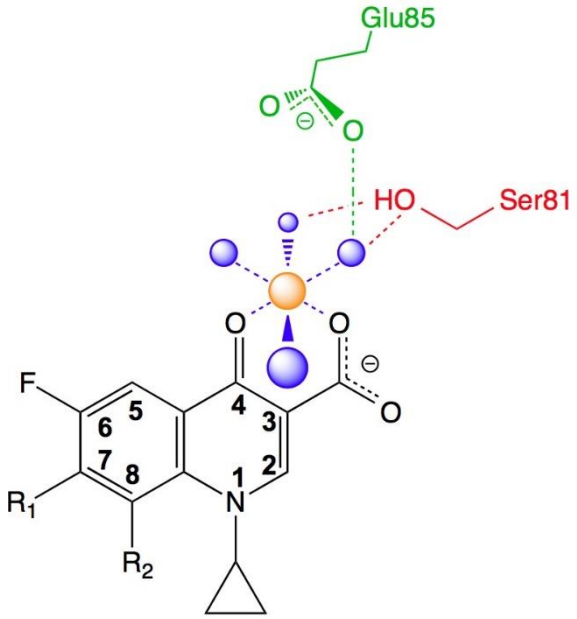

Figure 9. Schematic of the water-metal ion bridge. Residues are labeled according to their positions in *B. anthracis* topoisomerase IV. A Mg^{2+} ion is shown in orange, and coordinating water molecules are shown in blue. Blue dashed lines indicate the coordination sphere of the metal ion. Red and green dashed lines represent hydrogen bonding between water molecules and the serine and glutamic acid residues, respectively. Figure adapted from Aldred *et al.*[117]

of topoisomerase IIα poisons led to contributions to two other publications[122,123] that will not be discussed in this dissertation.

Chapter IV describes the actions of covalent topoisomerase II poisons with the catalytic core of human topoisomerase IIα. Results indicate that covalent poisons cannot enhance cleavage mediated by the catalytic core, but can still inhibit this enzyme if incubated with it prior to the addition of DNA. This suggests that these drugs are capable of interacting with multiple sites within the enzyme, but that not every interaction contributes to the stabilization of cleavage complexes. These results were published in conjunction with work describing the ability of the catalytic core to recognize supercoil geometry during cleavage.[124]

Chapter V describes the recognition of DNA geometry by *B. anthracis* gyrase and topoisomerase IV. Results demonstrate that gyrase can relax overwound DNA in a fast and processive manner while maintaining low levels of cleavage complexes, indicating that gyrase is well suited to work safely on (+)SC DNA ahead of replication forks and other tracking systems. Conversely, although topoisomerase IV relaxes overwound DNA faster than underwound molecules, it is unable to distinguish supercoil geometry during cleavage.

Chapter VI describes the activity of *M. tuberculosis* gyrase on (+)SC DNA. Like a canonical gyrase, the *M. tuberculosis* enzyme relaxes overwound DNA more rapidly than it introduces (-) supercoils into relaxed DNA, and it also maintains lower levels of cleavage complexes on (+)SC substrates. Furthermore, the use of several different gyrase constructs allowed the contributions of different domains of the enzyme to supercoil geometry recognition during cleavage to be investigated. Unlike the catalytic core of human topoisomerase IIα, the catalytic core of *M. tuberculosis* gyrase is unable to distinguish

supercoil handedness during cleavage. Instead, the ability to differentiate between the different substrates during the scission reaction appears to be embedded within the N-terminal domain.

Chapter VII describes the biochemical basis of interactions between quinolone antibacterials and *B. anthracis* gyrase and how these interactions are disrupted by the most common resistance mutations. Results indicate that the primary interaction occurs through the water-metal ion bridge, but that the bridge is anchored solely by the serine residue. Furthermore, altering the C7 and C8 groups of the quinolones can allow for new interactions with the enzyme and at least partially overcome resistance.

Conclusions and implications of the work presented in this dissertation are discussed in Chapter VIII.

CHAPTER II

METHODS

DNA Substrates

(-)SC pBR322 DNA was prepared from *E. coli* using a Plasmid Mega Kit (Qiagen) as described by the manufacturer. (+)SC pBR322 DNA was prepared by treating (-)SC molecules with recombinant *Archaeoglobus fulgidus* reverse gyrase.[125,126] The number of (+) supercoils induced by this process was comparable to the number of (-) supercoils in the original pBR322 preparations.[125] In all experiments that compared (-)SC with (+)SC DNA, the (-)SC plasmid preparations were processed identically to the (+)SC molecules except that reaction mixtures did not contain reverse gyrase. Relaxed pBR322 plasmid DNA was generated by treating (-)SC pBR322 with calf thymus topoisomerase I (Invitrogen) and purified as described previously.[118]

Human Topoisomerase IIα

Enzymes

Recombinant human wild-type topoisomerase IIα, mutant topoisomerase IIα$^{C392A/C405A}$, and truncated hTop2αΔ1175 (containing amino acids 1-1175) were expressed in *Saccharomyces cerevisiae* and purified as described previously.[85,127-129] The catalytic core of human topoisomerase IIα (containing residues 431-1193) was cloned into a GAL1-based vector that added an N-terminal tobacco etch virus protease-cleavable 6xHis-MBP tag.[130] Protein was expressed in yeast cells and purified using a Ni-nitriloacetic acid affinity

column (Qiagen) as described previously.[131,132] Enzymes were stored at -80 °C as a 1.5 mg/mL stock in 50 mM Tris-HCl, pH 7.8, 0.1 mM EDTA, 750 mM KCl, 5% glycerol. For all of the enzymes examined, the concentration of dithiothreitol (DTT) carried over from purification protocols was <2 μM in final reaction mixtures.

Drugs and other materials

Thymoquinone, 2-methyl-1,4-benzoquinone, 2,6-dimethyl-1,4-benzoquinone, 2,5-di-*t*-butyl-1,4-benzoquinone, 2,3,5-trimethyl-1,4-benzoquinone, and etoposide were purchased from Sigma-Aldrich. 2,5-Dimethyl-1,4-benzoquinone was purchased from Santa Cruz Biotechnology. Compounds were prepared as 20 or 40 mM stock solutions in 100% DMSO and stored at 4 ºC. In all cases, the activity of compounds in the DMSO stock solutions was stable for over 6 months. Ground black seed and black seed oil were obtained from Amazing Herbs. The ground black seed was dissolved at 187 mg/mL in 50% DMSO. Insoluble components were removed by centrifugation and the supernatant was stored at 4 ºC. Black seed oil was stored at room temperature and added directly to reaction mixtures. Light mineral oil was obtained from Fisher, stored at room temperature, and added directly to reaction mixtures.

Etoposide and benzoquinone were purchased from Sigma-Aldrich. Etoposide was prepared as a 20 mM stock solution in 100% DMSO and stored at room temperature. Benzoquinone was prepared as a 20 mM solution in water and stored at -20 °C. The quinolone CP-115,953 was a gift from Thomas D. Gootz and Paul R. McGuirk (Pfizer). It was stored at -20 °C as a 40 mM solution in 0.1 N NaOH and was diluted five-fold with

10 mM Tris-HCl, pH 7.9 immediately prior to use. Etoposide quinone was synthesized as described previously[133-135] and was stored at 4 °C as a 20 mM solution in 100% DMSO.

DNA cleavage

DNA cleavage reactions were performed as described previously.[136] Reaction mixtures contained 150 nM human topoisomerase IIα and 10 nM (-)SC pBR322 DNA in 20 µL of Topoisomerase IIα Cleavage Buffer [10 mM Tris-HCl (pH 7.9), 5 mM $MgCl_2$, 100 mM KCl, 0.1 mM Na_2EDTA, and 2.5% (v/v) glycerol]. Reactions were incubated at 37 °C for 6 min unless noted otherwise. Enzyme-DNA cleavage complexes were trapped by adding 2 µL of 5% SDS followed by 2 µL of 250 mM Na_2EDTA (pH 8.0) and 2 µL of 0.8 mg/mL Proteinase K. Reaction mixtures were incubated at 45 °C for 30 min to digest topoisomerase IIα. Samples were mixed with 2 µL of Agarose Loading Dye [60% sucrose in 10 mM Tris-HCl (pH 7.9), 0.5% bromophenol blue, and 0.5% xylene cyanol FF], heated at 45 °C for 2 min, and subjected to electrophoresis in 1% agarose gels in TAE [40 mM Tris-acetate (pH 8.3) and 2 mM Na_2EDTA] containing 0.5 µg/mL ethidium bromide. DNA cleavage was monitored by the conversion of the plasmid to linear molecules. DNA bands were visualized by ultraviolet light and quantified using an Alpha Innotech digital imaging system.

DNA cleavage reactions were carried out in the presence of 0–100 µM thymoquinone, 2-methyl-1,4-benzoquinone, 2,5-dimethyl-1,4-benzoquinone, 2,6-dimethyl-1,4-benzoquinone, 2,5-di-*t*-butyl-1,4-benzoquinone, 2,3,5-trimethyl-1,4-benzoquinone, or etoposide; 0–16 mg/mL black seed extract; or 2 µL of black seed oil or light mineral oil. Unless stated otherwise, compounds were added last to reaction mixtures. In some cases,

reactions contained 250 μM ATP or 100 μM DTT. Alternatively, DTT was added after the 6 min cleavage reaction, and samples were incubated for an additional 5 min.

DNA religation

DNA religation mediated by human topoisomerase IIα was monitored according to the procedure of Byl *et al.*[137] As described above for DNA cleavage assays, DNA cleavage/religation equilibria were established at 37 °C for 6 min in the presence of 0 or 50 μM thymoquinone, 2-methyl-1,4-benzoquinone, 2,5-dimethyl-1,4-benzoquinone, 2,6-dimethyl-1,4-benzoquinone, 2,5-di-*t*-butyl-1,4-benzoquinone, 2,3,5-trimethyl-1,4-benzoquinone, or etoposide. DNA religation was initiated by shifting samples from 37 to 0 °C. The shift to low temperature allows enzyme-mediated religation but prevents new rounds of DNA cleavage from occurring. Therefore, it results in a unidirectional sealing of the cleaved DNA. Reactions were stopped at time points up to 15 s by the addition of 2 μL of 5% SDS. Samples were processed and analyzed as described above. Religation was monitored by the loss of linear DNA.

Persistence of cleavage complexes

The persistence of topoisomerase IIα-DNA cleavage complexes was determined using the procedure of Gentry *et al.*[138] Initial reactions contained 750 nM topoisomerase IIα and 50 nM DNA in a total of 20 μL of Topoisomerase IIα Cleavage Buffer. Reactions were carried out in the absence of compound or in the presence of 50 μM thymoquinone or 8 mg/mL black seed extract. Reactions were incubated at 37 ºC for 6 min and then diluted 20-fold with Topoisomerase IIα Cleavage Buffer at 37 ºC. Samples (20 μL) were removed at times ranging from 0–8 h and stopped with 2 μL of 5% SDS. Samples were processed

and analyzed as described above. The persistence of cleavage complexes was determined by the loss of linear reaction product over time.

Bacterial Type II Topoisomerases

Enzymes

Wild-type *B. anthracis* gyrase and topoisomerase IV subunits (GyrA, GyrB, GrlA, and GrlB) were expressed and purified using a modification of a previously published protocol.[139] Genes were PCR-amplified from chromosomal DNA of the Sterne strain of *B. anthracis*. PCR products were cloned into the pET21b vector, which added an N-terminal 6xHis tag to each protein subunit. The $GyrA^{Ala\text{-}box}$ (in which the seven residues comprising the GyrA box were replaced with alanines), $GyrA^{S85L}$, $GyrA^{S85F}$, $GyrA^{E89K}$, and $GyrA^{E89A}$ constructs were generated using a QuikChange kit (Stratagene). The identities of all constructs were confirmed by DNA sequencing. Each subunit construct was individually transformed into *E. coli* strain BL21(DE3), and cells were grown overnight at 37 °C with shaking in LB medium containing 100 µg/mL ampicillin. Cultures were diluted 20-fold with fresh medium to yield 500-mL cultures, which were grown at 37 °C with shaking at 200 rpm until the optical density at 600 nm was 0.6. Protein expression was induced by adding IPTG to a final concentration of 0.2 mM, and cells were harvested at times optimized for each subunit (WT GyrA, $GyrA^{S85L}$, $GyrA^{S85F}$, $GyrA^{E89K}$, $GyrA^{E89A}$, and GrlA, 3 h; $GyrA^{Ala\text{-}box}$ and GrlB, 2 h; GyrB, 15 min). Pellets were resuspended in 30 mL of cold CelLytic B Buffer (Sigma). Cells were lysed by serial passage through an EmulsiFlex-C5 high-pressure homogenizer at >15,000 psi, cell debris was removed by centrifugation, and proteins were purified from the supernatant by passage through a 2-mL

Ni-nitrilotriacetic acid affinity column (Qiagen). Columns were washed according to the manufacturer's instructions. Proteins were eluted using 12 mL of buffer containing 20 mM Tris-HCl (pH 7.9), 500 mM NaCl, and 300 mM imidazole and exchanged into buffer containing 50 mM Tris-HCl (pH 7.5), 200 mM NaCl, 20% glycerol, and 5 mM DTT using 30 kDa molecular weight cut-off centrifugal concentrators (Amicon). Subunits were stored at -80 °C.

E. coli topoisomerase IV subunits (ParC and ParE) were purified as described previously[140,141] and stored at -80 °C.

Full-length *M. tuberculosis* gyrase subunits (GyrA and GyrB) were expressed and purified as described previously.[119] The GyrA$^{\text{Ala-box}}$ construct was generated using a QuikChange kit (Stratagene), and the identity was confirmed by DNA sequencing. The C-terminal deletion GyrA mutant (GyrA$^{\Delta\text{CTD}}$, residues 2-500) and catalytic core (a fusion of residues 426-675 of GyrB and residues 2-500 of GyrA) constructs were gifts from Dr. James Berger (Johns Hopkins University). GyrA, GyrB, GyrA$^{\text{Ala-box}}$, and GyrA$^{\Delta\text{CTD}}$ were individually cloned into a pET28b derivative that added an N-terminal tobacco etch virus protease (TEV)-cleavable 6xHis tag. The CC was cloned into a pET28b derivative that added an N-terminal TEV-cleavable 6xHis and maltose binding protein tag.[120] Each construct was individually transformed into *E. coli* strain Rosetta 2 pLysS, and cells were grown overnight at 37 °C with shaking in 2xYT medium containing 100 μg/mL kanamycin (GyrA$^{\text{Ala-box}}$ and GyrA$^{\Delta\text{CTD}}$) or ampicillin (catalytic core). Cultures were diluted 100-fold with fresh medium to yield 1-L cultures, which were grown at 30 °C with shaking at 150 rpm until the optical density at 600 nm was 0.3. Protein expression was induced by adding IPTG to a final concentration of 1 mM, and cells were harvested after 3 h. Pellets were

resuspended in 60 mL of cold CelLytic B Buffer (Sigma). Cells were lysed by sonication, cell debris was removed by centrifugation, and proteins were purified from the supernatant by passage through a 2-mL Ni-nitrilotriacetic acid affinity column (Qiagen). Columns were washed according to the manufacturer's instructions. Proteins were eluted using 12 mL of buffer containing 20 mM Tris-HCl (pH 7.9), 500 mM NaCl, 250 mM imidazole, and 10% glycerol. Fractions were pooled, concentrated, and incubated overnight at 4 °C with His-tagged TEV protease. The protease was subsequently removed by passage over a new Ni-nitrilotriacetic acid affinity column. The flow-through was collected, concentrated, and exchanged into buffer containing 50 mM Tris-HCl (pH 7.9), 300 mM KCl, and 30% glycerol using 30 kDa molecular weight cut-off centrifugal concentrators (Amicon). Subunits were stored at -80 °C.

Drugs and other materials

Ciprofloxacin was obtained from LKT Laboratories, stored at 4 °C as a 40 mM stock solution in 0.1 N NaOH, and diluted fivefold with 10 mM Tris-HCl (pH 7.9) immediately prior to use. Moxifloxacin was obtained from LKT Laboratories, and levofloxacin was obtained from Sigma Aldrich. Both drugs were stored at 4 °C as 20 mM stock solutions in 100% DMSO. Table 2 contains the full chemical names for the other compounds used. 8-Methyl-cipro, 8-methoxy-cipro, cipro-dione, 8-H-moxi, 8-methyl-moxi, moxi-dione, 3'-(AM)P-quinolone, and 3'-(AM)P-dione were synthesized as reported previously.[116,142] 8-methyl-cipro and 8-methoxy-cipro were stored at 4 °C as 40 mM stock solutions in 0.1 N NaOH and diluted five-fold with 10 mM Tris-HCl (pH 7.9) immediately prior to use.

Name in Dissertation	Full Chemical Name
3'-(AM)P-quinolone	1-Cyclopropyl-6-fluoro-1,4-dihydro-8-methyl-7-[(3S)-3-(aminomethyl)-1-pyrrolidinyl]-4-oxo-3-quinolinecarboxylic acid
3'-(AM)P-dione	3-amino-7-[(3S)-3-(aminomethyl)-1-pyrrolidinyl]-1-cyclopropyl-6-fluoro-8-methyl-2,4(1H,3H)-quinazolinedione
Cipro-dione	3-amino-7-(1-piperazinyl)-1-cyclopropyl-6-fluoro-2,4(1H,3H)-quinazolinedione
8-Methyl-cipro	1-Cyclopropyl-6-fluoro-1,4-dihydro-8-methyl-7-(1-piperazinyl)-4-oxo-3-quinolinecarboxylic acid
8-Methoxy-cipro	1-Cyclopropyl-6-fluoro-1,4-dihydro-8-methoxy-7-(1-piperazinyl)-4-oxo-3-quinolinecarboxylic acid
Moxi-dione	3-amino-7-[(4aS,7aS)-octahydro-6H-pyrrolo[3,4-b]pyridin-6-yl]-1-cyclopropyl-6-fluoro-8-methoxy-2,4(1H,3H)-quinazolinedione
8-H-moxi	1-Cyclopropyl-6-fluoro-1,4-dihydro-7-[(4aS,7aS)-octahydro-6H-pyrrolo[3,4-b]pyridin-6-yl]-4-oxo-3-quinolinecarboxylic acid
8-Methyl-moxi	1-Cyclopropyl-6-fluoro-1,4-dihydro-8-methyl-7-[(4aS,7aS)-octahydro-6H-pyrrolo[3,4-b]pyridin-6-yl]-4-oxo-3-quinolinecarboxylic acid

Table 2. Full chemical names of compounds used.

All other compounds were stored at 4 °C as 20 mM stock solutions in 100% DMSO. All other chemicals were analytical reagent grade.

DNA cleavage

DNA cleavage reactions were based on the procedure of Aldred *et al*.[116] Reactions with *B. anthracis* gyrase contained 500 nM wild-type, $GyrA^{S85L}$, $GyrA^{S85F}$, $GyrA^{E89K}$, or $GyrA^{E89A}$ gyrase or 250 nM $GyrA^{Ala\text{-}box}$ gyrase at a 1:2 GyrA:GyrB ratio and 10 nM (+)SC or (-)SC pBR322 in a total volume of 20 µL of 50 mM Tris-HCl (pH 7.5), 100 mM KGlu, 5 mM $MgCl_2$, and 50 µg/mL bovine serum albumin (BSA, Sigma). In some cases, a range of $MgCl_2$ concentrations (0-3 mM) were tested or $MgCl_2$ was replaced with $BaCl_2$ (2 mM), $NiCl_2$ (1 mM), or $MnCl_2$ (1 mM). Alternatively, $MgCl_2$ was replaced with $CaCl_2$ (20 mM) and a range of enzyme concentrations was tested. Reactions were incubated at 37 °C for 30 min. Enzyme-DNA cleavage complexes were trapped by adding 2 µL of 5% SDS followed by 2 µL of 250 mM Na_2EDTA and 2 µL of 0.8 mg/mL Proteinase K. Reaction mixtures were incubated at 45 °C for 30 min to digest the enzyme. Samples were mixed with 2 µL of Agarose Loading Dye and incubated at 45 °C for 2 min before loading on gels. Reaction products were subjected to electrophoresis in 1% agarose gels in TAE containing 0.5 µg/mL ethidium bromide and visualized as described above. DNA cleavage was monitored by the conversion of supercoiled plasmid to linear molecules and quantified by comparison to a control reaction in which an equal mass of DNA was digested by *Eco*RI (New England BioLabs).

DNA cleavage reactions with *B. anthracis* topoisomerase IV contained 100 nM enzyme (1:2 GrlA:GrlB ratio) and 10 nM (+)SC or (-)SC pBR322 in 20 µL of Topoisomerase IV

Cleavage Buffer [40 mM Tris-HCl (pH 7.9), 50 mM NaCl, and 12.5% glycerol] containing 10 mM $MgCl_2$. DNA cleavage reactions with *E. coli* topoisomerase IV contained 10 nM enzyme (1:1 ParC:ParE ratio) and 10 nM (+)SC or (-)SC pBR322 in 20 µL of Topoisomerase IV Cleavage Buffer containing 5 mM $MgCl_2$. Reactions with both enzymes were incubated at 37 °C for 10 min, then stopped, digested, and analyzed as described above.

DNA cleavage reactions with *M. tuberculosis* gyrase contained 100 nM wild-type, $GyrA^{Ala\text{-}box}$, or $GyrA^{\Delta CTD}$ gyrase (3:2 GyrA:GyrB ratio) or 100 nM CC and 10 nM (+)SC or (-)SC pBR322 in a total volume of 20 µL of 10 mM Tris-HCl (pH 7.5), 40 mM KCl, 6 mM $MgCl_2$, 0.1 mg/mL BSA, and 10 % glycerol. Reactions were incubated at 37 °C for 10 min, then stopped, digested, and analyzed as described above.

DNA supercoiling and relaxation

DNA supercoiling and relaxation assays were based on previously published protocols.[116,119] For assays with *B. anthracis* gyrase, GyrA and GyrB (1000 nM enzyme at a 1:1 GyrA:GyrB ratio) were incubated for 5 min at 37 °C in 100 mM Tris-HCl (pH 7.5), 350 mM KGlu, and 100 µg/mL BSA, then diluted twofold with a mixture containing DNA, Mg^{2+}, and ATP for a final reaction volume of 20 µL. The final concentrations of reactants were 500 nM gyrase, 5 nM (+)SC, (-)SC, or relaxed DNA, and 1.5 mM ATP in 50 mM Tris-HCl (pH 7.5), 5 mM $MgCl_2$, 175 mM KGlu, and 50 µg/mL BSA. Reactions were incubated at 37 °C for various times and stopped by the addition of 3 µL of a mixture of 0.77% SDS and 77.5 mM Na_2EDTA. Samples were mixed with 2 µL of Agarose Loading Dye and subjected to electrophoresis in 1% agarose gels in TBE [100 mM Tris-borate (pH

8.3) and 2 mM EDTA]. Gels were stained with 1 μg/mL ethidium bromide for 30 min. DNA bands were visualized with medium-range ultraviolet light on an Alpha Innotech digital imaging system.

Topoisomerase IV DNA relaxation assays contained 10 nM topoisomerase IV, 5 nM supercoiled pBR322, and 1 mM ATP in 20 μL of 40 mM HEPES (pH 7.6), 100 mM KGlu, 10 mM $Mg(OAc)_2$, and 50 mM NaCl. Reactions were incubated, stopped, and analyzed as described above.

M. tuberculosis gyrase supercoiling assays contained 25 nM gyrase, 5 nM supercoiled pBR322, and 1.5 mM ATP in 20 μL of 10 mM Tris-HCl (pH 7.5), 40 mM KCl, 6 mM $MgCl_2$, 0.1 mg/mL BSA, and 10 % glycerol. Reactions were incubated, stopped, and analyzed as described above.

Two-dimensional gel electrophoresis

In some cases, supercoiling reaction products were analyzed by two-dimensional gel electrophoresis as described previously.[125] The first dimension was run for 2 h as described in the preceding section. The gel was then soaked in TBE containing 4.5 μg/mL chloroquine for 2 h with gentle shaking followed by electrophoresis in the orthogonal direction (90° clockwise) for 2 h in fresh TBE containing 4.5 μg/mL chloroquine. Gels were stained and DNA bands were visualized as described above.

Single-molecule assays

An ~5 kb region of pET28b was amplified by PCR using primers that incorporated cut sites for *Bsa*I to create DNA with unique, nonpalindromic sticky ends as described previously.[143] One end of the linear substrate was ligated to an ~500 bp DNA handle

functionalized with multiple biotin moieties, while the other end was ligated to a similar handle containing multiple digoxigenin moieties. An 18×5×0.08 mm flow chamber was constructed using a pair of glass coverslips joined together by two strips of double-sided adhesive film. The chamber was incubated with DNA at a final concentration of ~1 pM. The digoxigenin-containing end of the DNA was immobilized to the surface of the chamber with anti-digoxigenin antibodies. The biotin-containing end was attached to an ~1 μm diameter streptavidin-coated magnetic bead (Dynal). The resulting DNA construct could then be torsionally constrained and manipulated using magnetic tweezers.

A magnetic tweezers apparatus similar to that described by Ribeck and Saleh[144] was used to manipulate DNA topology and apply small stretching forces to the substrate. DNA extension was recorded at a rate of 200 frames per second using video-based tracking of bead images at a magnification of 125 nm per pixel. To verify tethering of single DNA molecules, beads were rotated at a force of 3.5 pN. Single coilable DNA molecules denature when underwound and form a plectoneme when overwound, following characteristic extension-rotation curves for both conformational changes.[145]

DNA relaxation reactions were carried out at 22 °C and utilized 1 nM gyrase and 1 mM ATP in 50 mM Tris-HCl pH 7.5, 5 mM $MgCl_2$, 175 mM KGlu, 50 μg/mL BSA, and 0.1% Tween-20 (to prevent sticking of the magnetic beads). Positive supercoils were generated at forces <5 pN by rotating the magnetic bead in increments of +50 rotations. Under these conditions, supercoiling reduces DNA extension due to the formation of plectonemes. Relaxation of the (+)SC DNA resulted in extension of the substrate. The magnetic tweezers apparatus was programmed to automatically apply +50 rotations when the DNA extension

exceeded a set threshold, typically 20-50 nm below the maximum (fully unwound) extension.

A simple detection routine was employed to quantify burst events within recorded data. A candidate point within an activity burst was defined as a point at which the change in mean extension over 100 ms (20 data points) on either side of the point was greater than 100 nm. After the window of the activity burst was defined, it was narrowed by excluding any points that were within one standard deviation of the mean extension 20 ms before or after the burst. The end points of the burst were defined by re-including one data point ahead of and one data point behind this narrowed region. Burst rates were obtained by linear regression of the raw data. Burst sizes were estimated by dividing the change in extension over the burst event by the average extension change resulting from relaxation of a single plectonemic supercoil. The bursting events were independent of force and were therefore pooled in the distributions.

CHAPTER III

POISONING HUMAN TOPOISOMERASE IIα WITH THYMOQUINONE, A NATURAL PRODUCT

Introduction

Nigella sativa is an annual flowering plant that is indigenous to Pakistan, India, and Mediterranean countries.[146] The seeds of *N. sativa* (often referred to as black seed or black cumin) are used as a spice in Eastern cooking.[147,148] Black seed has also been utilized as a medicinal herb in Middle Eastern, Northern African, and Indian cultures for over 3000 years.[146,147,149] Seeds from *N. sativa* were found in Tutankhamun's tomb, indicating that their use in Egypt dates back at least to *c*. 1325 B.C.[149] Historically, the herb has been used to treat a number of illnesses associated with inflammation, including asthma, bronchitis, fever, arthritis, and rheumatism.[150-152] More recently, it has been shown to have anticancer activity in animal and cellular models.[147,153-158]

The major and most well-studied bioactive compound in *N. sativa* is thymoquinone.[146] This compound is found in the essential oil, which comprises approximately 0.4% of the seed.[147] A high proportion of the essential oil (estimates range from 28–57%) is thymoquinone. Since thymoquinone was first isolated in the 1960s, a number of studies have investigated its antioxidant and cellular effects.[159] The compound displays anti-inflammatory and pro-apoptotic properties.[146,159] In addition, it causes cell cycle arrest and inhibits the growth of cancer cells with minimal effects on non-malignant lines.[146,160-162]

Thymoquinone is similar in structure to 1,4-benzoquinone (Figure 10), a benzene metabolite that increases levels of DNA cleavage mediated by human type II

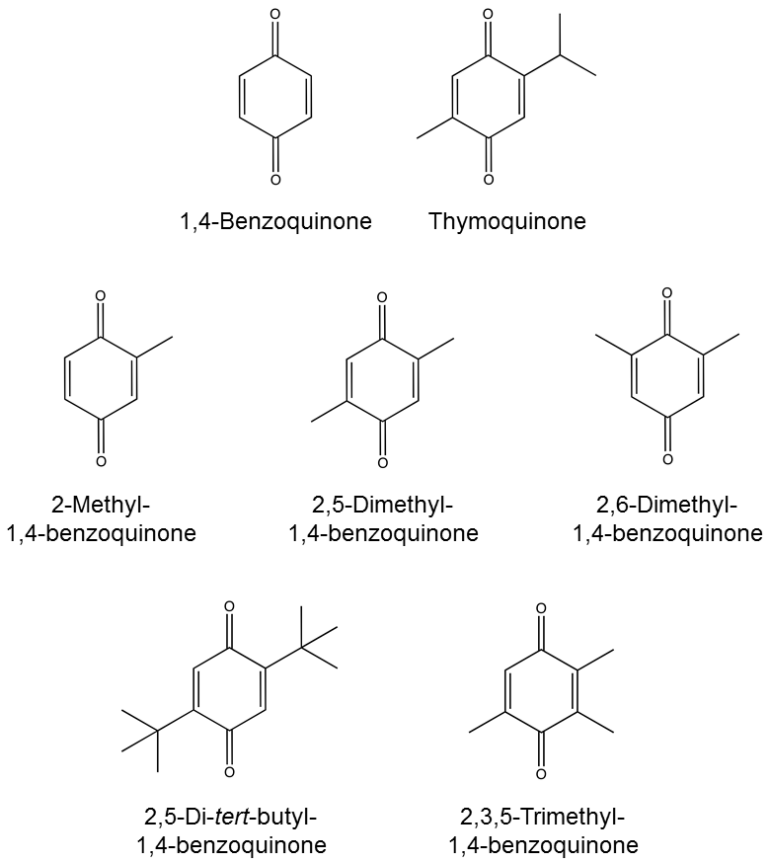

Figure 10. Structures of 1,4-benzoquinone, thymoquinone, and related compounds.

topoisomerases.[87] Because thymoquinone has anticancer properties and has structural similarities to known topoisomerase II poisons, the effects of the compound on the activity of human topoisomerase IIα were determined.

Results and Discussion

Effects of thymoquinone on DNA cleavage mediated by topoisomerase IIα

First, the ability of thymoquinone to stabilize cleavage complexes mediated by topoisomerase IIα was investigated. Thymoquinone increased levels of DNA cleavage mediated by human topoisomerase IIα ~5-fold in a dose-dependent manner (Figure 11, left). At all concentrations examined, cleavage induced by the compound was similar to or greater than that of etoposide, a commonly used anticancer drug. Maximal DNA scission was observed at ~50 μM thymoquinone and the cleavage-religation equilibrium was reached at ~6 min (right).

Type II topoisomerases do not require ATP for DNA cleavage or religation (the above reactions did not contain ATP). However, because of the large conformational changes that accompany DNA strand passage, the cofactor is required to promote overall catalytic activity.[27,163] Therefore, the effects of thymoquinone on topoisomerase IIα activity were assessed in the presence of ATP (Figure 11, left, inset). Although the relative enhancement of DNA cleavage was somewhat lower in the presence of ATP, thymoquinone still poisoned the enzyme.

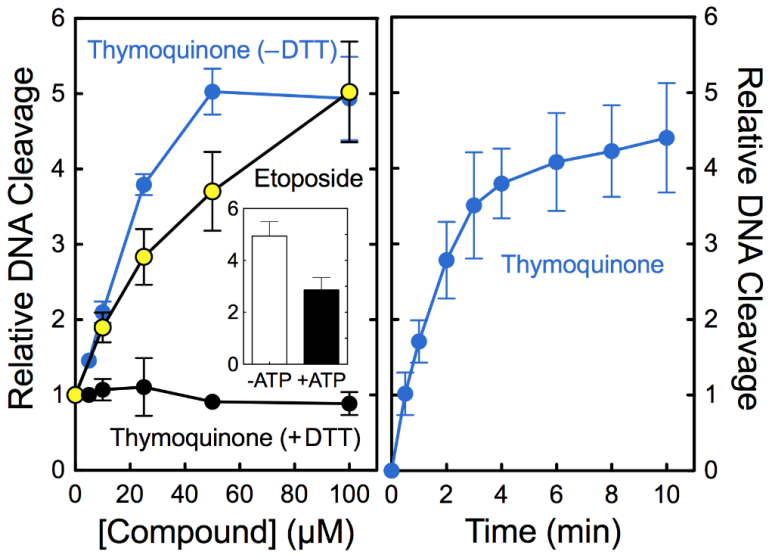

Figure 11. Thymoquinone enhances DNA cleavage mediated by human topoisomerase IIα. Left: Concentration dependence of thymoquinone-induced DNA cleavage in the absence (–DTT, blue) or presence (+DTT, black) of 100 μM DTT. Results for etoposide (yellow) are shown for comparison. Inset: Thymoquinone enhances topoisomerase IIα-mediated DNA cleavage in the presence of ATP. DNA cleavage induced by 100 μM thymoquinone is shown in the absence (white) or presence (black) of 250 μM ATP. Right: Time course of thymoquinone-induced DNA cleavage. DNA cleavage levels were calculated relative to a 6 min no-drug control reaction. Error bars represent standard deviations for at least three independent experiments.

Characterization of thymoquinone as a covalent poison

Thymoquinone is structurally related to 1,4-benzoquinone, the archetypical covalent topoisomerase II poison (see Figure 10).[87] This similarity suggests that thymoquinone is also a covalent poison. Therefore, several experiments were carried out to determine whether this hypothesis was correct.

First, a number of compounds related to thymoquinone (shown in Figure 10) were tested for the ability to enhance DNA scission mediated by human topoisomerase IIα (Figure 12). If thymoquinone is a covalent poison, altering ring substituents should lead to predictable changes in cleavage activity. 2-Methyl-1,4-benzoquinone, which lacks the electron-donating isopropyl group of thymoquinone, should be more reactive than thymoquinone and therefore be a more potent topoisomerase II poison. As seen in Figure 12, this was the case: 2-methyl-1,4-benzoquinone induced cleavage at much lower concentrations. Replacing the isopropyl moiety of thymoquinone with a methyl group, which is less electron donating, should also result in a compound that is more reactive than the parent compound (but less so than 2-methyl-1,4-benzoquinone). 2,5-Dimethyl-1,4-benzoquinone and 2,6-dimethyl-1,4-benzoquinone both displayed this predicted intermediate activity.

In contrast to the above, substitution of the methyl and isopropyl groups with tertiary butyl groups, which are more electron donating, should decrease the reactivity of the parent compound. 2,5-Di-*tert*-butyl-1,4-benzoquinone, which contained these substitutions, displayed no ability to enhance enzyme-mediated DNA cleavage. Finally, the ability of covalent poisons to induce DNA scission generally requires at least two available acylation sites on the compound.[85,88,89] Consistent with this requirement, 2,3,5-trimethyl-

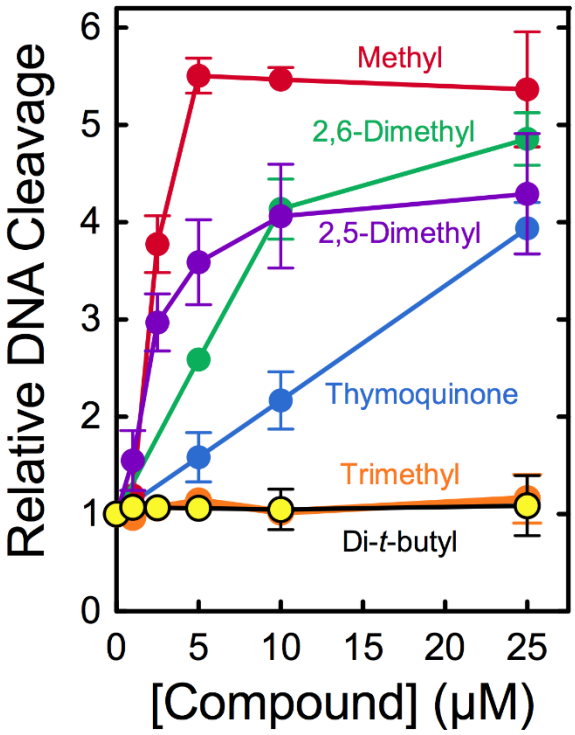

Figure 12. Effects of thymoquinone derivatives on DNA cleavage mediated by human topoisomerase IIα. Results are shown for 2-methyl-1,4-benzoquinone (red); 2,5-dimethyl-1,4-benzoquinone (purple); 2,6-dimethyl-1,4-benzoquinone (green); 2,3,5-trimethyl-1,4-benzoquinone (orange); and 2,5-di-*tert*-butyl-1,4-benzoquinone (yellow). DNA cleavage levels were calculated relative to a no-drug control reaction. Thymoquinone (blue) is shown for comparison. Error bars represent standard deviations for at least three independent experiments, except for 2,3,5-trimethyl-1,4-benzoquinone and 2,5-di-*tert*-butyl-1,4-benzoquinone, for which error bars represent the standard error of the mean of two independent replicates.

1,4-benzoquinone, which has only one available acylation site, displayed no activity against topoisomerase IIα.

Previous studies have shown that covalent poisons can accommodate a greater range of structural alterations than interfacial poisons.[70,71,87-89,135,164] This suggests that covalent poisons act more as chemical modification reagents than "ligands" that require specific binding pockets on the enzyme. The above notwithstanding, increased reactivity among the compounds examined also correlated with decreased substituent bulk (methyl > dimethyl > methyl + isopropyl > di-*t*-butyl). Thus, it is possible that changes in activity in this series are due to steric, rather than electronic, effects. If this were the case, the observed activity patterns would not be conclusive support that thymoquinone is a covalent poison.

Therefore, a second experiment was carried out in which the effects of DTT on thymoquinone and its derivatives were examined. As predicted for covalent poisons, which contain reactive groups that are sensitive to reducing agents, 100 μM DTT abrogated the ability of thymoquinone to increase DNA cleavage when added to reaction mixtures (Figure 11, left, and Figure 13). Similarly, the inclusion of DTT in reaction mixtures abolished the activity of 2-methyl-1,4-benzoquinone, 2,5-dimethyl-1,4-benzoquinone, and 2,6-dimethyl-1,4-benzoquinone (Figure 13).

Once covalent poisons have generated protein crosslinks within topoisomerase II, their redox state no longer affects their activity. Consequently, the addition of reducing agents to assay mixtures after DNA cleavage-religation equilibria have been established with a covalent poison should not reverse the cleavage enhancement. As seen in Figure 13, 100 μM DTT had no significant effect on the activity of thymoquinone, 2-methyl-1,4-

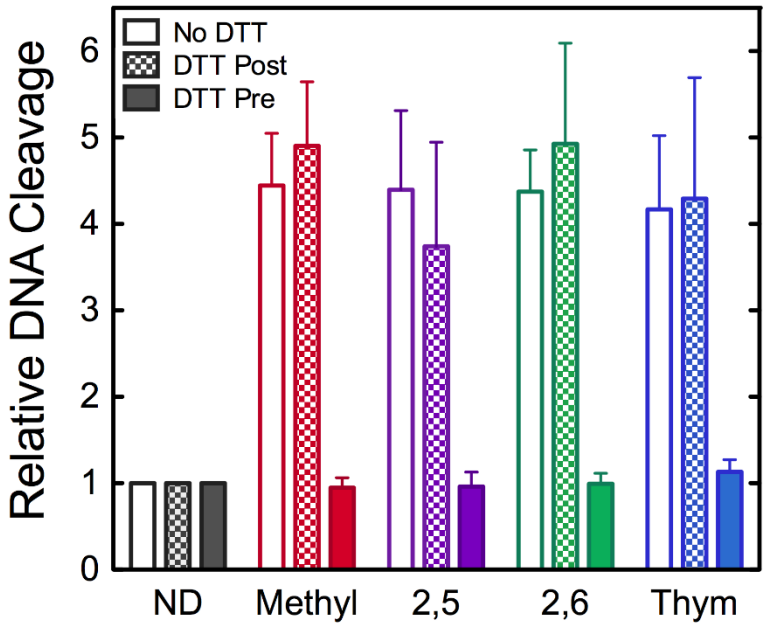

Figure 13. Effects of DTT on DNA cleavage enhancement by thymoquinone derivatives. Cleavage reactions were carried out in the absence of DTT (open bars), in the presence of 100 µM DTT added after establishment of cleavage-religation equilibria (checked bars), or in the presence of 100 µM DTT added at the start of the 6-min cleavage reaction (filled bars). Results are shown for 50 µM 2-methyl-1,4-benzoquinone (Methyl, red); 2,5-dimethyl-1,4-benzoquinone (2,5, purple); 2,6-dimethyl-1,4-benzoquinone (2,6, green); and thymoquinone (Thym, blue). DNA cleavage levels were calculated relative to a no-drug control reaction (ND, black). Error bars represent standard deviations for at least three independent experiments.

benzoquinone, 2,5-dimethyl-1,4-benzoquinone, or 2,6-dimethyl-1,4-benzoquinone once adducts were formed.

In a third experiment, 50 μM thymoquinone was incubated with human topoisomerase IIα prior to the addition of DNA (Figure 14, left). As expected for a covalent poison, thymoquinone inactivated the enzyme ($t_{1/2} \approx 5$ min).

Finally, in a fourth experiment, topoisomerase IIα was incubated with thymoquinone and digested with trypsin. The resulting peptides were analyzed by MALDI mass spectrometry (data not shown). Mass changes in several peptides were observed following treatment with thymoquinone. Although this finding indicates that thymoquinone covalently modifies topoisomerase IIα, sites of adduction could not be assigned. This is most likely due to the fact that thymoquinone has two sites for potential acylation and generates protein crosslinks. A similar issue was previously reported for the analysis of topoisomerase IIα peptides following incubation with 1,4-benzoquinone.[85] In this case, sites of adduction were identified using plumbagin (a *para*-quinone that has only a single site for acylation) and were confirmed by mutagenesis studies.[85] This study established that quinones can adduct human topoisomerase IIα at Cys392 and Cys405. It also showed that topoisomerase $IIα^{C392A/C405A}$ is partially (~40-50%) resistant to covalent poisons (such as 1,4-benzoquinone, PCB quinones, and curcumin oxidation products) but not to interfacial poisons.[71,85]

Therefore, the ability of thymoquinone to increase the level of DNA cleavage mediated by topoisomerase $IIα^{C392A/C405A}$ was compared to that of the wild-type enzyme. As seen in Figure 14 (right), levels of cleavage were ~40% lower with the mutant enzyme.

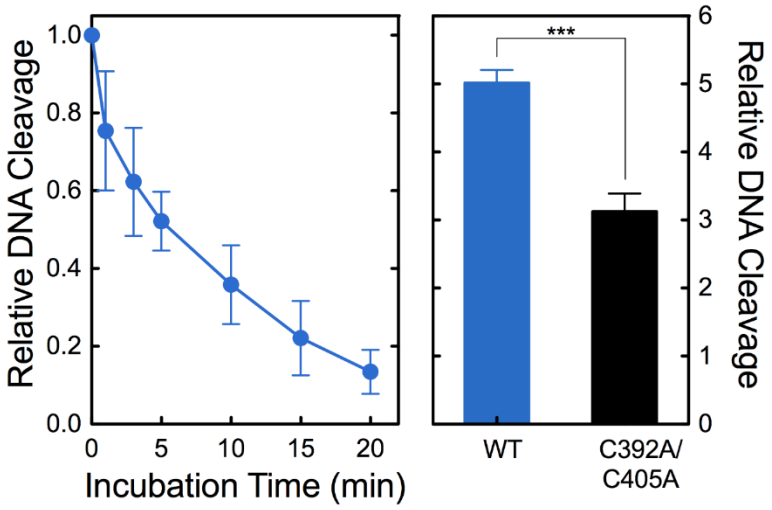

Figure 14. Thymoquinone is a covalent topoisomerase IIα poison. Left: Thymoquinone inactivates human topoisomerase IIα when incubated with the enzyme prior to the addition of DNA. Cleavage activity was monitored in the presence of 50 μM thymoquinone. DNA cleavage levels were calculated relative to cleavage induced when thymoquinone and the enzyme were not incubated prior to reaction initiation. Error bars represent standard deviations for at least three independent experiments. Right: Human topoisomerase $IIα^{C392A/C405A}$ is partially resistant to thymoquinone. Cleavage enhancement was monitored in the presence of 50 μM thymoquinone. DNA cleavage levels are shown for the wild-type enzyme (blue) and topoisomerase $IIα^{C392A/C405A}$ (black). Error bars represent standard deviations for at least three independent experiments. ***p = 0.0001

Taken together, the above results provide strong evidence that thymoquinone and related compounds are covalent topoisomerase II poisons.

Effects of thymoquinone on DNA religation

Interfacial topoisomerase II poisons typically increase levels of DNA cleavage complexes by inhibiting the religation of cut strands.[20,82,83] In contrast, covalent poisons have varying abilities to inhibit the topoisomerase II DNA religation reaction. Thymoquinone displayed a modest effect on the rate of topoisomerase II religation (decreased by ~35–50%), while etoposide (an interfacial poison) inhibited the reaction by at least 10-fold (Figure 15). The thymoquinone derivatives 2-methyl-1,4-benzoquinone, 2,5-dimethyl-1,4-benzoquinone, and 2,6-dimethyl-1,4-benzoquinone displayed no appreciable ability to inhibit religation (Figure 15, inset).

Effects of thymoquinone on the stability of cleavage complexes

Upon dilution, DNA cleavage complexes formed with human topoisomerase IIα rapidly re-establish equilibria ($t_{1/2}$ < 1 min) in which levels of DNA cleavage are significantly decreased (Figure 16). Covalent poisons trap the DNA within the enzyme by crosslinking the N-terminal domains; therefore, the re-equilibration seen in the absence of the poison should not take place. As predicted, no significant decrease in thymoquinone-induced cleavage complexes was seen 8 h after dilution (Figure 16).

Ability of black seed extract to poison topoisomerase IIα

In culinary and medicinal applications, thymoquinone is typically consumed as either ground black seed or black seed oil.[146-149] Therefore, the effects of both on the DNA

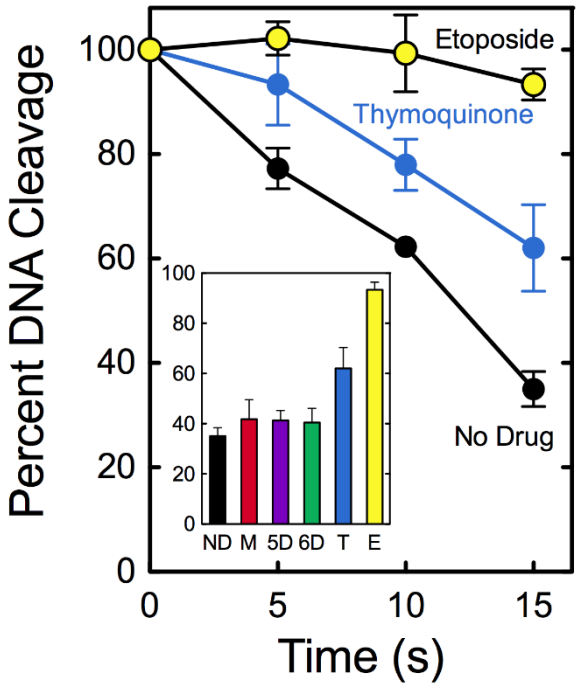

Figure 15. Effects of thymoquinone on religation mediated by human topoisomerase IIα. DNA cleavage reactions were initiated in the absence of compound (No Drug, black) or in the presence of 50 µM thymoquinone (blue). Results with 50 µM etoposide (yellow) are shown for comparison. DNA cleavage levels prior to the induction of religation were set to 100%. Inset: Levels of DNA cleavage remaining at 15 s after the induction of religation are shown for reactions containing no drug (ND, black) or 50 µM 2-methyl-1,4-benzoquinone (M, red); 2,5-dimethyl-1,4-benzoquinone (5D, purple); 2,6-dimethyl-1,4-benzoquinone (6D, green); thymoquinone (T, blue); or etoposide (E, yellow). Error bars represent standard deviations for at least three independent experiments.

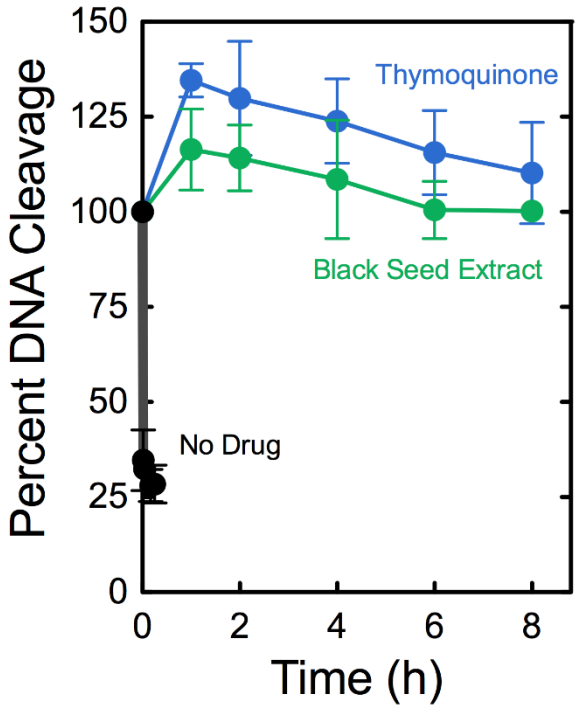

Figure 16. Effects of thymoquinone and black seed extract on the persistence of topoisomerase IIα-DNA cleavage complexes. Assays were carried out in the absence of compound (No Drug, black) or in the presence of 50 µM thymoquinone (blue) or 8 mg/mL black seed extract (green). DNA cleavage at time zero was set to 100%. Error bars represent standard deviations for at least three independent experiments.

cleavage activity of human topoisomerase IIα were determined (Figure 17). Black seed extract increased enzyme-mediated DNA cleavage ~4-fold in a dose-dependent fashion. Levels of cleavage enhancement were consistent with the estimated thymoquinone concentration in the extract. Furthermore, as seen with thymoquinone, cleavage complexes formed in the presence of black seed extract remained stable for more than 8 h following dilution in persistence assays (see Figure 16).

The inclusion of 2 μL of black seed oil in reaction mixtures also increased levels of DNA cleavage (~4-fold) mediated by human topoisomerase IIα (Figure 17, inset). In contrast, no cleavage enhancement was observed when light mineral oil was included instead.

Taken together, results with the black seed extract and oil imply that thymoquinone is a topoisomerase II poison even in its more complex natural formulation.

Conclusions

A number of topoisomerase II poisons derived from natural sources display chemotherapeutic or chemopreventive activity.[5,16,20,22,62-67,69-72,75] Thymoquinone is the primary active compound in black seed, a Mediterranean plant with a rich history of use as a medicinal herb.[146,147,159] Given the structural similarity between thymoquinone and established topoisomerase II poisons, the activity of the compound against human topoisomerase IIα was determined. Results discussed here indicate that thymoquinone is a covalent topoisomerase II poison, even in its herbal formulation. Thus, thymoquinone can be added to the growing list of dietary and medicinal natural products with activity against human type II topoisomerases.

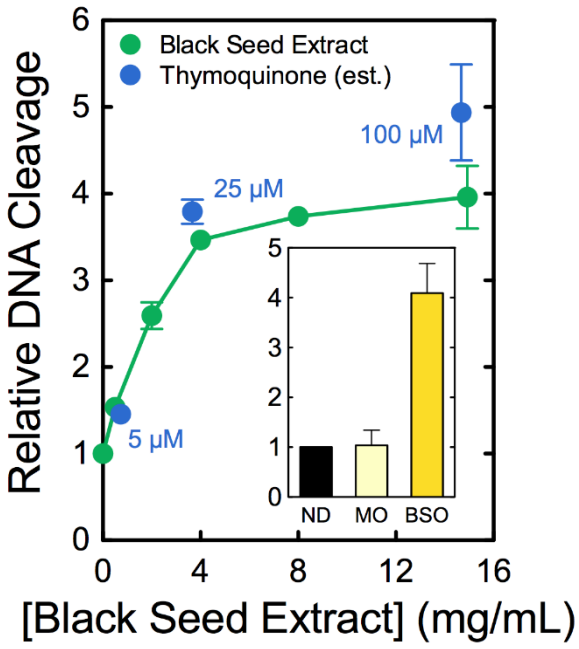

Figure 17. Effects of black seed extract on DNA cleavage mediated by human topoisomerase IIα (green). Cleavage results for 5, 25, and 100 µM thymoquinone (blue) are overlaid at concentrations of black seed extract estimated to contain the corresponding amounts of thymoquinone.[147] Inset: DNA cleavage is shown in the absence of compound (ND, black) or in the presence of 2 µL (in a total reaction volume of 20 µL) of light mineral oil (MO, light yellow) or black seed oil (BSO, yellow). DNA cleavage levels were calculated relative to a no-drug control reaction. Error bars represent standard deviations for at least three independent experiments.

CHAPTER IV

DRUG INTERACTIONS WITH THE CATALYTIC CORE OF HUMAN TOPOISOMERASE IIα

Introduction

As described in Chapter I, human topoisomerase IIα functions as a homodimeric protein. Based on homology with DNA gyrase, the enzyme can be divided into three domains: the N-terminal domain, the catalytic core, and the C-terminal domain.[3,5,14,20-22,40] The N-terminal domain contains the site of ATP binding and hydrolysis. ATP binding triggers dimerization of the N-terminal domain, which helps capture the T-segment and closes the N-terminal protein gate.[165] This action induces the transport of the T-segment through the open gate in the G-segment.[3,5,14,20-22,40,165] The catalytic core of topoisomerase IIα contains the active site tyrosine that covalently attaches to the DNA during scission. It also forms a second protein gate that allows the T-segment to exit the enzyme following strand passage. The C-terminal domain is the least well understood region of topoisomerase IIα. It is highly variable and contains nuclear localization sequences and phosphorylation sites.[14,20,40] Although not necessary for catalytic activity, the C-terminal domain is involved in the recognition of DNA geometry during strand passage and provides different type II topoisomerases with unique capabilities. In human topoisomerase IIα, the C-terminal domain allows the enzyme to relax (+)SC DNA 10 times faster than it does (-)SC molecules.[125,166] In contrast, topoisomerase IIβ relaxes (+) and (-) supercoils at the same rate.[125,166]

The mechanism of action and site of interaction of interfacial poisons are well documented.[3,5,14,20-22,40] However, the mechanistic basis for the actions of covalent poisons is less well known. It has been proposed that the ability of covalent poisons to close the N-terminal gate plays an important role in mediating their ability to increase levels of DNA cleavage complexes.[89,90] However, modified residues have been identified in both the N-terminal gate and the catalytic core.[70,85] To address the proposed role of the N-terminal gate in the actions of covalent poisons, the effects of benzoquinone and thymoquinone on the DNA cleavage activity of the catalytic core of human topoisomerase IIα were determined.

Results and Discussion

Role of the N-terminal gate of human topoisomerase IIα in mediating the actions of covalent poisons

To explore the role of the N-terminal gate in the actions of covalent poisons, the effects of benzoquinone[87] and thymoquinone[121] on DNA cleavage mediated by wild-type topoisomerase IIα and the catalytic core were examined. Effects on cleavage mediated by a truncated human enzyme lacking the C-terminal domain (hTop2αΔ1175) were also determined as a control. Benzoquinone and thymoquinone displayed similar abilities to increase the level of cleavage complexes formed with full-length topoisomerase IIα or hTop2αΔ1175 (Figure 18). This finding demonstrates that the C-terminal domain plays no significant role in mediating the actions of covalent topoisomerase II poisons. Conversely, neither compound displayed any ability to enhance DNA cleavage mediated by the catalytic core. This result indicates that the N-terminal gate of topoisomerase IIα is critical

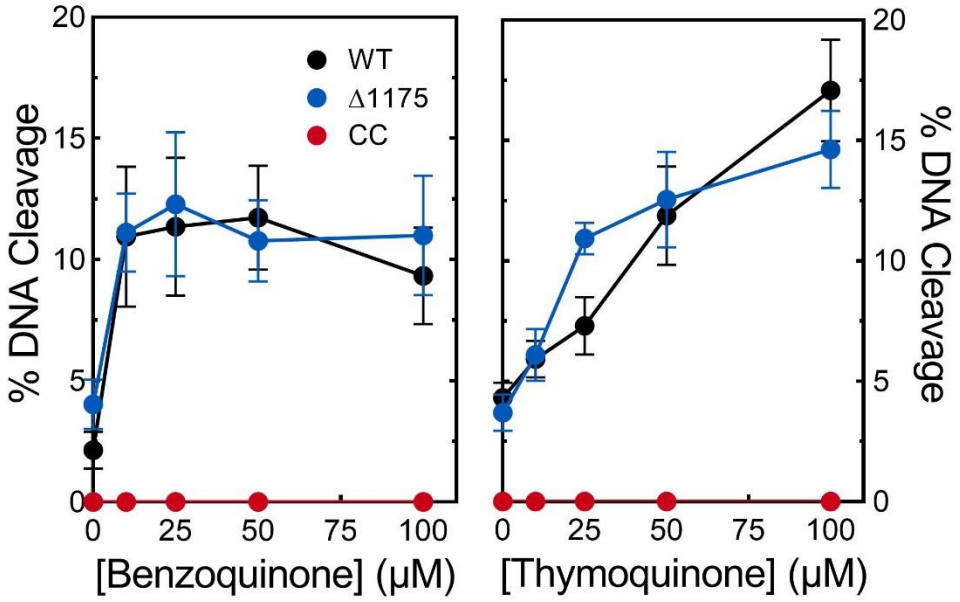

Figure 18. Covalent poisons do not enhance DNA cleavage mediated by the catalytic core of human topoisomerase IIα. Effects of benzoquinone (left) and thymoquinone (right) on DNA cleavage mediated by wild-type human topoisomerase IIα (black), the catalytic core (red), and hTop2αΔ1175 (blue) are shown. Error bars represent the standard deviation of at least three independent experiments.

for the actions of covalent poisons. In contrast, interfacial poisons act at the DNA-enzyme interface[167] and would not be expected to require the N-terminal gate for their activity. As seen in Figure 19, the interfacial poisons etoposide and CP-115,953 were able to enhance DNA cleavage with full-length topoisomerase IIα, hTop2αΔ1175, and the catalytic core.

A hallmark characteristic of covalent poisons is the ability to inactivate the enzyme when the two are incubated prior to the addition of DNA.[88,89] Even though this inactivation could be explained by the closure of the N-terminal gate (thus preventing DNA from entering the active site of topoisomerase II),[85,90] this proposed mechanism is controversial. Indeed, treatment of human topoisomerase IIα with benzoquinone or PCB quinones blocks the ability of the enzyme to cleave oligonucleotides that are able to bind to the protein and diffuse into the active site without entering through the protein gate.[85] This finding implies that mechanisms besides the proposed closing of the N-terminal gate may contribute to enzyme inactivation by covalent poisons.

To address this controversy, benzoquinone and thymoquinone were incubated with wild-type topoisomerase IIα, hTop2αΔ1175, or the catalytic core prior to the addition of plasmid, and the effects on DNA cleavage were assessed. Assays with the catalytic core were carried out in the presence of Ca^{2+} to raise baseline levels of DNA cleavage. As seen in Figure 20, benzoquinone and thymoquinone inactivated all three enzymes. Thus, while covalent poisons require the N-terminal gate to stimulate DNA cleavage mediated by topoisomerase II, they do not require this portion of the protein to inactivate the enzyme. Although the closing of the N-terminal gate may contribute to topoisomerase II inactivation, clearly other mechanisms can produce a similar effect.

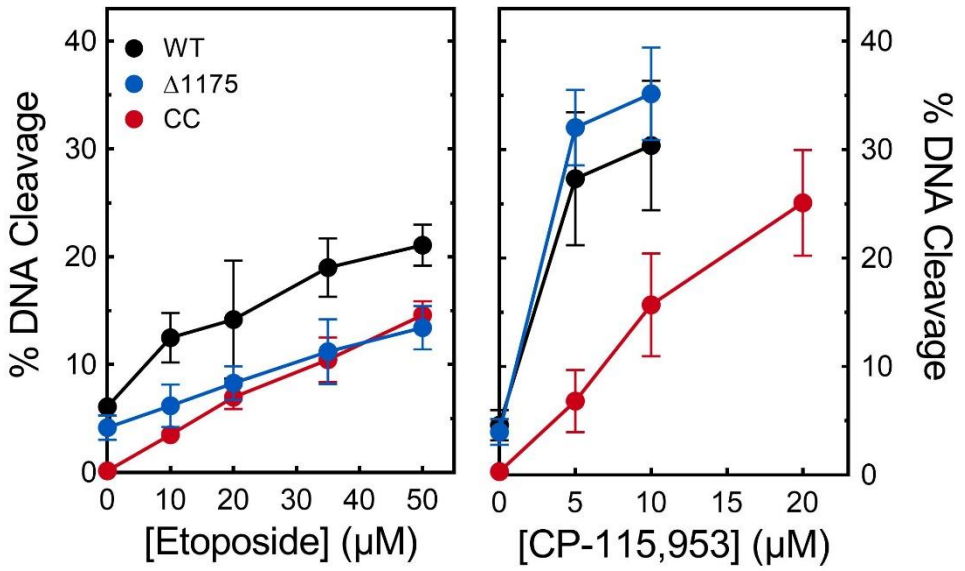

Figure 19. Interfacial poisons are able to enhance DNA cleavage mediated by the catalytic core of human topoisomerase IIα. Effects of etoposide (left) and CP-115,953 (right) on DNA cleavage mediated by wild-type human topoisomerase IIα (black), the catalytic core (red), and hTop2αΔ1175 (blue) are shown. Error bars represent the standard deviation of at least three independent experiments.

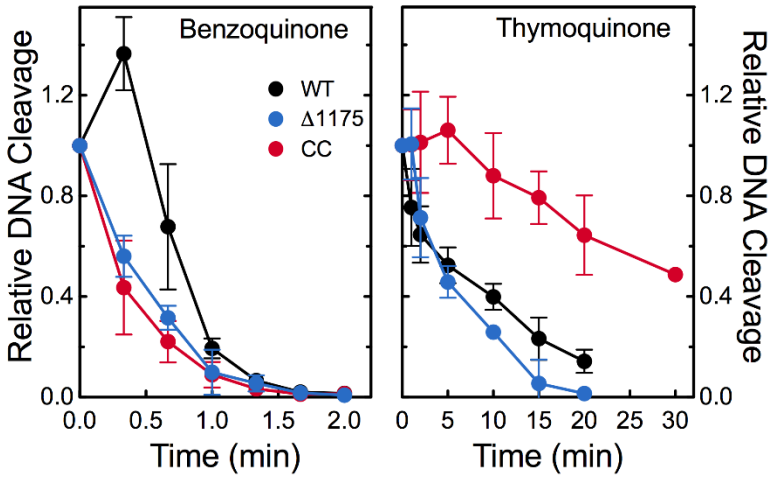

Figure 20. Covalent poisons inactivate human topoisomerase IIα enzymes when incubated with the protein prior to the addition of DNA. The DNA cleavage activities of wild-type human topoisomerase IIα (black), the catalytic core (red), and hTop2αΔ1175 (blue) were monitored in the presence of 50 μM benzoquinone (left) or 50 μM thymoquinone (right). DNA cleavage levels were calculated relative to cleavage induced when the drug and the enzyme were not incubated prior to DNA addition. Error bars represent the standard deviation of at least three independent experiments.

Mechanism of action of etoposide quinone

Etoposide has been linked to the generation of treatment-related acute myeloid leukemias,[39,47,80,168] and etoposide quinone, a metabolite of etoposide,[134,169] has been implicated in this process.[170] Although etoposide is an interfacial topoisomerase II poison, several studies indicate that etoposide quinone acts primarily as a covalent poison.[135,171,172] However, it is not known whether the metabolite can interact in an interfacial manner as well.

Previous studies indicate that the pendant E-ring of etoposide is critical to its actions as an interfacial poison (Figure 21).[82,173,174] Substitution of either the 3'- or 5'-methoxy groups with a hydroxyl moiety has little effect on drug activity.[171,175] Thus, the catechol metabolite of etoposide displays an activity (and mechanism) similar to that of the parent drug. Removal of the 4'-hydroxyl moiety or substitution by a methoxy group greatly compromises the activity of etoposide.[82,173] However, it is not known whether substitution by a carbonyl group (as observed in etoposide quinone) affects the ability of etoposide to function as an interfacial poison.

The experiments shown in Figure 18 provide a method for determining whether etoposide quinone can function as an interfacial poison in addition to acting as a covalent poison. If etoposide quinone functions purely as a covalent poison, it should have no effect on DNA cleavage mediated by the catalytic core. However, if it retains the ability to act as an interfacial poison in addition to its actions as a covalent poison, it should display at least some activity against the catalytic core. As seen in Figure 21, etoposide quinone retains partial activity against the catalytic core of human topoisomerase IIα. However, this activity could be due to a portion of the etoposide quinone preparation being reduced over

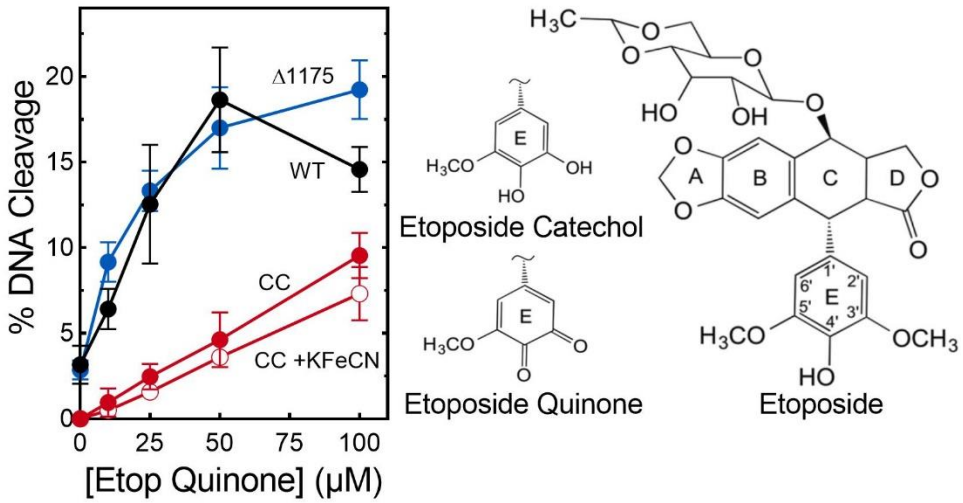

Figure 21. Etoposide quinone enhances DNA cleavage mediated by the catalytic core of human topoisomerase IIα. The effects of etoposide quinone on DNA cleavage mediated by wild-type human topoisomerase IIα (black), the catalytic core (red), and hTop2αΔ1175 (blue) are shown. The structure of etoposide and the E-rings of etoposide catechol and etoposide quinone are depicted at right. Error bars represent the standard deviation of at least three independent experiments.

time to the catechol, which is an interfacial topoisomerase II poison. To address this possibility, the effect of 10 μM $K_3[Fe(CN)_6]$ on the ability of etoposide quinone to enhance DNA cleavage mediated by the catalytic core was assessed. The oxidant, which converts the catechol to the quinone,[171] had little effect on the actions of etoposide quinone against the catalytic core, indicating that the observed activity is due to the quinone form. Although etoposide quinone functions primarily as a covalent poison, these findings indicate that it still retains a modest ability to act as an interfacial topoisomerase II poison.

Conclusions

The N-terminal gate and the catalytic core of type II topoisomerases work coordinately to capture, cleave, and transport DNA during the DNA strand passage reaction. Although this coordination is essential for proper enzyme function, it has obscured the individual contributions of these two domains to important aspects of drug mechanism. The use of different topoisomerase IIα constructs provided considerable insight into the actions of covalent topoisomerase II poisons (Figure 22). Whereas the N-terminal gate is necessary for the enhancement of DNA cleavage by these compounds, residues within the catalytic core may be responsible for the inhibition of catalytic function that follows the incubation of covalent poisons with topoisomerase II prior to the addition of DNA. Finally, the ability of interfacial poisons, but not covalent poisons, to enhance DNA cleavage mediated by the catalytic core allowed for the further characterization of the mechanism of action of etoposide quinone. Although this important drug metabolite functions primarily as a covalent poison, it still retains the ability to act in an interfacial manner.

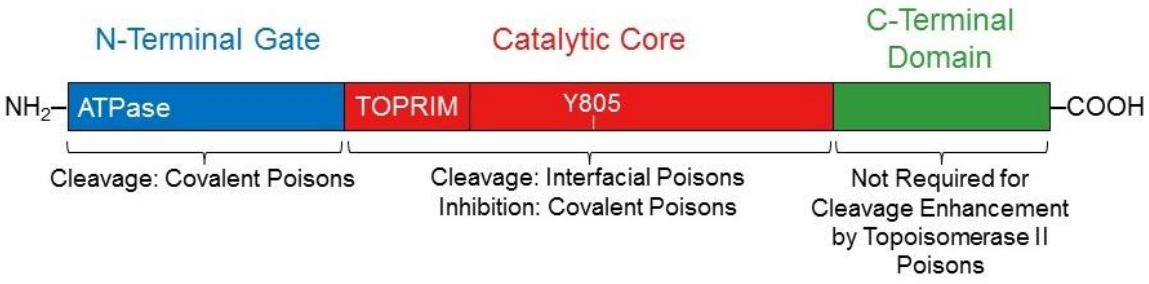

Figure 22. Domains of human topoisomerase IIα and their involvement in drug activity. The enzyme is divided into three domains: the N-terminal gate (blue, amino acid residues 1-430), which contains the ATPase site; the catalytic core (red, residues 431-1193), which contains the TOPRIM domain (the portion that binds the catalytic divalent metal ions) and the DNA cleavage/ligation active site tyrosine residue (Y805); and the C-terminal domain (green, residues 1194-1531). Contributions of each domain to the activities of topoisomerase II poisons are indicated.

CHAPTER V

RECOGNITION OF DNA GEOMETRY BY *B. ANTHRACIS* GYRASE AND TOPOISOMERASE IV

Introduction

Despite the similarities between topoisomerase IV and gyrase discussed in Chapter I, differences in the C-terminal domains of the A subunits (GrlA/ParC and GyrA) confer each enzyme with a unique array of catalytic activities.[49] Because the C-terminal domain of GrlA/ParC allows topoisomerase IV to interact with distal DNA segments, the enzyme uses a "canonical" strand passage mechanism in which it captures existing intra- or intermolecular DNA crossovers (Figure 23).[48] This allows the enzyme to relax (*i.e.*, remove) (+) or (-) supercoils, which results in a respective decrease or increase in DNA linking number. It also allows the enzyme to remove DNA knots and tangles in a highly efficient manner.[48,49]

In contrast to the canonical mechanism used by all other type II topoisomerases, gyrase uses a mechanism in which the C-terminal domain of the GyrA subunit wraps DNA, inducing a (+) crossover between the G- and T-segment that mimics a (+) supercoil (Figure 23).[48,176-181] This "wrapping" mechanism has three important implications for gyrase activity. First, the captured G- and T-segments are proximal to one another.[182] Therefore, gyrase greatly favors the catalysis of intramolecular strand passage reactions: the enzyme can efficiently alter superhelical density but is very poor at removing knots and tangles.[182,183] Second, because gyrase always acts on the induced (+) crossover, it works in a unidirectional manner: in the presence of ATP, the enzyme can remove (+), but not (-),

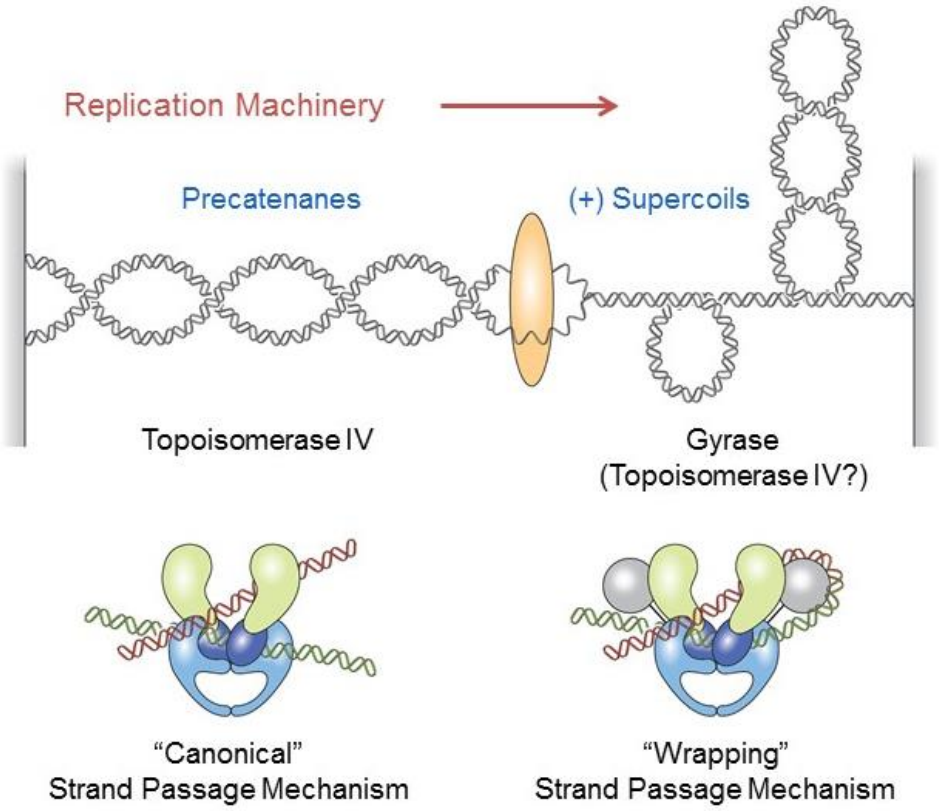

Figure 23. Cellular functions and DNA strand passage mechanisms of gyrase and topoisomerase IV. Gyrase removes (+)SC DNA ahead of the replication machinery and also introduces (-) supercoils into the genome. Topoisomerase IV may assist in the removal of (+) supercoils, but primarily acts to resolve precatenanes behind the fork and unlink daughter chromosomes. Topoisomerase IV uses a "canonical" DNA strand passage mechanism and gyrase uses a "wrapping" mechanism to support their decatenation and supercoiling activities, respectively. Artwork by Ethan Tyler, NIH Medical Arts.

supercoils and always causes a decrease in DNA linking number.[48,184] Third, the ability of gyrase to create and subsequently remove (+) supercoils allows the enzyme to decrease the linking number beyond that of relaxed DNA. Thus, among all known topoisomerases, gyrase is the only enzyme able to negatively supercoil DNA.[16,49]

As a result of their individual properties, gyrase and topoisomerase IV have distinct functions during DNA replication (Figure 23).[49,185-187] Gyrase works primarily ahead of the fork to remove (+) supercoils generated by the replicative helicase and to restore the negative superhelicity of the bacterial chromosome.[4,5] Although topoisomerase IV can alter superhelical density and help to alleviate torsional stress that accumulates ahead of the fork,[56-58] its critical function is to decatenate (*i.e.*, untangle) daughter chromosomes following DNA replication.[48,59-61] During DNA synthesis, topoisomerase IV works primarily behind the fork to remove catenanes following replication. Despite the fact that gyrase (possibly assisted by topoisomerase IV) plays an essential role in relaxing overwound DNA ahead of the replication machinery and that quinolone-stabilized cleavage complexes formed ahead of these moving forks are potentially the most dangerous for the cell,[20,188-190] little is known about how these enzymes remove (+) supercoils or form cleavage complexes on overwound DNA. Therefore, the activities of *B. anthracis* gyrase and topoisomerase IV on (+)SC DNA were characterized.

Results and Discussion

Activity of B. anthracis *gyrase on (+)SC DNA*

As discussed above, gyrase plays two important roles in the cell: it alleviates stress ahead of DNA tracking systems and it generates (-) supercoils to help maintain the correct superhelical density of the bacterial chromosome. Although the supercoiling activity of gyrase has been well documented,[176,184,191-197] virtually nothing is known about the ability of the enzyme to remove (+) supercoils from DNA. Therefore, the ability of *B. anthracis* gyrase to relax a (+)SC plasmid and subsequently convert it to a (-)SC molecule was assessed. The initial substrate contained 15-17 (+) supercoils, which is comparable to the number of (-) supercoils present in the original plasmid isolated from *E. coli*.[125]

As shown in Figure 24 (top), gyrase rapidly relaxed the overwound plasmid and removed all of the (+) supercoils within 2 min. To further investigate the speed and processivity of this reaction, relaxation was monitored over a 90 s time course (Figure 24, middle). In a fully processive reaction, the enzyme catalyzes the complete relaxation of the substrate with little evidence of intermediate topoisomers. Conversely, in a fully distributive reaction, the enzyme relaxes the entire substrate population synchronously and the complete range of intermediate topoisomers are observed. Although the gyrase-catalyzed relaxation of (+) supercoils is not entirely processive, relatively few (+)SC intermediate topoisomers were observed (further discussed below).

In contrast, the conversion of relaxed plasmid to (-)SC DNA by gyrase occurred much more slowly (Figure 24). The enzyme took ~45 min to fully underwind the plasmid population. Additionally, the supercoiling reaction was much more distributive than the relaxation reaction. Similar rates for the supercoiling reaction were observed

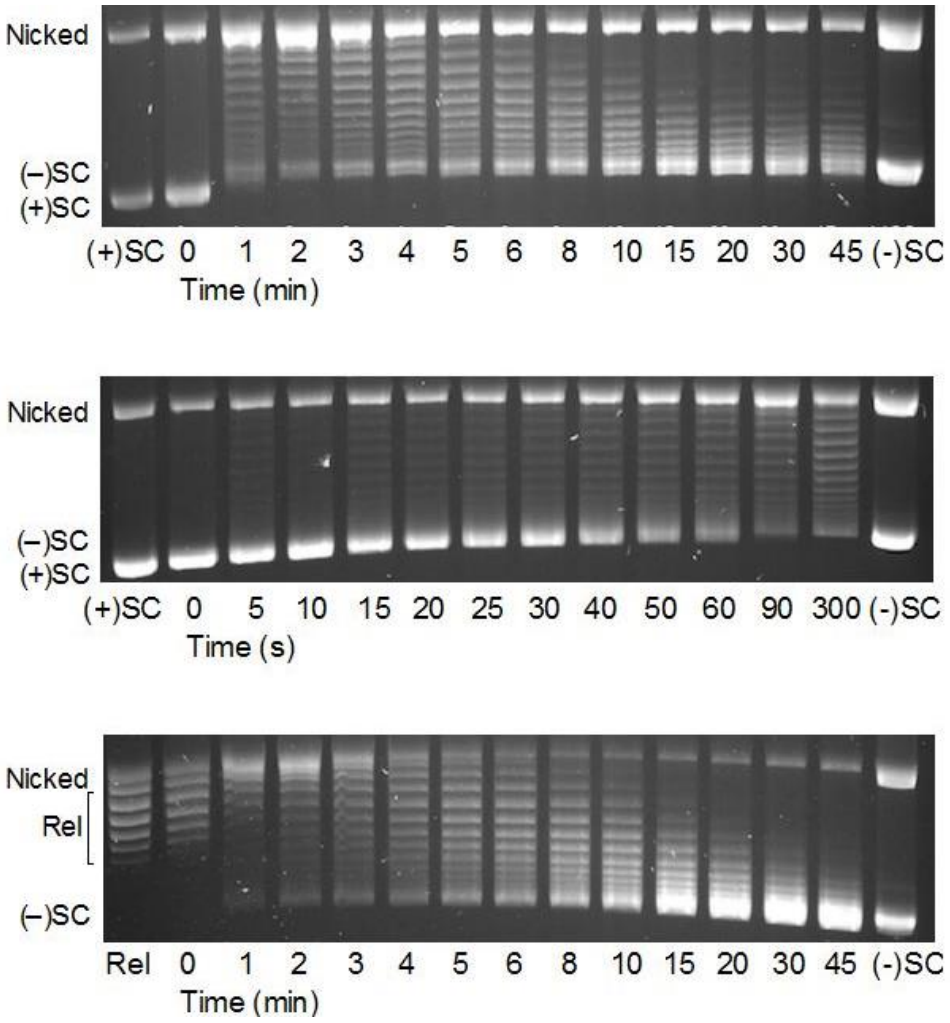

Figure 24. *B. anthracis* gyrase removes (+) supercoils more rapidly than it introduces (-) supercoils into relaxed DNA. Top: Gyrase activity on (+)SC DNA. A time course is shown for the relaxation of (+) supercoils followed by the introduction of (-) supercoils. (+)SC and (-)SC standards are shown. Middle: Expanded time course for the relaxation of (+)SC DNA by gyrase. Bottom: Time course for the introduction of (-) supercoils into relaxed DNA (Rel) by gyrase. Gel images are representative of at least three independent experiments.

whether the initial DNA substrate was (+)SC (Figure 24, top) or relaxed (Figure 24, bottom). This highlights the clear distinction between the rates of relaxation and supercoiling.

A number of DNA topoisomers were apparent in the later stages of the relaxation reaction (Figure 24, middle), and it was difficult to discern their supercoil handedness on a one-dimensional gel. These topoisomers may represent (+)SC molecules that have yet to be fully relaxed or molecules that have already been relaxed and are partially (-)SC. Therefore, the products of relaxation reactions were analyzed by two-dimensional gel electrophoresis. As seen in Figure 25, all of the (+)SC topoisomers were gone by ~90 s. This confirms the above conclusion that, under the conditions employed, gyrase completely removes all (+) supercoils in <2 min. It also indicates that the time required to fully relax (+)SC DNA is 10–20-fold shorter than that required for gyrase to fully negatively supercoil the bulk of the relaxed molecules. Despite these rate differences, a small proportion of DNA molecules become (-)SC within 30 s (Figure 25, see also Figure 24), suggesting the presence of a gyrase population that is capable of acting much faster than the majority of enzyme molecules.

Single-molecule measurements of gyrase activity

To further explore the rate at which gyrase removes (+) supercoils and to address possible different modes of enzyme activity, magnetic tweezers[145] were utilized to measure gyrase-catalyzed relaxation of (+)SC DNA (Figure 26). Gyrase typically relaxed (+)SC DNA in discrete, rapid bursts (Figure 26, A and B). The time between bursts was highly variable, leading to a wide distribution of average relaxation rates (Figure 27). In contrast to a previous study with *E. coli* gyrase,[195] relaxation rates for the *Bacillus* enzyme were

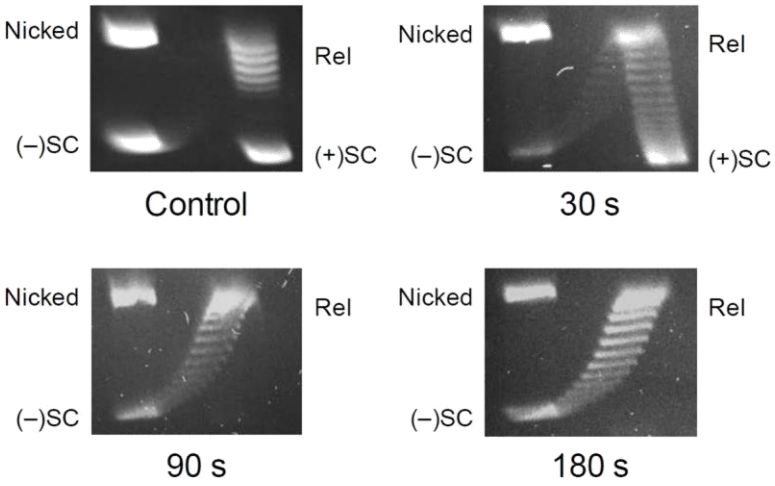

Figure 25. Two-dimensional gel analysis of gyrase activity on (+)SC DNA. A control gel showing mobility of nicked, (+)SC, relaxed (Rel), and (-)SC DNA is shown at the top left. DNA products generated after 30 s (top right), 90 s (bottom left), and 180 s (bottom right) reactions are shown. Gel images are representative of at least three independent experiments.

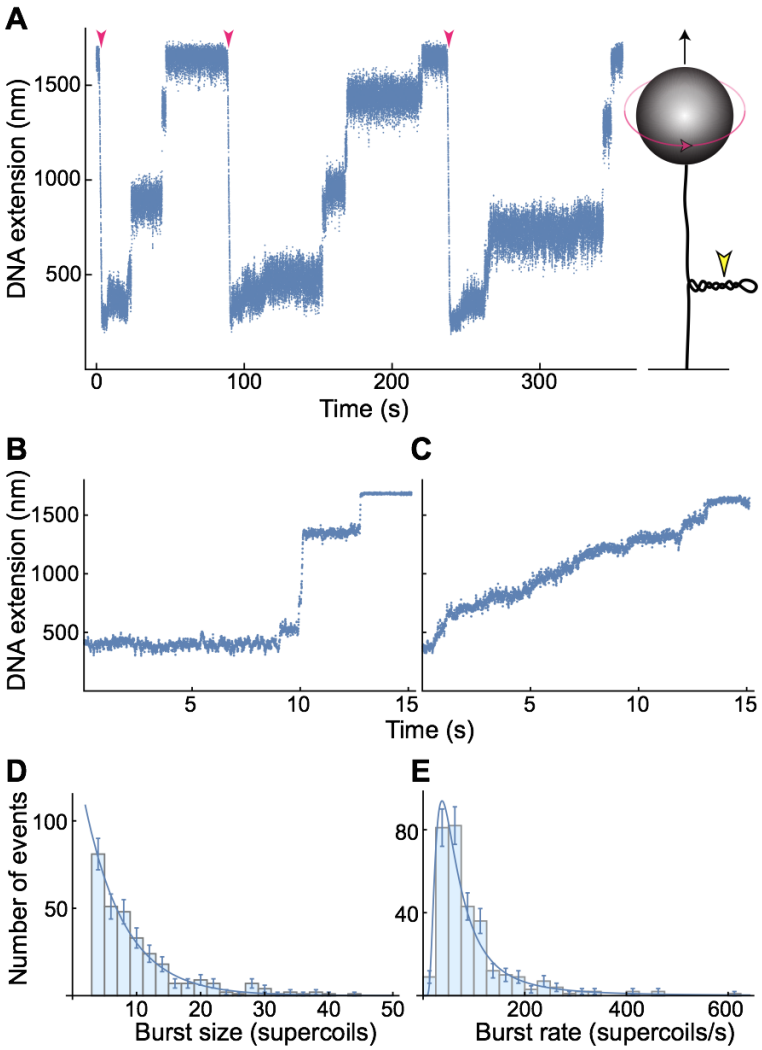

Figure 26. Single-molecule measurements of gyrase activity. (A) Representative measurement of gyrase activity over time using magnetic tweezers. A cartoon of the experimental setup (not to scale) is shown at right: a single DNA molecule (black line) is torsionally constrained by attachment to a slide and manipulated by the attached magnetic bead (grey sphere). Both the upward force (black arrow) on the bead and its rotation (red arrow) are controlled through an externally applied magnetic field. Counterclockwise bead rotation increases the linking number of the DNA, generating (+) supercoils. DNA extension (determined by bead height above slide surface) decreases in proportion to plectoneme supercoiling (yellow arrowhead). Results are shown at left for a single DNA molecule that was extended by a constant upward magnetic force of 1 pN. Upon introduction of 50 (+) supercoils (red arrowheads), the DNA extension was reduced as a plectoneme formed. Gyrase removed supercoils in a series of discrete steps and the DNA returned to its initial length, initiating the onset of another measurement cycle. (B, C) Gyrase relaxes (+) DNA supercoils using two distinct modes of activity. Representative traces in which the enzyme removed multiple supercoils either in rapid bursts ("burst mode" relaxation, B), or at a steady rate ("steady mode" relaxation, C), are shown. The DNA was under constant tension of 3.5 pN and 2.2 pN in B and C, respectively. (D, E) Characterization of burst mode

relaxation. Distributions include measurements of 307 individual burst events. In each event, gyrase rapidly removed four or more supercoils. Burst size distribution (D) fits a single exponential curve. Burst rate distribution (E) fits an inverse gamma function with shape parameter $\alpha=2.1\pm0.2$ and scale parameter $\beta=114\pm11$ supercoils/s. Error bars represent the square-root of the number of observed events; these errors were accounted for in the determination of the best-fit parameters (±SE).

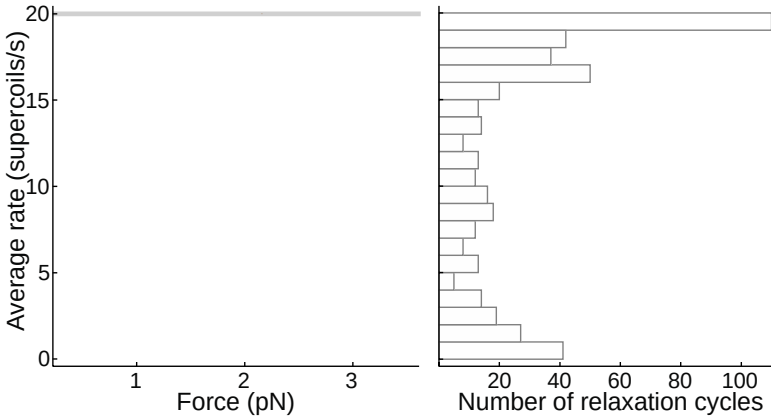

Figure 27. Average (+) supercoil relaxation rates. Left: Average rate at which gyrase removed 50 (+) supercoils at various forces. The differences in activities at any given force are larger than the differences among forces. The upper limit of the average measurable rate (20 supercoils/s) is indicated by the gray line. Colors indicate measurements on different single DNA molecules. Right: Distribution of average relaxation rates measured at left. The average rate was ≥10 supercoils/s in 319 out of 492 relaxation cycles and ≥20 supercoils/s in 110 cycles.

independent of force. The existence of at least two distinct activity modes further contributed to this variability (Figures 26B,C and 28). Gyrase removed multiple supercoils in rapid bursts ("burst mode") or at a steady rate ("steady mode"). Heterogeneous activity is a well-documented aspect of some enzymes observed in single-molecule studies[198] and is a possible source of plasticity for an enzyme that performs multiple necessary functions.

B. anthracis gyrase relaxed 50 (+) supercoils at an average rate of ≥10 supercoils/s in 319 out of 492 measurements (65%) and ≥20 supercoils/s in 110 measurements (22%) (Figure 27). This represents a lower bound for the average relaxation rate, because gyrase frequently removed (+) supercoils as rapidly as they were introduced, even up to 60 supercoils per second. Moreover, the enzyme often paused, leading to broadly distributed average velocities that are significantly slower than the burst relaxation rate between pauses.

To characterize gyrase relaxation activity in "burst mode," enzyme processivity and speed were measured (Figure 26D and 26E). The mean burst size of 6.2 ± 0.4 supercoils corresponds to three catalytic cycles executed in rapid succession, and bursts were often much larger. The burst size distribution was described by a simple exponential decay function, indicating that the number of sequential catalytic cycles is random. The mean burst rate was 107 ± 23 supercoils/s, which is comparable to the rate of (+) supercoil production by *E. coli* DNA polymerase.[199] The burst rate distribution was described by an inverse gamma function, as expected for an enzyme taking a finite number of discrete steps.[200]

Gyrase relaxed all 50 (+) supercoils introduced during each measurement cycle. This strongly indicates that a single enzyme can process the entire plectoneme (Figure 26A)

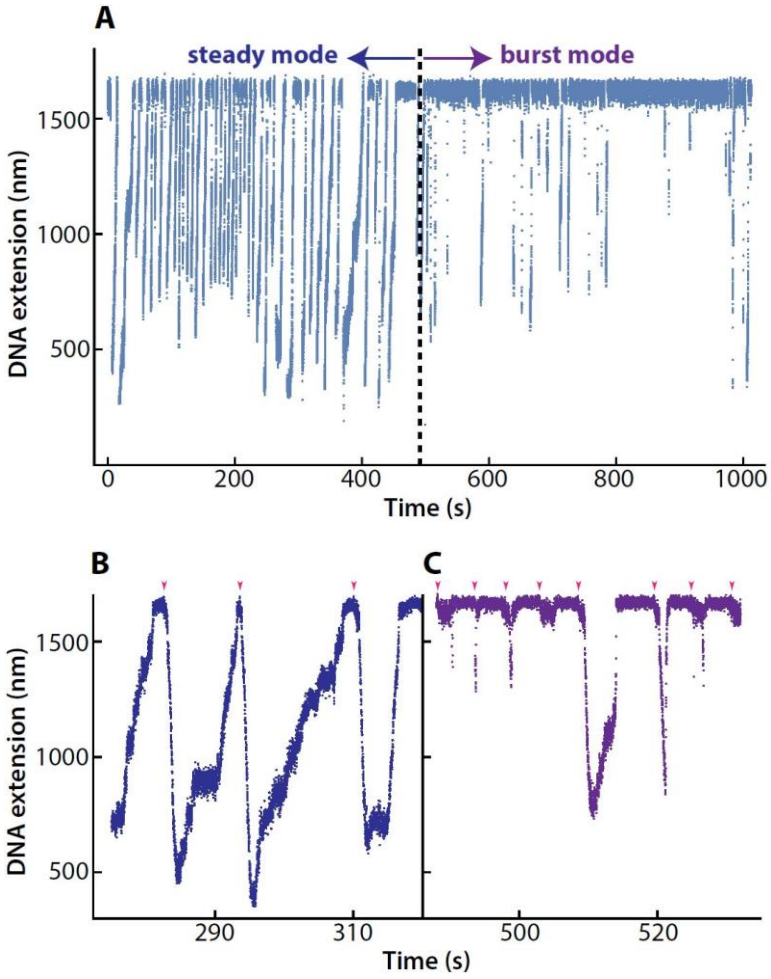

Figure 28. Evidence of single-molecule heterogeneity: switching between two distinct modes of gyrase activity. (A) During the course of 128 sequential relaxation cycles, gyrase switches from predominantly steady mode relaxation to predominantly burst mode relaxation. The dashed line near 500 s indicates the approximate time of the relaxation mode change. For visual clarity, each relaxation cycle is separated in time by 2.5 s, corresponding to the time to introduce 50 supercoils. The DNA was under constant tension of 2.2 pN. (B, C) Expanded detail of events shown in A. Four sequential steady mode relaxation cycles (B) and eight sequential burst mode relaxation cycles (C) are shown. In burst mode, gyrase often relaxed (+) supercoils at a rate at least as fast as they were introduced [50 (+) supercoils in 2.5 s, indicated by red arrowheads]. The raw data show that back-to-back bursts frequently removed 50 supercoils in under 2.5 s with an intrinsic burst rate exceeding 60 supercoils/s. During the fifth relaxation cycle gyrase exhibited both steady-mode and burst-mode activity, demonstrating dynamic heterogeneity of a single enzyme.

from a unique binding site at its distal end, which potentially favors binding because it is sterically accessible and presents a preferred binding geometry.

Finally, *B. anthracis* gyrase relaxed (+) supercoils in at least two modes of activity (Figure 26, B and C). The burst size distribution (Figure 26E) points to an underlying stochastic process, which is inconsistent with the regular repetition of single steps and short pauses that would constitute a steady velocity. Thus, the "burst" and "steady" modes are recognizably different. Furthermore, switching between these modes was observed even within uninterrupted relaxation events (Figure 28), indicating dynamic switching between relaxation modes by a single enzyme.

Contribution of DNA wrapping to relaxation of (+) supercoils by gyrase

A previous single-molecule study that examined *E. coli* gyrase suggested that variable reaction rates observed for the enzyme under different conditions might reflect the use of two different mechanisms.[195] The enzyme could act through the classic wrapping mechanism, in which only proximal DNA segments were captured, or by a canonical type II topoisomerase mechanism that favored capture of distal segments. Clearly, gyrase must use the wrapping mechanism in order to introduce (-) supercoils. However, it is not obvious how it achieves its rapid rates of (+) supercoil relaxation. Indeed, canonical type II enzymes that do not wrap DNA, such as human topoisomerase IIα and *E. coli* topoisomerase IV, have been shown to rapidly remove (+) supercoils.[58,125,200,201] Thus, gyrase could potentially use a canonical mechanism to efficiently relax overwound DNA. Alternatively, it could rely on the wrapping mechanism for this activity, as (+)SC DNA would be an ideal substrate for generating a (+) wrap around the GyrA C-terminal domain.

To distinguish between these possibilities, a previously described *E. coli* GyrA mutant[178] was recapitulated in *B. anthracis*. In this construct, $GyrA^{Ala\text{-}box}$, the seven amino acids of the GyrA-box were replaced with alanine residues. The GyrA-box is necessary for DNA wrapping by gyrase, and mutation or removal of this motif in *E. coli* gyrase resulted in an enzyme that was no longer able to introduce (-) supercoils into DNA, similar to a gyrase construct in which the entire GyrA C-terminal domain was removed.[177] As seen in Figure 29 (top and middle), *B. anthracis* $GyrA^{Ala\text{-}box}$ gyrase is unable to convert relaxed to (-)SC DNA and, like canonical type II topoisomerases, has gained the ability to relax (-)SC DNA in the presence of ATP. The conclusion from these findings is that disrupting the GyrA-box of *B. anthracis* gyrase restricts the enzyme to using a canonical type II topoisomerase strand passage mechanism.

As shown in Figure 29 (bottom), $GyrA^{Ala\text{-}box}$ gyrase could still remove (+) supercoils, but acted more distributively and much more slowly than the wild-type enzyme. The mutant enzyme took at least 45 min to fully relax overwound DNA (as compared to <2 min for wild-type gyrase, see Fig 2). While these results demonstrate that gyrase can remove (+) supercoils using a canonical mechanism, they strongly suggest that the enzyme uses a wrapping mechanism to achieve high rates of processive (+) supercoil removal.

Recognition of DNA geometry during strand passage by B. anthracis *gyrase and topoisomerase IV*

Previous studies indicate that some, but not all, canonical type II topoisomerases are able to discern the geometry of DNA supercoils during the strand passage reaction. For example, human topoisomerase IIα, but not topoisomerase IIβ or *Chlorella* virus topoisomerase II, relaxes (+)SC DNA ~10-fold faster than comparably (-)SC

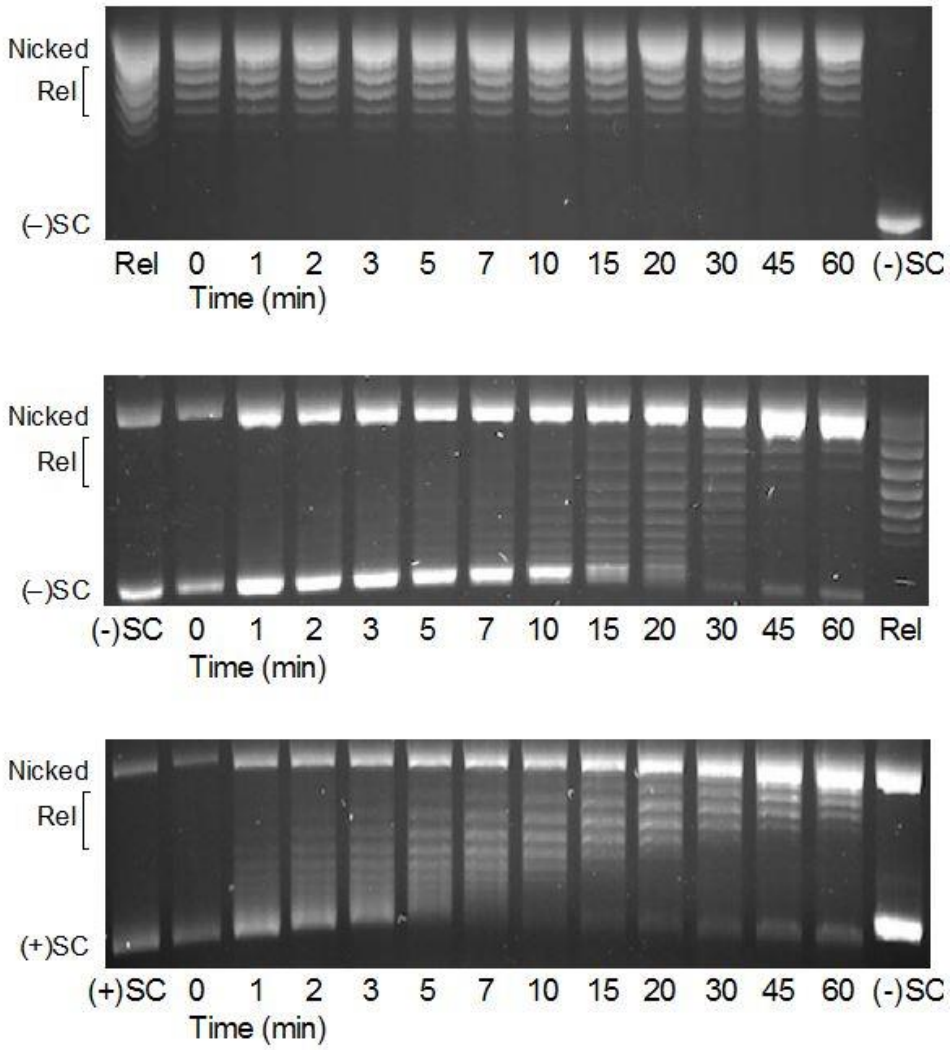

Figure 29. GyrA$^{\text{Ala-box}}$ gyrase acts as a canonical type II topoisomerase. Top: GyrA$^{\text{Ala-box}}$ gyrase does not supercoil relaxed DNA. Relaxed (Rel) and (-)SC DNA standards are shown. Middle: GyrA$^{\text{Ala-box}}$ gyrase slowly relaxes (-)SC DNA. Bottom: GyrA$^{\text{Ala-box}}$ gyrase slowly and distributively relaxes (+)SC DNA. Gel images are representative of at least three independent experiments.

plasmid.[125,166,202] Furthermore, topoisomerase IV from the Gram-negative bacterium *E. coli* also removes (+) supercoils ≥10-fold faster.[58,201,203] In the case of topoisomerase IV, the difference between rates reflects (at least in part) the ability of the enzyme to carry out a processive reaction on overwound DNA, while its reaction on underwound molecules is distributive.

To determine whether type II topoisomerases from Gram-positive bacteria can discern DNA supercoil geometry during strand passage, the ability of *B. anthracis* topoisomerase IV to remove (+) and (-) supercoils was examined (Figure 30). As determined by the loss of supercoiled DNA, the enzyme relaxed overwound DNA ~3-fold faster than comparably underwound molecules. Results with *B. anthracis* topoisomerase IV differ from those with the *E. coli* enzyme in two respects. First, the difference in the rates of relaxation of (+)SC *vs.* (-)SC supercoiled DNA is smaller. Second, the Gram-positive enzyme acted processively on both substrates, which may partly account for the smaller difference in relaxation rates.

Gyrase cannot remove (-) supercoils in the presence of ATP;[48] thus, it is impossible to determine whether the wild-type enzyme has an intrinsic ability to distinguish supercoil geometry during strand passage. However, because $GyrA^{Ala\text{-}box}$ gyrase can carry out relaxation with both substrates, the mutant enzyme was used to investigate this issue. Although the distributive nature of these reactions makes them difficult to quantify, it is clear from Figure 29 that $GyrA^{Ala\text{-}box}$ gyrase removes (+) faster than (-) supercoils. Therefore, even in the absence of DNA wrapping, *B. anthracis* gyrase displays an innate capacity to recognize supercoil geometry during strand passage.

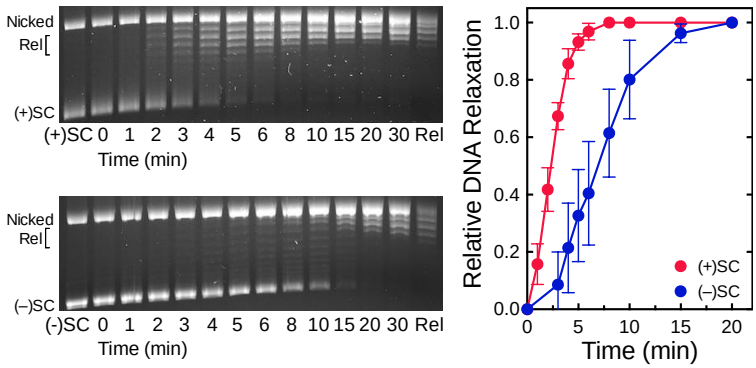

Figure 30. *B. anthracis* topoisomerase IV relaxes (+)SC DNA faster than (-)SC DNA. Left: Relaxation of (+)SC (top) and (-)SC (bottom) DNA by topoisomerase IV. (+)SC, (-)SC, and relaxed (Rel) standards are shown. Gel images are representative of at least three independent experiments. Right: Quantification of experiments shown at left. Relative amounts of relaxed DNA in each experiment were determined by monitoring the loss of the SC band in comparison to SC DNA present in the 0 min sample. Error bars represent standard deviations for at least three independent experiments.

Recognition of DNA geometry during cleavage by B. anthracis *gyrase and topoisomerase IV*

Cleavage complexes formed ahead of replication forks and other DNA tracking systems are most likely to be converted to non-ligatable DNA strand breaks.[20,188-190] Because these systems overwind the DNA as they open the double helix, the abilities of *B. anthracis* gyrase and topoisomerase IV to cleave (+)SC DNA were compared. Quinolone antibacterials were included in most reactions because of their clinical importance and because they substantially raise levels of cleavage complexes, facilitating quantification.[50,68,73,76]

Gyrase recognizes DNA supercoil geometry during cleavage. In the presence of ciprofloxacin, the enzyme maintained ~3-fold lower levels of cleavage complexes on (+)SC as compared to (-)SC DNA (Figure 31, left). This geometry recognition also occurred in the presence of two other clinically relevant quinolones, moxifloxacin and levofloxacin (Figure 31, left, inset), or in the absence of drug (Figure 31, right).

To determine whether DNA wrapping is necessary for gyrase to distinguish supercoil geometry during DNA cleavage, the ability of $GyrA^{Ala\text{-}box}$ gyrase to cleave (+)SC and (-)SC DNA was assessed (Figure 32). Similar to the wild-type enzyme, $GyrA^{Ala\text{-}box}$ gyrase maintained lower levels of cleavage complexes on (+)SC DNA in the presence or absence of ciprofloxacin. Therefore, as was the case for relaxation, the intrinsic ability of gyrase to recognize DNA supercoil geometry is independent of wrapping.

Results with gyrase are similar to those observed for eukaryotic and viral type II topoisomerases.[124,125,166,188,202] In contrast, it has been reported that *E. coli* topoisomerase IV maintains ~20-fold higher levels of cleavage complexes on (+)SC DNA in the presence

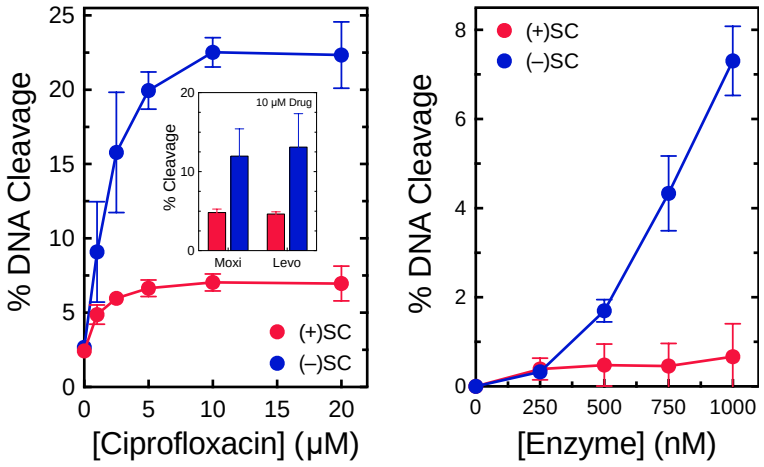

Figure 31. Wild-type gyrase maintains lower levels of cleavage complexes on (+)SC DNA. Left: Levels of cleavage complexes generated by gyrase on (+)SC DNA (red) or (-)SC DNA (blue) in the presence of ciprofloxacin. Inset: Levels of cleavage complexes generated by gyrase in the presence of 10 μM moxifloxacin (Moxi) or levofloxacin (Levo). Right: Levels of cleavage complexes generated by varying concentrations of gyrase on (+)SC DNA (red) or (-)SC DNA (blue) in the absence of quinolones. Error bars represent standard deviations for at least three independent experiments.

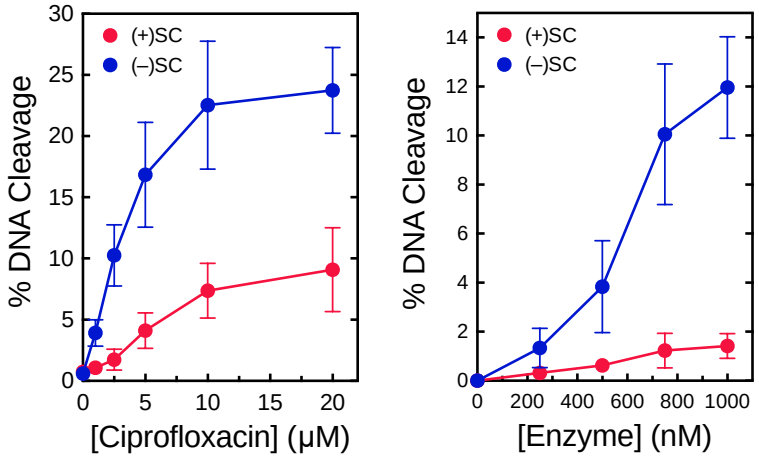

Figure 32. GyrA$^{Ala\text{-}box}$ gyrase maintains lower levels of cleavage complexes on (+)SC DNA. Left: Levels of cleavage complexes generated by GyrA$^{Ala\text{-}box}$ gyrase on (+)SC DNA (red) or (-)SC DNA (blue) in the presence of ciprofloxacin. Right: Levels of cleavage complexes generated by GyrA$^{Ala\text{-}box}$ gyrase on (+)SC DNA (red) or (-)SC DNA (blue) in the absence of quinolones. Error bars represent standard deviations for at least three independent experiments.

of a quinolone.[58] To determine whether this is also the case in a Gram-positive species, the ability of *B. anthracis* topoisomerase IV to discern supercoil geometry during cleavage in the presence of ciprofloxacin was assessed. As seen in Figure 33 (left), the *Bacillus* enzyme displayed little ability to distinguish between (+)SC and (-)SC substrates: it maintained similar levels of cleavage complexes with both.

These results are markedly different than those reported for *E. coli* topoisomerase IV.[58] Although this disparity may represent divergence between Gram-positive and Gram-negative species, it could also reflect differences in the methodologies used in the present and previous studies. The previous study used a competition experiment that monitored simultaneous cleavage of one (-)SC and one (+)SC plasmid of different lengths. In contrast, the experiments described here monitored cleavage in parallel assays that utilized the same plasmid molecules that were equally, but oppositely, supercoiled. Because competition experiments can be inordinately influenced by enzyme-DNA binding affinities, off rates, etc., the ability of *E. coli* topoisomerase IV to discern supercoil geometry was re-examined using independent cleavage assays. As seen in Figure 33 (right), results with the *E. coli* enzyme were similar to those observed with *B. anthracis* topoisomerase IV. If anything, *E. coli* topoisomerase IV maintained slightly higher levels of cleavage complexes on (-)SC substrates.

Conclusions

Even though the bacterial chromosome is globally underwound by ~6%,[2,6-8] localized regions of overwound DNA are generated by critical nucleic acid processes. For example, DNA becomes (+)SC ahead of advancing replication forks, transcription complexes, and DNA helicases.[1,204-207] In bacterial cells, (+) supercoils are removed by gyrase, possibly

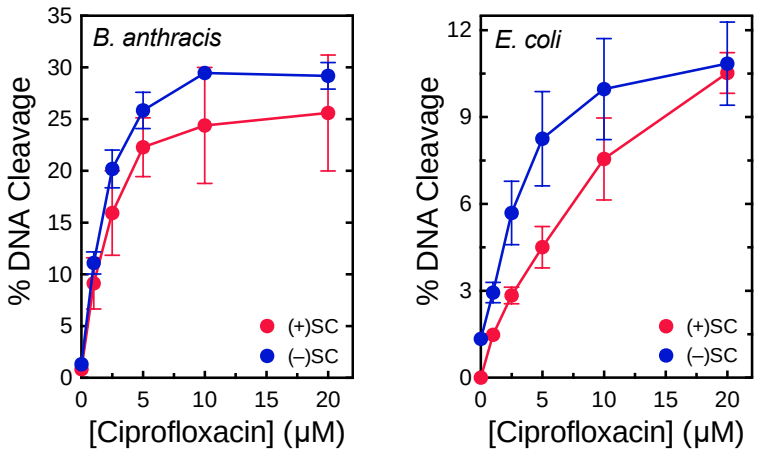

Figure 33. Topoisomerase IV maintains similar levels of cleavage complexes on (+)SC and (-)SC DNA. Left: Levels of cleavage complexes generated by *B. anthracis* topoisomerase IV on (+)SC DNA (red) or (-)SC DNA (blue) in the presence of ciprofloxacin. Right: Levels of cleavage complexes generated by *E. coli* topoisomerase IV on (+)SC DNA (red) or (-)SC DNA (blue) in the presence of ciprofloxacin. Error bars represent standard deviations for at least three independent experiments.

aided by topoisomerase IV, and quinolone-stabilized cleavage complexes most likely to cause permanent genomic damage are formed on overwound DNA.[20,188-190] Despite the essential roles of these enzymes on (+)SC DNA, little is known about the actions of gyrase and topoisomerase IV on overwound substrates. Results of the present study provide novel insights into these critical enzyme activities.

Gyrase is usually described by its ability to introduce negative supercoils, but *B. anthracis* gyrase actually removes (+) supercoils much more rapidly than it introduces (-) supercoils. Additionally, its relaxation of overwound DNA is generally processive, while its introduction of (-) supercoils into relaxed DNA occurs in a highly distributive manner. The ability of gyrase to wrap DNA is critical for both functions. Wrapping is absolutely required for the negative supercoiling activity of the enzyme, but it is also necessary in order for gyrase to carry out rapid, processive relaxation of (+)SC DNA. In the absence of wrapping, gyrase was able to relax both overwound and underwound molecules. However, it removed (+) supercoils more quickly than (-) supercoils, indicating that the enzyme has an inherent ability to recognize supercoil geometry during strand passage. Similarly, *B. anthracis* topoisomerase IV relaxed overwound DNA ~3-fold faster than underwound DNA. This rate difference is not as great as that reported for *E. coli* topoisomerase IV,[58,201,203] possibly because the *B. anthracis* enzyme is able to act processively on both substrates.

Although gyrase and topoisomerase IV both catalyze strand passage faster with (+)SC substrates, they differ in their ability to distinguish the handedness of DNA supercoils during DNA cleavage. Whereas gyrase maintains lower levels of cleavage complexes on overwound DNA, topoisomerase IV maintains similar levels of these complexes with over-

and underwound molecules. As a result, gyrase maintains substantially lower levels of cleavage complexes on (+)SC DNA than topoisomerase IV. This recognition of DNA geometry allows gyrase to act as a safer enzyme ahead of the replication fork. It may be a less important consideration for topoisomerase IV, because the enzyme works primarily behind the fork. Thus, the abilities of these enzymes to recognize DNA geometry make them well suited for their individual physiological roles.

CHAPTER VI

RECOGNITION OF DNA GEOMETRY BY *M. TUBERCULOSIS* GYRASE

Introduction

The majority of bacterial species encode both gyrase and topoisomerase IV. However, some species have only gyrase. Among these are several disease-causing organisms, including *Treponema pallidum* (syphilis),[208] *Helicobacter pylori* (stomach and intestinal ulcers),[209] *Campylobacter jejuni* (gastroenteritis),[210] *Mycobacterium leprae* (leprosy),[211] and *M. tuberculosis* (tuberculosis, TB).[212] TB is one of the top ten causes of death worldwide, with an estimated 10.4 million new cases and 1.4 million deaths in 2015.[213] Additionally, drug resistance is becoming increasingly problematic. Of the new cases in 2015, it is estimated that 480,000 were caused by multidrug-resistant tuberculosis (MDR-TB), which can cost as much as $20,000 to treat.[213] Moxifloxacin and gatifloxacin, fourth-generation quinolone antibacterials, are crucial drugs in MDR-TB treatment regimens, highlighting the potential of gyrase as a drug target in these infections.

As the only type II topoisomerase in the cell, gyrase in *M. tuberculosis* must carry out the activities of both gyrase and topoisomerase IV. Therefore, it is functionally distinct from the "canonical" gyrases found in other species. Because gyrase can be an important target for TB treatment, and because several disease-causing organisms encode a single "non-canonical" gyrase, it is critical to understand how these enzymes function on their DNA substrates. It is particularly important to determine how they act on overwound DNA, because, as discussed in Chapter V, quinolone-stabilized cleavage complexes on (+)SC DNA have the potential to be more dangerous for the cell. As a first step toward

characterizing the interactions between a non-canonical gyrase and overwound DNA, the relaxation and supercoiling activity of *M. tuberculosis* gyrase was assessed. Furthermore, mutant *M. tuberculosis* enzymes were used to define the contributions of each region of the enzyme to the recognition of DNA geometry during cleavage.

Results and Discussion

Activity of M. tuberculosis *gyrase on (+)SC DNA*

The type II topoisomerase in *M. tuberculosis* is defined as a gyrase based on its ability to introduce (-) supercoils into relaxed DNA.[214] However, the enzyme has a higher decatenation activity than observed in a canonical gyrase and is therefore a "hybrid" of gyrase and topoisomerase IV. Like other gyrases, the ability of this enzyme to supercoil relaxed DNA is well documented,[214-216] but no studies have investigated its actions on (+)SC DNA. To determine how a hybrid type II topoisomerase interacts with overwound DNA, the ability of *M. tuberculosis* gyrase to convert a (+)SC plasmid to a (-)SC molecule was investigated. As shown in Figure 34, gyrase rapidly relaxed the overwound DNA and subsequently introduced (-) supercoils in a slower, more distributive manner. This pattern of activity is similar to that observed for *B. anthracis* gyrase (see Figure 24). Therefore, like the canonical gyrase, the enzyme from *M. tuberculosis* functions differently on (+)SC and relaxed DNA.

As discussed in Chapter V, gyrase and topoisomerase IV differ in their ability to recognize DNA geometry during cleavage. This may be related to the position of each enzyme relative to the replication fork. Gyrase, ahead of the fork, is often working on

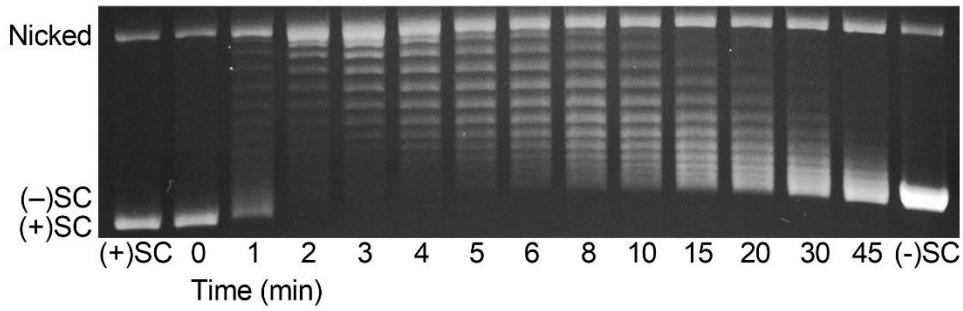

Figure 34. *M. tuberculosis* gyrase rapidly removes (+) supercoils and then slowly introduces (-) supercoils. A time course is shown for the relaxation of (+) supercoils followed by the introduction of (-) supercoils. (+)SC and (-)SC standards are shown. Gel image is representative of at least three independent experiments.

overwound DNA and has the potential to create dangerous cleavage complexes, so it is advantageous for this enzyme to maintain low levels of cleavage complexes on (+)SC DNA. Topoisomerase IV does not distinguish between overwound and underwound DNA during cleavage, possibly because it primarily works behind the fork and is less likely to encounter moving DNA tracking systems. However, as a hybrid enzyme, *M. tuberculosis* gyrase must be able to function in both locations and could conceivably function as a gyrase or as a topoisomerase IV with regard to DNA cleavage. To resolve this issue, the ability of *M. tuberculosis* gyrase to cleave (+)SC and (-)SC DNA was determined (Figure 35). Like the canonical gyrase (see Figure 31), *M. tuberculosis* gyrase maintained lower levels of cleavage complexes on overwound DNA both in the absence and presence of drugs. These results suggest that although gyrase in this species has adapted to perform some of the functions of topoisomerase IV, it still retains the characteristics that make gyrase a safe enzyme to function ahead of replication forks and DNA tracking systems.

Contributions of the GyrA-box and the C-terminal domain to the recognition of DNA geometry during cleavage

The replacement of the seven amino acids of the GyrA box with alanine residues has been reported to prevent wrapping by *E. coli* gyrase[178] and, as shown in Chapter V, the parallel mutant in *B. anthracis* gyrase prevents supercoiling by the enzyme but does not change the ability of gyrase to recognize DNA geometry during cleavage (see Figures 29 and 32). To determine whether *M. tuberculosis* gyrase is similarly able to recognize DNA geometry in the absence of the ability to wrap DNA, a corresponding $GyrA^{Ala\text{-}box}$ mutant was made, and its ability to cleave either (+)SC or (-)SC DNA was assessed. As shown in

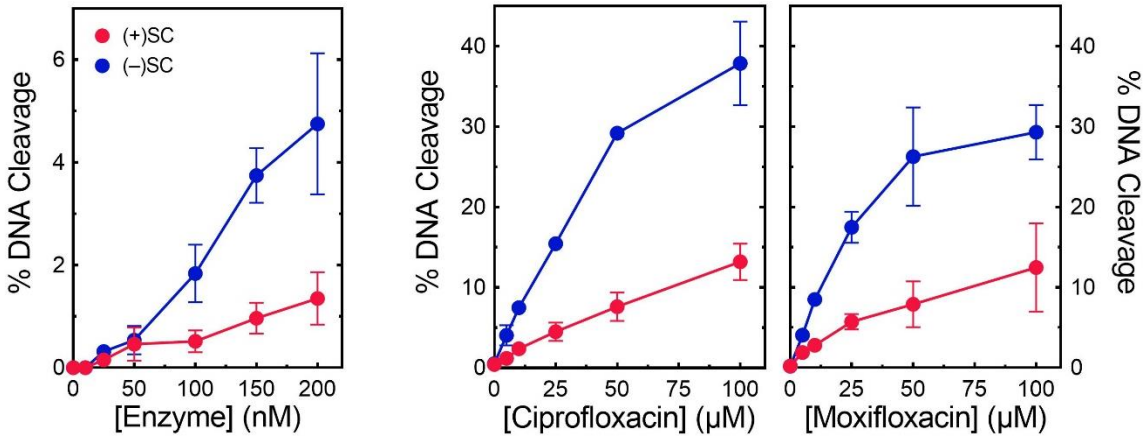

Figure 35. *M. tuberculosis* wild-type gyrase maintains lower levels of cleavage complexes on (+)SC DNA. Left: Levels of cleavage complexes generated by varying concentrations of gyrase on (+)SC DNA (red) or (-)SC DNA (blue) in the absence of quinolones. Middle and right: Levels of cleavage complexes generated by gyrase on (+)SC DNA (red) or (-)SC DNA (blue) in the presence of ciprofloxacin (middle) or moxifloxacin (right). Error bars represent the standard deviations for at least three independent experiments.

Figure 36, GyrA$^{\text{Ala-box}}$ gyrase retains the ability to distinguish DNA geometry during cleavage and maintains 2–4-fold lower levels of cleavage complexes on (+)SC DNA.

A previous study with *E. coli* gyrase showed that removal of the entire C-terminal domain (CTD) of GyrA changed gyrase to a "conventional" type II topoisomerase: it was no longer able to introduce (-) supercoils into relaxed DNA, but it gained the ability to relax (-)SC DNA and had a higher decatenation activity than the parent enzyme.[177] However, the effects of this alteration on DNA cleavage have not been examined. For human topoisomerase IIα, removal of the CTD does not change the ability of the enzyme to discern supercoil handedness during cleavage.[166] To determine the role of the CTD in DNA geometry recognition by bacterial enzymes during cleavage, *M. tuberculosis* gyrase in which the CTD was deleted (GyrA$^{\Delta\text{CTD}}$ gyrase, which contains residues 2-500 of GyrA) was assessed for its ability to cleave both DNA substrates (Figure 37). GyrA$^{\Delta\text{CTD}}$ gyrase was still able to maintain lower levels of cleavage complexes on (+)SC DNA. Therefore, like the human enzyme, the ability of *M. tuberculosis* gyrase to distinguish supercoil handedness during the cleavage reaction does not rely on the CTD.

Ability of the catalytic core to distinguish DNA geometry during cleavage

It is not obvious which portion of *M. tuberculosis* gyrase is responsible for the recognition of DNA geometry during cleavage. Although the DNA scission occurs within the catalytic core of the enzyme (defined as residues 426-675 of GyrB and residues 2-500 of GyrA), the N-terminal gate region (residues 2-425 of GyrB) is crucial for capturing the T-segment and therefore could have an important role in distinguishing supercoil handedness. Previous work with the catalytic core from human topoisomerase IIα showed that the N-terminal gate was not required for the recognition of supercoil geometry during

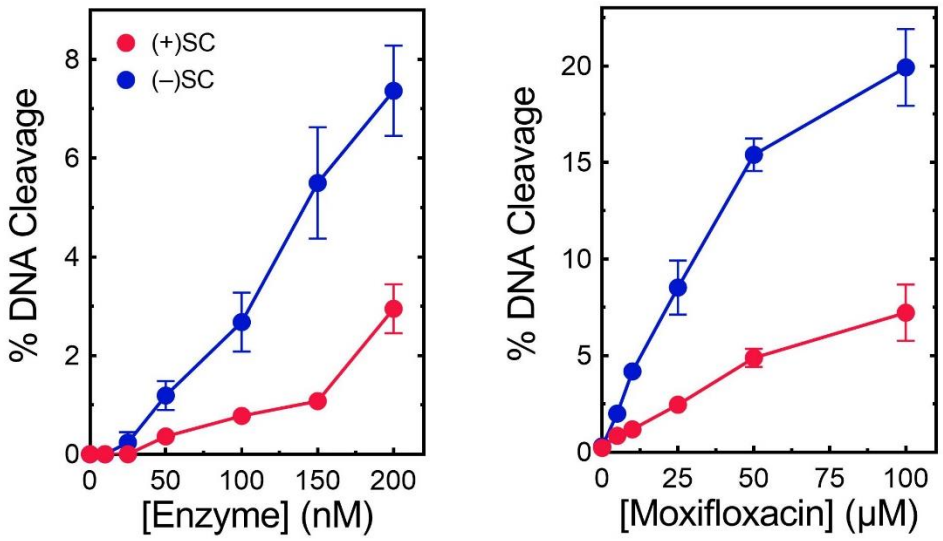

Figure 36. *M. tuberculosis* GyrA$^{\text{Ala-box}}$ gyrase maintains lower levels of cleavage complexes on (+)SC DNA. Left: Levels of cleavage complexes generated by varying concentrations of GyrA$^{\text{Ala-box}}$ gyrase on (+)SC DNA (red) or (-)SC DNA (blue) in the absence of quinolones. Right: Levels of cleavage complexes generated by GyrA$^{\text{Ala-box}}$ gyrase on (+)SC DNA (red) or (-)SC DNA (blue) in the presence of moxifloxacin. Error bars represent the standard deviations for at least three independent experiments.

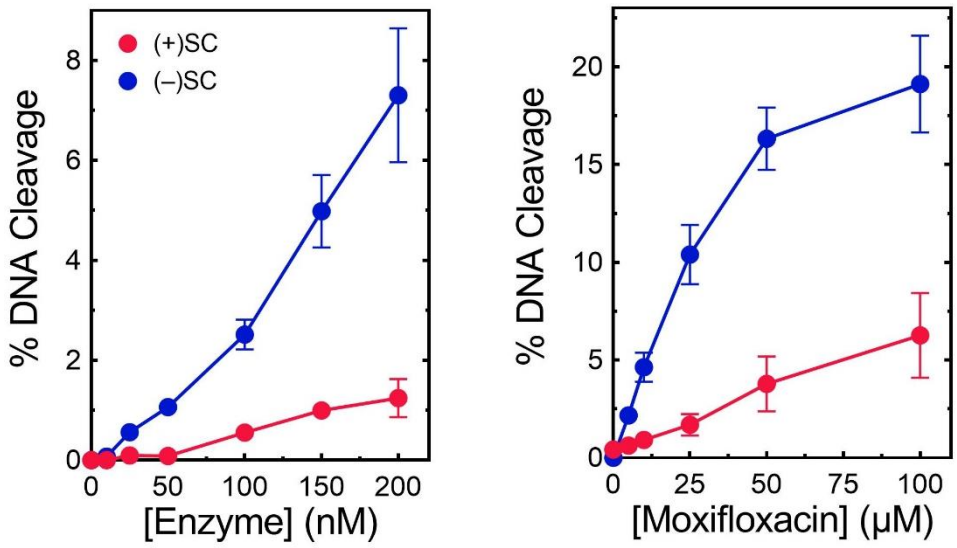

Figure 37. *M. tuberculosis* GyrA$^{\Delta CTD}$ gyrase maintains lower levels of cleavage complexes on (+)SC DNA. Left: Levels of cleavage complexes generated by varying concentrations of GyrA$^{\Delta CTD}$ gyrase on (+)SC DNA (red) or (-)SC DNA (blue) in the absence of quinolones. Right: Levels of cleavage complexes generated by GyrA$^{\Delta CTD}$ gyrase on (+)SC DNA (red) or (-)SC DNA (blue) in the presence of moxifloxacin. Error bars represent the standard deviations for at least three independent experiments.

cleavage.[124] To determine if this is also the case in a bacterial type II topoisomerase, the ability of the catalytic core of *M. tuberculosis* to cleave (+)SC and (-)SC was evaluated (Figure 38). Unlike the full-length or GyrA$^{\Delta CTD}$ gyrase, the catalytic core did not distinguish between overwound and underwound DNA but maintained similar levels of cleavage complexes on both substrates. Therefore, the ability of *M. tuberculosis* gyrase to recognize DNA geometry during cleavage must be embedded in the N-terminal region.

Conclusions

In *M. tuberculosis* and other species encoding a single type II topoisomerase, gyrase must carry out the functions usually associated with topoisomerase IV. Thus, gyrase from these species has a mix of characteristics from canonical gyrases (ability to negatively supercoil DNA) and topoisomerase IV (ability to decatenate DNA). Results here show that *M. tuberculosis* gyrase retains many features of a canonical gyrase that make it a safer enzyme to function ahead of moving DNA tracking systems. In particular, it is able to rapidly remove (+) supercoils, while its introduction of (-) supercoils occurs more slowly and distributively. Furthermore, it is able to distinguish between (+)SC and (-)SC DNA during the cleavage reaction and maintains significantly lower levels of cleavage complexes on overwound DNA. The N-terminal gate region of the enzyme is required for the discernment of supercoil handedness, suggesting that the capture of the transport segment may influence how gyrase maintains cleavage complexes on substrates with different topologies. The involvement of the N-terminal region in geometry recognition also points to a mechanistic difference between *M. tuberculosis* gyrase and human topoisomerase IIα,[124] implying that bacterial and eukaryotic topoisomerases may utilize distinct methods for sensing the supercoil geometry of their substrates.

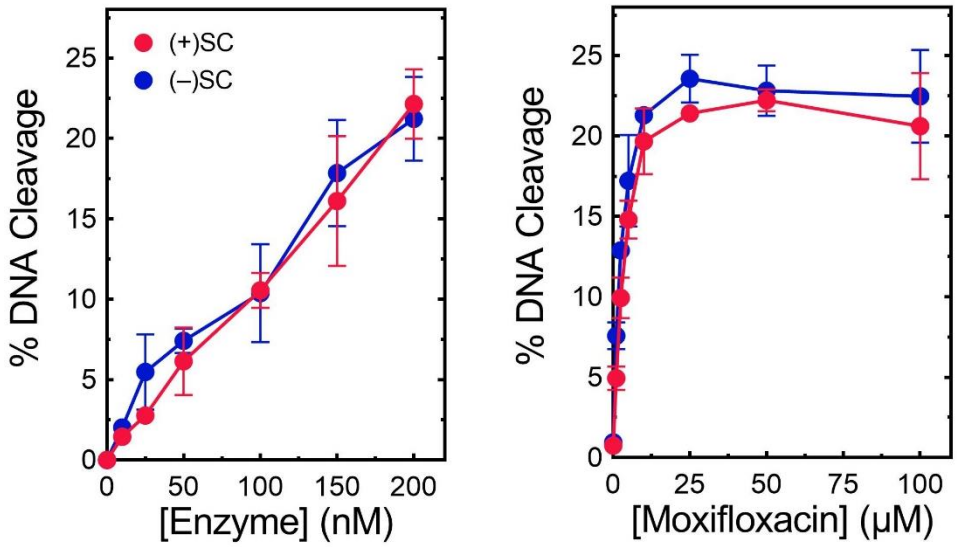

Figure 38. The catalytic core of *M. tuberculosis* gyrase maintains similar levels of cleavage complexes on (+)SC and (-)SC DNA. Left: Levels of cleavage complexes generated by varying concentrations of the catalytic core on (+)SC DNA (red) or (-)SC DNA (blue) in the absence of quinolones. Right: Levels of cleavage complexes generated by the catalytic core on (+)SC DNA (red) or (-)SC DNA (blue) in the presence of moxifloxacin. Error bars represent the standard deviations for at least three independent experiments.

CHAPTER VII

QUINOLONE INTERACTIONS WITH *B. ANTHRACIS* GYRASE AND THE BASIS OF DRUG RESISTANCE

Introduction

Although gyrase and topoisomerase IV are both targets for quinolones, the relative contributions of each enzyme to cytotoxicity appear to be both species- and drug-dependent.[73,101-106] As a generalization, gyrase is the primary cellular target for most quinolones in Gram-negative species, whereas topoisomerase IV plays a more important role in many Gram-positive bacteria. This trend notwithstanding, based on laboratory studies, gyrase appears to be the primary target for clinically relevant quinolones in *Bacillus anthracis*, a Gram-positive organism that is the causative agent of anthrax.[107-109]

As described in the introduction, the majority of the studies that described the water-metal ion bridge as the primary interaction between bacterial type II topoisomerases and quinolones have been carried out with topoisomerase IV from *B. anthracis* and *E. coli*.[116-118] While recent biochemical and structural studies demonstrated the existence and role of the water-metal ion bridge in quinolone interactions with *M. tuberculosis* gyrase,[119,120] this enzyme is unusual in two respects. First, as discussed in Chapter VI, it is the only type II topoisomerase encoded by *M. tuberculosis* and is therefore functionally distinct from "canonical" gyrases (having to carry out the cellular functions of both gyrase and topoisomerase IV).[212,216] Second, it lacks the highly conserved serine residue and depends solely on the acidic residue to anchor the bridge.[119,120] Given the importance of gyrase as the primary target for quinolones in many pathogenic species, it is critical to

understand how these drugs interact with a canonical enzyme and how specific mutations lead to resistance. Therefore, the existence and potential role of the water-metal ion bridge in *B. anthracis* gyrase were assessed.

Results and Discussion

Characterization of wild-type B. anthracis *gyrase and GyrA mutants*

As reported for other bacterial species, the most common gyrase mutations in quinolone-resistant strains of *B. anthracis* are found at the conserved serine and acidic acid residues ($GyrA^{S85}$ and $GyrA^{E89}$). In laboratory strains selected for resistance against ciprofloxacin and/or moxifloxacin (two widely prescribed quinolone antibacterials), approximately 80% of the isolates carried a $GyrA^{S85L}$ mutation (either alone or in combination with other gyrase/topoisomerase IV amino acid changes).[108,111] The only other mutation reported to cause resistance without any other gyrase/topoisomerase IV changes was a $GyrA^{E89K}$ substitution.[108,111] Therefore, studies were focused on $GyrA^{S85L}$ gyrase and $GyrA^{E89K}$ gyrase. In addition, enzymes with $GyrA^{S85F}$ or $GyrA^{E89A}$ substitutions were characterized. The S85F mutation recapitulates the most common quinolone resistance mutation seen in *B. anthracis* topoisomerase IV, which has been examined previously.[116] This mutation is not observed in gyrase due to differences in the codon used for the serine residue. The E89A mutation represents a control for the double charge change in $GyrA^{E89K}$ to determine whether resistance is due to the loss of glutamic acid or the conversion of a negative to a positive charge at that position.

As a first step toward comparing the wild-type and mutant enzymes, their ability to supercoil relaxed DNA was assessed. As seen in Figure 39, the serine mutant enzymes and

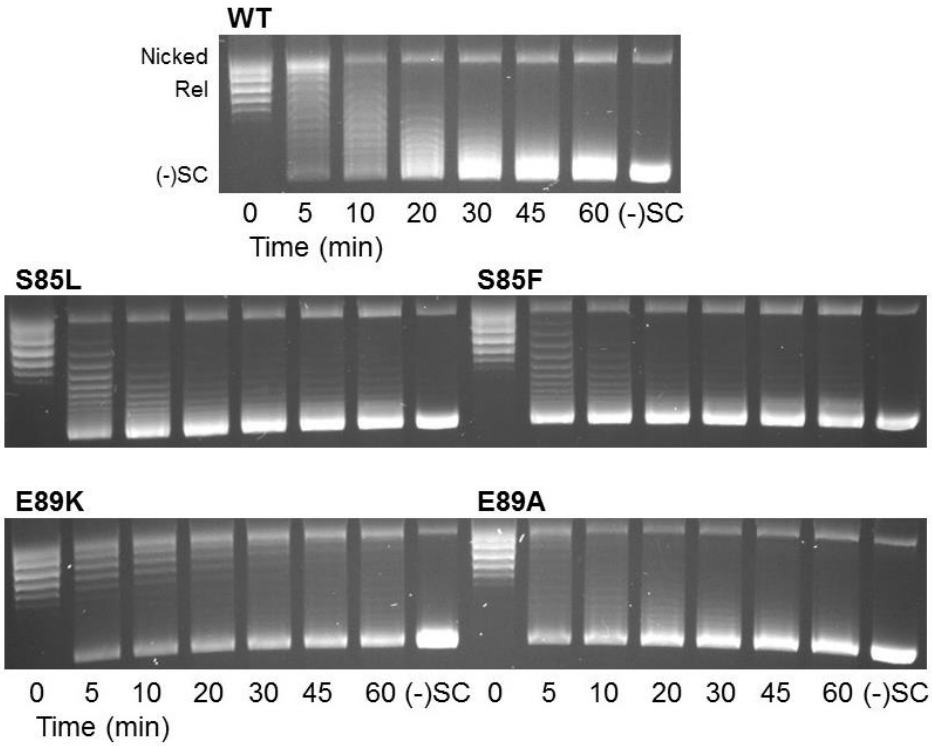

Figure 39. Supercoiling activities of wild-type *B. anthracis* gyrase and mutant enzymes. A time course is shown for the introduction of (-) supercoils into relaxed DNA by wild-type gyrase (top), enzymes with S85L and S85F mutations (middle), and enzymes with E89K and E89A mutations (bottom). Positions of nicked, relaxed (Rel), and (-)SC DNA are marked on the top image. Gel images are representative of at least three independent experiments.

the E89A mutant gyrase maintain a wild-type ability to supercoil DNA. Consistent with previous reports, the overall catalytic activity of the E89K mutant enzyme was decreased as compared to wild-type gyrase. This may be the reason why mutations at this position are observed less frequently than those at the serine residue.

Because quinolones kill cells primarily by increasing levels of gyrase- and/or topoisomerase IV-mediated DNA cleavage, the ability of the above enzymes to cleave DNA was determined (Figure 40). All of the mutant enzymes displayed an activity similar to or higher than that of wild-type gyrase. These DNA cleavage patterns are similar to those reported for the corresponding mutations in topoisomerase IV[116,117] and strongly suggest that quinolone resistance in *B. anthracis* gyrase is not due to a general loss of enzymatic activity.

Effects of quinolones and related compounds on DNA cleavage mediated by wild-type gyrase and mutant enzymes

Although GyrA mutations at S85 and E89 have been observed in quinolone-resistant *B. anthracis* cultures, a direct causal link between these mutations and quinolone resistance in gyrase has yet to be established. Therefore, the abilities of ciprofloxacin and moxifloxacin to enhance DNA cleavage mediated by wild-type, S85L, S85F, E89K, and E89A gyrase were determined. The S85L, S85F, and E89K mutant enzymes all displayed high resistance to both quinolones (Figure 41). These mutations decreased the relative potencies of both drugs between ~10- and 70-fold (Table 3), as measured by the drug concentration required to increase levels of cleavage complexes 3-fold (CC_3). The mutations had a smaller effect on the potency of moxifloxacin as compared to ciprofloxacin. Additionally, at 250 μM, moxifloxacin was able to induce levels of cleavage

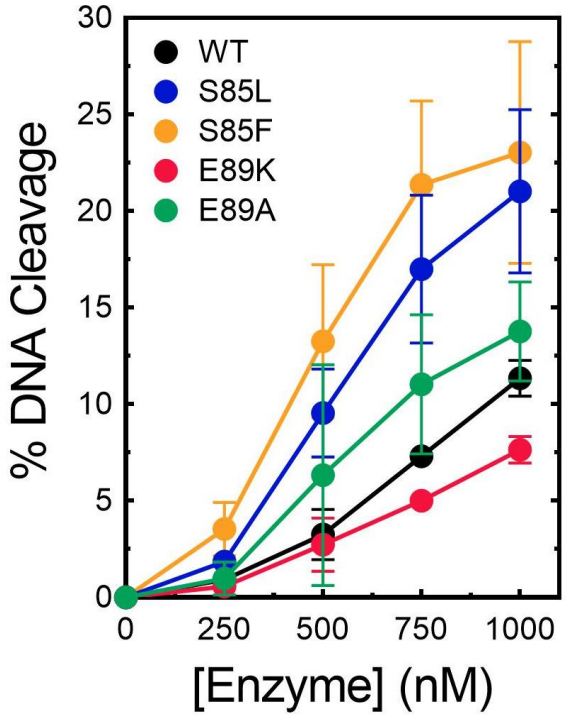

Figure 40. Cleavage activities of wild-type *B. anthracis* gyrase and mutant enzymes. The abilities of wild-type (black), $GyrA^{S85L}$ (blue), $GyrA^{S85F}$ (orange), $GyrA^{E89K}$ (red), and $GyrA^{E89A}$ (green) gyrase to cleave DNA in the absence of drugs are shown. Assays were carried out in the presence of 20 mM $CaCl_2$ to facilitate quantitation. Error bars represent the standard deviation of at least three independent experiments.

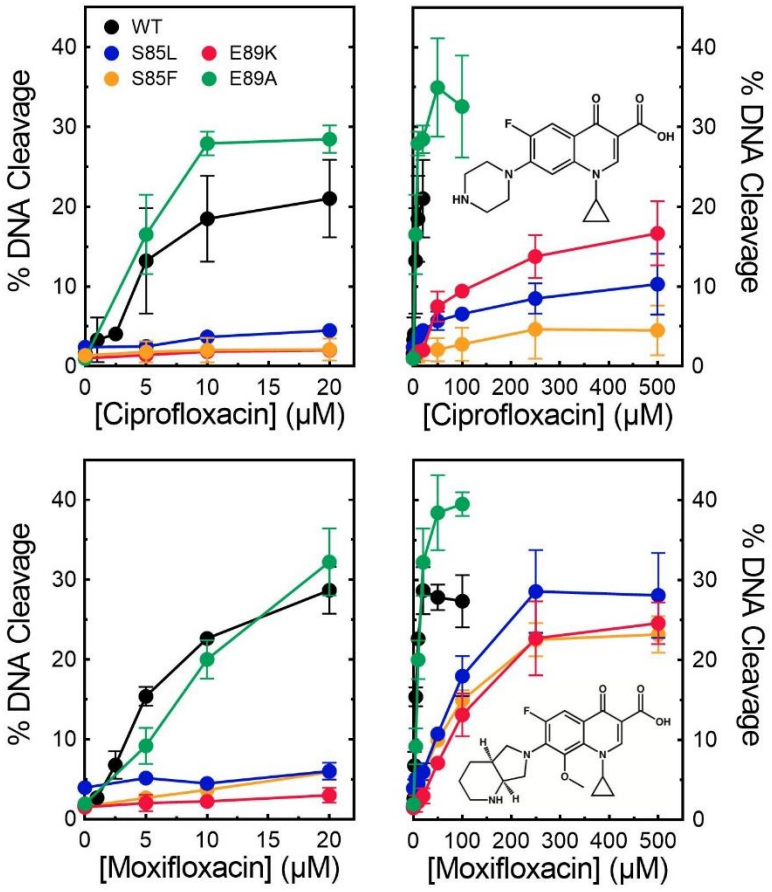

Figure 41. Effects of ciprofloxacin and moxifloxacin on DNA cleavage mediated by wild-type gyrase and mutant enzymes. The abilities of wild-type (black), GyrA^{S85L} (blue), GyrA^{S85F} (orange), GyrA^{E89K} (red), and GyrA^{E89A} (green) gyrase to cleave DNA in the presence of ciprofloxacin (top) and moxifloxacin (bottom) are shown. Drug structures are shown in right panels. Error bars represent the standard deviation of at least three independent experiments.

	CC_3 (μM)				
Drug	**WT**	**S85L**	**S85F**	**E89K**	**E89A**
Ciprofloxacin	2.75	150	200	25	0.75
Moxifloxacin	1.75	60	15	30	2.5
3'-(AM)P-quinolone	0.2	0.6	0.2	0.75	0.2
3'-(AM)P-dione	0.3	1.75	0.3	0.4	0.4
Cipro-dione	185	20	15	85	125
Moxi-dione	380	>500	>500	>500	480

Table 3. Relative potencies of quinolones and related compounds against wild-type gyrase and mutant enzymes. CC_3 is the drug concentration required to increase levels of cleavage 3-fold over baseline.

with the mutant enzymes close to those generated with wild-type gyrase and 20 μM drug (the highest drug concentration that could be used without producing multiple cleavage events per plasmid). In contrast, ciprofloxacin was not able to induce wild-type levels of cleavage with the mutant enzymes, even at concentrations as high as 500 μM.

The E89K mutation introduces a double charge change in the vicinity of quinolone binding. To determine whether resistance associated with this mutation is due to the loss of the glutamic acid or to the introduction of an opposite charge at this position, the effects of quinolones on DNA cleavage mediated by $GyrA^{E89A}$ gyrase were examined (Figure 41). Unlike the other mutants examined, this enzyme displayed no resistance to either ciprofloxacin or moxifloxacin. This implies that the basis for quinolone resistance caused by the E89K mutation is the disruptive charge inversion. This is in marked contrast to results with *B. anthracis* topoisomerase IV, in which the equivalent E→K and E→A mutations displayed similar levels of resistance.[117] These findings suggest potentially important differences in the way that quinolones interact with gyrase and topoisomerase IV in *B. anthracis*.

In addition to ciprofloxacin and moxifloxacin, the activity of 3'-(AM)P-quinolone against the wild-type and mutant enzymes was also examined. Unlike the C7 groups of clinically relevant quinolones, the 3'-(AM)P substituent can interact directly with bacterial type II topoisomerases.[217] This interaction potentially obviates the requirement for the proposed water-metal ion bridge in mediating drug-enzyme interactions.[116,117,142] Consistent with this hypothesis, 3'-(AM)P-quinolone displayed high activity against all of the mutant enzymes with little change in potency compared to wild-type (Figure 42, top left). Even when the 3'-(AM)P group was moved to a quinazolinedione skeleton (which

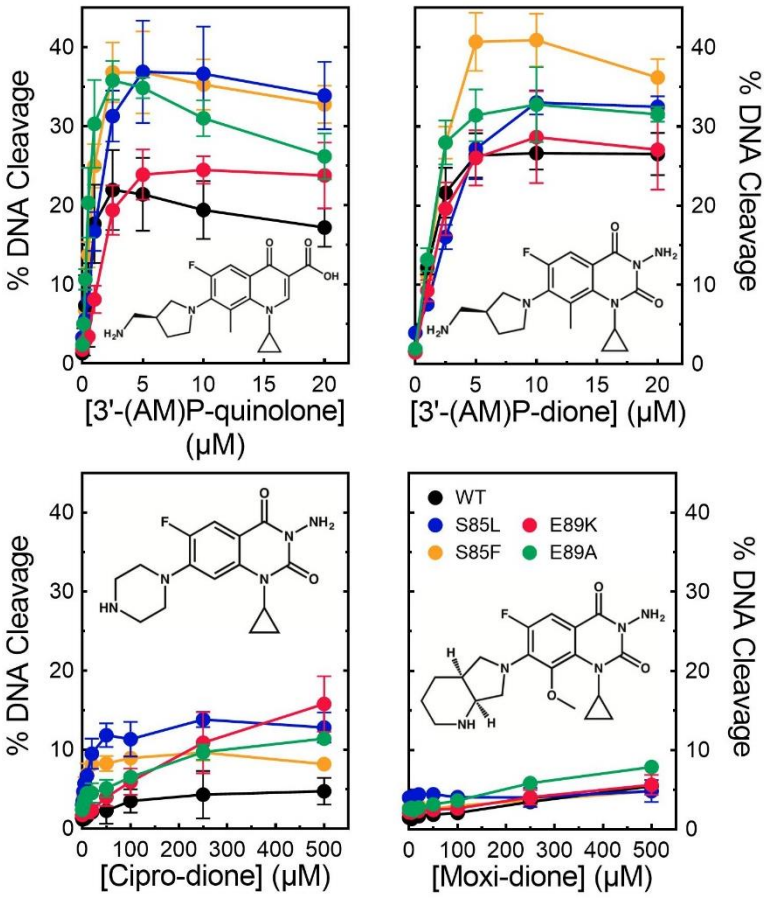

Figure 42. Effects of 3'-(AM)P-quinolone and quinazolinediones on DNA cleavage mediated by wild-type gyrase and mutant enzymes. The abilities of wild-type (black), $GyrA^{S85L}$ (blue), $GyrA^{S85F}$ (orange), $GyrA^{E89K}$ (red), and $GyrA^{E89A}$ (green) gyrase to cleave DNA in the presence of 3'-(AM)P-quinolone (top left), 3'-(AM)P-dione (top right), cipro-dione (bottom left), and moxi-dione (bottom right) are shown. Drug structures are shown in each panel. Error bars represent the standard deviation of at least three independent experiments.

lacks the C3/C4 keto acid required to form a water-metal ion bridge), the compound retained high activity against wild-type gyrase as well as quinolone-resistant mutant enzymes (Figure 42, top right). Conversely, when the C7/C8 substituents of ciprofloxacin and moxifloxacin (piperazinyl/H and diazabicyclononyl/methoxyl groups, respectively) were transferred to a quinazolinedione core, the resulting diones lost the majority of their activity against all of the enzymes, including the wild-type gyrase (Figure 42, bottom). These findings with "cipro-dione" and "moxi-dione" emphasize the importance of the C3/C4 keto acid in mediating the activity of clinically relevant quinolones against gyrase.

Based on results with *B. anthracis*[116,117] and *E. coli*[118] topoisomerase IV, the critical role of the C3/C4 keto acid of quinolones may be to facilitate binding to the enzyme or to position the drug appropriately for stabilizing cleavage complexes. To distinguish between these possibilities, the ability of cipro-dione and moxi-dione to compete with 5 μM 3'-(AM)P-dione in a DNA cleavage assay was assessed. If the C3/C4 keto acid is important for binding, the removal of this group should prevent effective competition.[116,117] Conversely, if the group is used for positioning the drug in the active site, the drugs should compete efficiently.[118] As seen in Figure 43, neither drug was able to substantially decrease levels of DNA cleavage induced by 3'-(AM)P-dione. Even at concentrations as high as 250 μM (corresponding to a 50-fold molar excess), cipro-dione and moxi-dione decreased cleavage by <50%. These results provide evidence that the C3/C4 keto acid is crucial for binding of quinolones to *B. anthracis* gyrase.

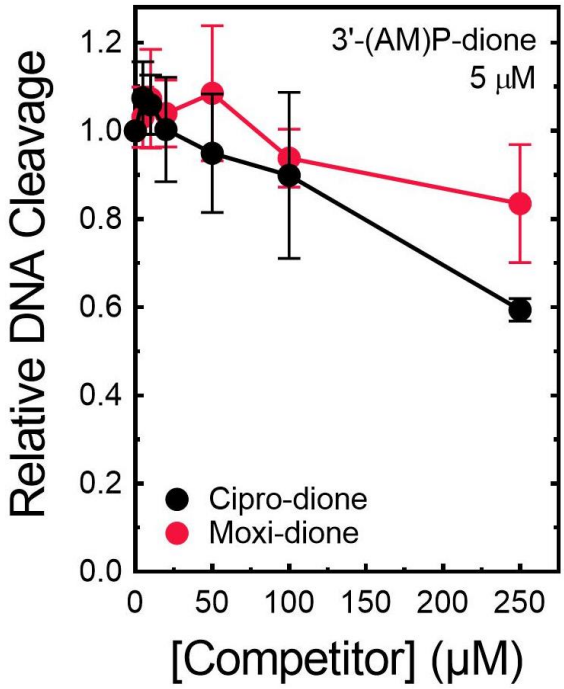

Figure 43. Abilities of cipro-dione and moxi-dione to compete with 3'-(AM)P-dione for binding to wild-type gyrase. The abilities of increasing concentrations of cipro-dione (black) and moxi-dione (red) to bind to the wild-type enzyme and prevent cleavage enhancement by 5 μM 3'-(AM)P-dione were determined. Drugs were added simultaneously to reaction mixtures. The small levels of cleavage seen in the presence of cipro-dione or moxi-dione alone were subtracted out from the levels of cleavage seen with both drugs, and the corrected cleavage level is plotted relative to the level observed with 3'-(AM)P-dione only. Error bars represent the standard deviation of at least three independent experiments.

Evidence for a water-metal ion bridge in mediating interactions between clinically relevant quinolones and B. anthracis *gyrase*

The importance of the C3/C4 keto acid for drug binding coupled with the effects of the resistance mutations strongly suggest that *B. anthracis* gyrase utilizes the water-metal ion bridge to mediate interactions with quinolones. Therefore, three approaches were utilized to determine whether this was the case. First, the requirement for metal ions to support quinolone-stabilized DNA cleavage mediated by wild-type gyrase was examined. Although DNA scission could utilize a variety of metal ions other than Mg^{2+} (data not shown), not all ions could support DNA cleavage induced by quinolones. For example, as seen in Figure 44, ciprofloxacin and moxifloxacin were unable to induce cleavage in the presence of Ba^{2+} and Ni^{2+}. In contrast, substantial levels of cleavage were observed with 3'-(AM)P-dione, which does not require a metal ion for activity. These findings indicate that quinolones require a non-catalytic divalent metal ion in order to function against *B. anthracis* gyrase.

Second, it was determined whether mutations at S85 or E89 of GyrA altered the metal ion requirements for quinolone-induced DNA cleavage. In the presence of Mg^{2+}, high quinolone concentrations could (at least partially) overcome drug resistance with the S85L and E89K mutants (see Figure 41). However, in the presence of Mn^{2+}, ciprofloxacin and moxifloxacin were unable to induce cleavage with these mutant enzymes (Figure 45). This is despite the fact that Mn^{2+} supported the activity of both quinolones against the wild-type enzyme and the non-resistant E89A mutant as well as the activity of 3'-(AM)P-dione against all of the enzymes examined. The finding that resistance mutations at S85 and E89 restrict the variety of metal ions that clinically relevant quinolones can use to enhance DNA

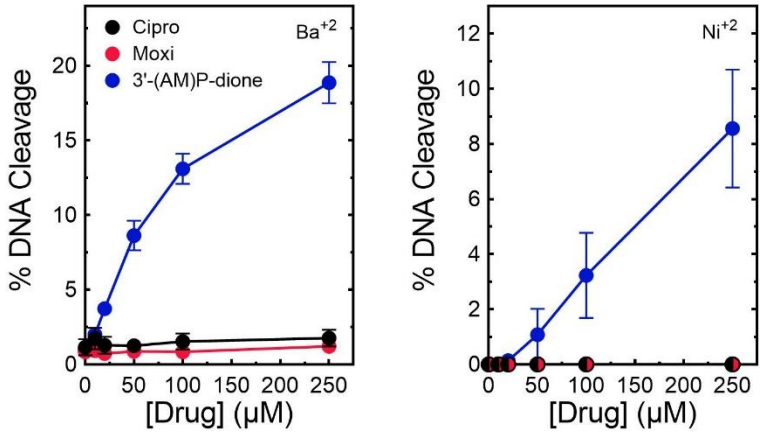

Figure 44. Effects of alternative metal ions on drug-induced DNA cleavage mediated by wild-type gyrase. The abilities of ciprofloxacin (black), moxifloxacin (red), and 3'-(AM)P-dione (blue) to induce cleavage by wild-type gyrase in the presence of Ba^{2+} (left) or Ni^{2+} (right) are shown. Error bars represent the standard deviation of at least three independent experiments.

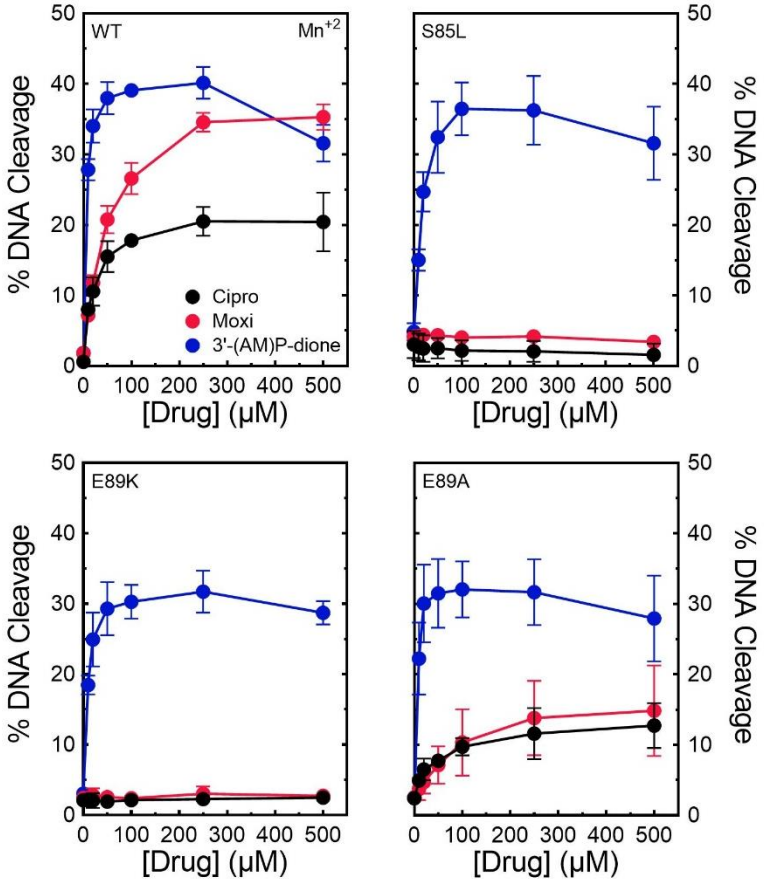

Figure 45. Effects of Mn^{2+} on drug-induced DNA cleavage mediated by wild-type gyrase and mutant enzymes. The abilities of ciprofloxacin (black), moxifloxacin (red), and 3'-(AM)P-dione (blue) to induce cleavage by wild-type gyrase (top left) or enzymes with S85L (top right), E89K (bottom left), or E89A (bottom right) mutations in the presence of Mn^{2+} are shown. Error bars represent the standard deviation of at least three independent experiments.

cleavage further implicates a role for a non-catalytic divalent metal ion in mediating interactions between the drug and *B. anthracis* gyrase.

Third, enzymes with mutations at S85 and E89 were assessed to determine whether the substitutions affected the affinity of the metal ion required for quinolone actions against gyrase. These experiments monitored DNA cleavage levels over a range of 0-3 mM Mg^{2+}. In order to facilitate direct comparisons between the wild-type and mutant enzymes, DNA cleavage levels were normalized to those observed in reactions containing 3 mM $MgCl_2$. Compared to wild-type gyrase, the S85L and E89K mutants decreased the affinity of Mg^{2+} in reactions that contained ciprofloxacin (Figure 46, left). Concentrations of the metal ion required to induce half-maximal and maximal levels of cleavage rose ~2.5-fold. In contrast, the E89A mutation, which does not cause quinolone resistance, had no effect on metal ion usage. As a control, parallel titrations were carried out with 3'-(AM)P-dione (Figure 46, right). No decrease in metal ion affinity was observed with any of the mutant enzymes. In fact, the quinazolinedione required lower levels of Mg^{2+} with the E89 mutants.

The studies described above indicate that quinolones require a divalent metal ion for their actions and that resistance mutations restrict the usage and decrease the affinity of the coordinating metal ion. Taken together, these findings provide strong evidence that quinolone interactions with *B. anthracis* gyrase are mediated by the water-metal ion bridge. However, these results point to an important distinction between the amino acids used to anchor the bridges in *B. anthracis* gyrase and topoisomerase IV. Whereas the serine residue is a critical bridge anchor in both enzymes, it appears that the glutamic acid residue is used only in topoisomerase IV. This is based on the fact that the conversion of this residue to an

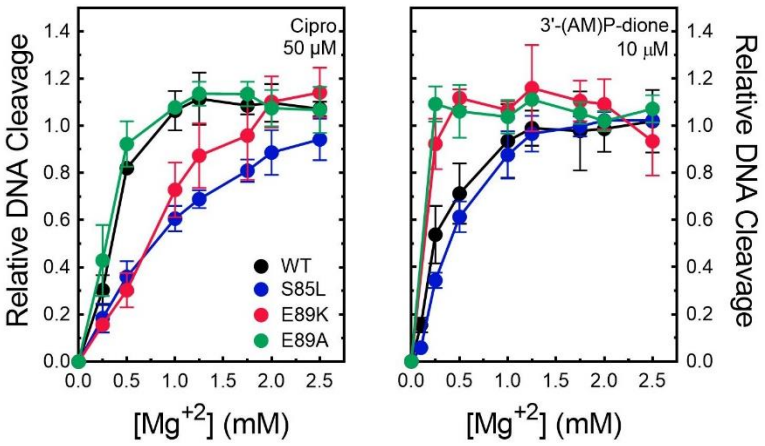

Figure 46. Effects of GyrA mutations on Mg^{2+} concentrations required to support maximum levels of drug-induced cleavage. Results are shown for ciprofloxacin (left) and 3'-(AM)P-dione (right) with wild-type gyrase (black) or enzymes with S85L (blue), E89K (red), or E89A (green) mutations. Cleavage levels with each drug-enzyme pair were normalized to levels observed with 3 mM $MgCl_2$. Error bars represent the standard deviation of at least three independent experiments.

alanine causes resistance and altered utilization of metal ions in topoisomerase IV[117] but does neither in gyrase.

Role of the water-metal ion bridge in mediating quinolone-gyrase interactions

Two lines of evidence imply that the water-metal ion bridge is used primarily to mediate binding interactions between clinically relevant quinolones and *B. anthracis* gyrase: high concentrations of quinolones can overcome the effects of resistance mutations (Figure 41) and removal of the C3/C4 keto acid greatly diminishes drug affinity for the enzyme (Figure 43). To determine whether this is the case, a competition assay that utilized S85L or E89K gyrase was employed. These experiments monitored the ability of 0-50 μM ciprofloxacin and moxifloxacin to compete with DNA cleavage induced by 5 μM 3'-(AM)P-dione. These three drugs display similar potencies against wild-type *B. anthracis* gyrase (see Figures 41 and 42). Therefore, if the resistance mutations do not reduce drug affinity, cleavage levels induced by 3'-(AM)P-dione should drop by 50% at ~5 μM quinolone. As seen in Figure 47, this was not the case. Even at a 10-fold molar excess of ciprofloxacin or moxifloxacin, DNA scission decreased <50%. These results provide strong evidence that the water-metal ion bridge provides the primary binding contact between clinically relevant quinolones and *B. anthracis* gyrase.

Effects of the C8 substituent on quinolone activity and resistance

Previous studies demonstrated that the substituent at C8 can make important contributions to quinolone activity against *B. anthracis* topoisomerase IV[142] and *M. tuberculosis* gyrase.[119] Therefore, a series of ciprofloxacin- and moxifloxacin-based compounds containing a –H, –methyl, or –methoxyl substituent at C8 were assessed for

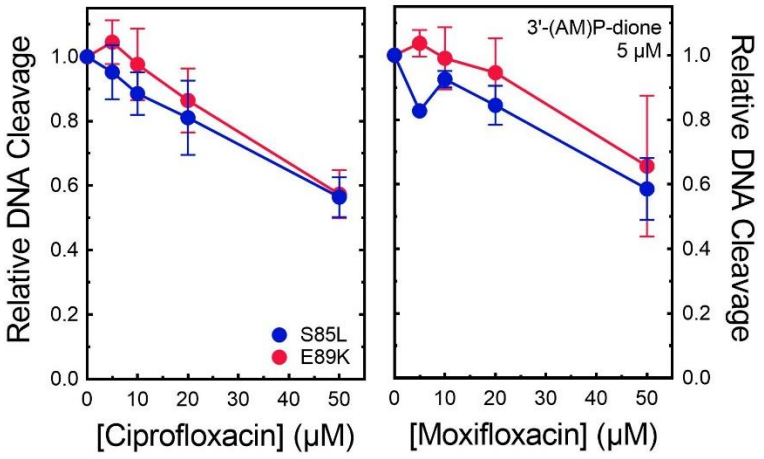

Figure 47. Abilities of ciprofloxacin and moxifloxacin to compete with 3'-(AM)P-dione for binding to quinolone-resistant enzymes. The abilities of increasing concentrations of ciprofloxacin (left) and moxifloxacin (right) to bind to S85L (blue) or E89K (red) gyrase and prevent cleavage enhancement by 5 μM 3'-(AM)P-dione were determined. Drugs were added simultaneously to reaction mixtures. The levels of cleavage seen in the presence of ciprofloxacin or moxifloxacin alone were subtracted out from the levels of cleavage seen with both drugs, and the corrected cleavage level is plotted relative to the level observed with 3'-(AM)P-dione only. Error bars represent the standard deviation of at least three independent experiments.

their activities against wild-type, S85L, and E89K gyrase. Compared to ciprofloxacin (which contains a C8-H group), 8-methyl-cipro and 8-methoxy-cipro displayed considerably higher potencies and efficacies against the wild-type and mutant enzymes (Figure 48). In fact, 8-methoxy-cipro was able to overcome resistance at ~20 μM drug. Although less striking, similar results were seen with the moxifloxacin series (Figure 49). Compared to the parent compound (which contains a C8-methoxyl group), 8-H-moxi displayed much lower efficacy against all of the enzymes and was unable to overcome resistance even at high concentrations. In contrast, 8-methyl-moxi displayed high potency and efficacy that were similar to (or slightly higher than) those of moxifloxacin. These results demonstrate that the substituent at C8 affects the actions of quinolones against *B. anthracis* gyrase.

Conclusions

Results described in this chapter provide strong evidence that the primary interaction between clinically relevant quinolones and *B. anthracis* gyrase occurs through the water-metal ion bridge (Figure 50). Furthermore, the function of the bridge in gyrase is to facilitate binding of the drug to the enzyme. This is as opposed to *E. coli* topoisomerase IV, which uses the bridge to position quinolones but does not require it for drug binding.[118]

The bridge "anchors" in *B. anthracis* gyrase are distinct from those in topoisomerase IV and in *M. tuberculosis* gyrase. In *B. anthracis* topoisomerase IV, both the serine and the glutamic acid residues are used to anchor the bridge, and loss of either anchor causes quinolone resistance.[116,117] Because *M. tuberculosis* gyrase lacks the serine residue, the only available anchor is the glutamic acid, so this residue provides the principal contact for quinolone binding.[119] Conversely, in *B. anthracis* gyrase, the water-metal ion bridge seems

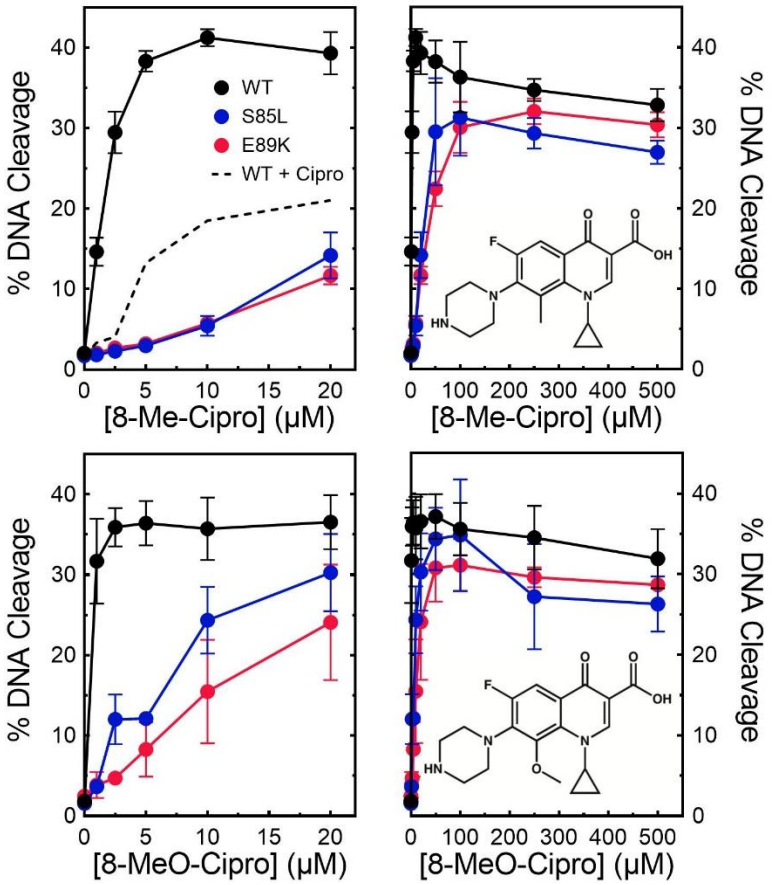

Figure 48. Effects of different C8 groups on ciprofloxacin-induced DNA cleavage mediated by wild-type gyrase and quinolone-resistant mutants. The abilities of 8-methyl-ciprofloxacin (top) and 8-methoxy-ciprofloxacin (bottom) to enhance cleavage mediated by wild-type (black), $GyrA^{S85L}$ (blue), $GyrA^{S85F}$ (orange), $GyrA^{E89K}$ (red), and $GyrA^{E89A}$ (green) gyrase were determined. Cleavage induced by ciprofloxacin with wild-type gyrase is shown by the dotted black line in the top left panel. Drug structures are shown in right panels. Error bars represent the standard deviation of at least three independent experiments.

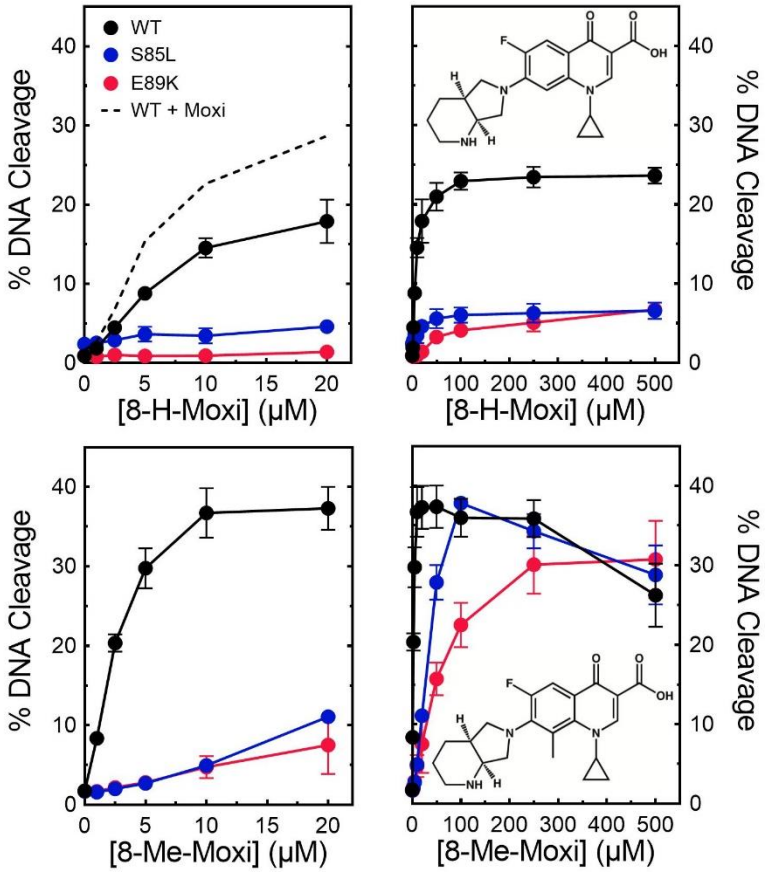

Figure 49. Effects of different C8 groups on moxifloxacin-induced DNA cleavage mediated by wild-type gyrase and quinolone-resistant mutants. The abilities of 8-H-moxifloxacin (top) and 8-methyl-moxifloxacin (bottom) to enhance cleavage mediated by wild-type (black), $GyrA^{S85L}$ (blue), $GyrA^{S85F}$ (orange), $GyrA^{E89K}$ (red), and $GyrA^{E89A}$ (green) gyrase were determined. Cleavage induced by moxifloxacin with wild-type gyrase is shown by the dotted black line in the top left panel. Drug structures are shown in right panels. Error bars represent the standard deviation of at least three independent experiments.

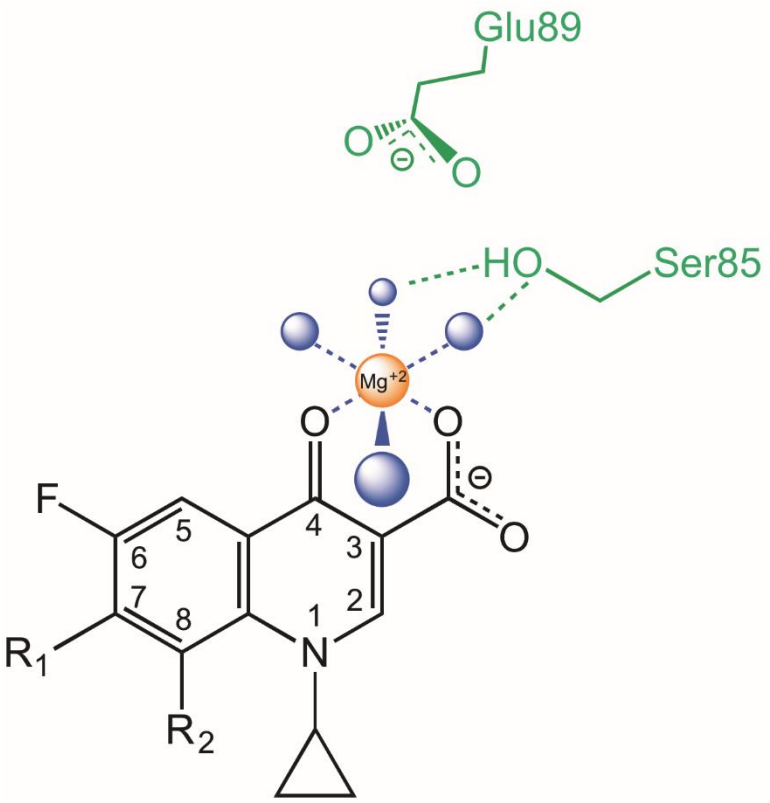

Figure 50. Simplified schematic of the water-metal ion bridge used to mediate interactions between quinolones and *B. anthracis* gyrase. Only interactions with the protein (and not DNA) are shown. A representative quinolone core is depicted in black, the non-catalytic Mg^{2+} in orange, water molecules in blue, and the serine and acidic residues in green. Blue lines indicate the octahedral coordination sphere of the divalent metal ion interacting with four water molecules and the C3/C4 keto acid of the quinolone. The green dashed lines represent hydrogen bonds between the serine side chain hydroxyl group and the water molecules. In contrast to *B. anthracis* and *E. coli* topoisomerase IV, the glutamic acid residue does not appear to act as a bridge anchor. Adapted from Aldred *et al*.[117]

to be primarily coordinated through the serine residue. In this case, quinolone resistance in gyrase harboring an E89K mutation is likely due to the disruptive charge inversion rather than the loss of an anchor. These findings point to subtle, but critical, differences in the drug binding pockets of gyrase and topoisomerase IV from different species that give rise to distinct quinolone interactions.

In accord with the above, it is possible to introduce interactions that overcome drug resistance differentially. For example, changing the C8 substituent of ciprofloxacin (which is the primary prophylactic and first-line drug used to treat anthrax)[218,219] from a hydrogen to a methoxyl group greatly improves the efficacy of the drug against wild-type and quinolone-resistant *B. anthracis* gyrase. However, in *M. tuberculosis* gyrase, the drug derivative best able to overcome resistance is the C8-methyl form of moxifloxacin.[119]

Taken together, these results present an opportunity to shift the paradigm for the development and use of new quinolones. Historically, these drugs were developed as broad-spectrum antibacterials. However, by analyzing drug interactions with gyrase and topoisomerase IV from individual bacteria, it should be possible to identify specific quinolone derivatives that are able to overcome target-mediated resistance in those pathogenic species.

CHAPTER VIII

CONCLUSIONS AND IMPLICATIONS

Natural Products and Covalent Topoisomerase II Poisons

Natural products are the single most productive source of lead compounds that have been used for drug development.[220,221] In fact, natural products and their derivatives have led to the development of almost half of the anticancer drugs approved worldwide,[221,222] and a number of topoisomerase II poisons derived from natural sources display chemotherapeutic or chemopreventive activity.[5,16,20,22,62-67,69-72] Chapter III describes the characterization of thymoquinone, the major active compound in black seed, both in its pure and herbal forms. Black seed has a rich history of use as a medicinal herb, and both black seed and thymoquinone have been reported to have anticancer properties.[146,147,153-158,160-162] Results in Chapter III show that thymoquinone acts as a covalent poison against human topoisomerase IIα. Furthermore, the herbal formulations that are actually used in culinary and medical applications (ground black seed and black seed oil) also display activity against the enzyme. These results suggest that black seed and other medicinal herbs may be exerting their beneficial effects partly through topoisomerases. The continued investigation of natural products with activity against topoisomerases can lead to a better understanding of the biochemical basis for their health benefits, provide new insights into enzyme mechanism, and potentially lead to new therapeutics.

Results in Chapter IV provide new information about the mechanism of action of covalent topoisomerase II poisons. Although it had been proposed that the N-terminal gate

was important for the activity of covalent poisons,[89,90] it had also been shown that covalent poisons could modify residues within both the N-terminal region and within the catalytic core.[70,85] The use of complementary constructs containing different regions of topoisomerase IIα allowed the actions of covalent poisons to be more fully investigated. As discussed in Chapter IV, the N-terminal gate of topoisomerase IIα is required for the stabilization of cleavage complexes by benzoquinone and thymoquinone, which are both covalent poisons. However, benzoquinone and thymoquinone retained the ability to inhibit the catalytic core of topoisomerase IIα prior to the addition of DNA, indicating that there are at least two distinct classes of interactions that covalent poisons can make with the enzyme that have different effects on enzyme activity. This may partly explain why it has been difficult to pinpoint the important residues for the activity of covalent poisons: these compounds likely interact with multiple residues in both the N-terminal gate and the catalytic core, but not every residue is important for the stabilization of cleavage complexes. Future studies to determine which residues within the catalytic core are necessary for the inhibitory effects of covalent poisons could provide important information about how these compounds interact with the protein near the DNA-binding site and shed light on the mechanistic basis of this hallmark feature of covalent poisons.

Recognition of DNA Geometry by Bacterial Type II Topoisomerases

Although gyrase is typically described as the "only known topoisomerase able to generate negative supercoiling",[16] results discussed in Chapters V and VI show that gyrase from both *B. anthracis* and *M. tuberculosis* actually removes (+) supercoils dramatically faster than it introduces (-) supercoils into relaxed DNA. This likely reflects the cellular requirement for rapid removal of (+) supercoils during replication. To this point, the

bacterial DNA replication machinery typically moves at a rate of 500-1000 nucleotides/s,[199] which creates ~50-100 (+) supercoils/s ahead of the fork. As determined by single-molecule experiments, the average burst rate of relaxation of (+) supercoils by *B. anthracis* gyrase exceeds 100 supercoils/s. This rate is therefore within the physiological range, even if only a single molecule of gyrase were acting ahead of a replication fork.

The two functions of gyrase

The two critical cellular functions of gyrase are bounded by distinct temporal constraints (Figure 51). The "acute function" of the enzyme is to remove (+) supercoils that rapidly accumulate immediately ahead of replication forks and other DNA tracking systems. This localized activity must occur within a short window of time in order to allow these essential nucleic acid processes to continue. Therefore, it requires an exceptionally high rate. In contrast, the "steady-state function" of gyrase is to maintain the proper superhelical density of the bacterial chromosome. Because local overwinding that occurs as a result of individual nucleic acid events has a relatively minor effect on global supercoiling, the maintenance of topological homeostasis can take place over a protracted time scale.

Despite the fact that gyrase removes (+) supercoils much more quickly than it introduces (-) supercoils into relaxed DNA, both reactions utilize the same wrapping mechanism to achieve optimal rates. Why, then, does relaxation take place so much faster than supercoiling? One possible explanation is that the relaxation of (+)SC DNA is energetically favorable, whereas the introduction of (-) supercoils is energetically unfavorable.[2] Alternatively, overwound DNA should intrinsically provide gyrase with the (+) supercoils needed to wrap around the C-terminal domain of GyrA. In contrast, when

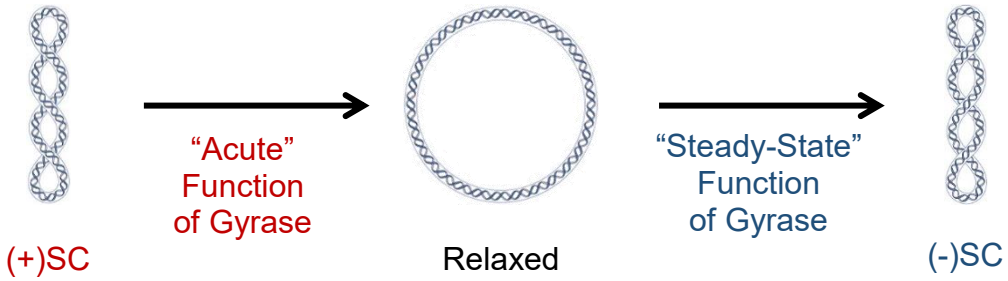

Figure 51. The two critical cellular functions of gyrase. Gyrase has two important functions within the cell that must occur on different time scales. The "acute" function of the enzyme is to remove (+) supercoils that accumulate ahead of DNA tracking machinery, which must occur rapidly in order to keep up with the moving forks. The "steady-state" function of gyrase is to introduce (-) supercoils into the genome to maintain its overall superhelical density.

acting on relaxed or (-)SC DNA, the enzyme must first induce a (+) supercoil before continuing through its cycle. This necessity could negatively impact both the rate and the processivity of the strand passage reaction.

On the basis of the above, I propose that (+)SC DNA may actually be the preferred substrate for gyrase. This raises an interesting teleological question: did the initial evolutionary pressure to develop the wrapping mechanism stem from the need to introduce (-) supercoils or to remove (+) supercoils? Although it is impossible to definitively resolve this issue, I suggest that the latter may be the case. Replication in bacterial systems takes place *via* two forks moving away from a single origin, each at a rate of 500-1000 nucleotides/s.[199] This is in contrast to human cells, in which tens of thousands of origins fire and replication forks move at a much slower rate of ~30 nucleotides/s.[223] As a result, bacterial cells have a unique requirement for a topoisomerase that can remove (+) supercoils at an especially high rate. Conversion of gyrase to a canonical type II topoisomerase by mutating the GyrA-box dramatically reduces the rate of (+) supercoil removal. Furthermore, single-molecule experiments indicate that the maximal rate of (+) supercoil relaxation by gyrase is several-fold faster than that of topoisomerase IV.[58,201,203] Therefore, it appears that a canonical type II enzyme may not be able to act rapidly enough to keep up with the bacterial replication fork. As eukaryotic species evolved, the accompanying slower rates of fork movement, coupled with the emergence of multiple topoisomerases (both type I and type II) that were able to relax (+) supercoils, dispensed with the need for such a rapidly acting enzyme.

The wrapping mechanism developed for (+) supercoil removal concomitantly conferred gyrase with the ability to introduce (-) supercoils. As discussed above, this

activity plays a critical role in maintaining the topological state of the bacterial chromosome. The requirement for globally underwound DNA endured in eukaryotes, but the advent of histones and higher-order chromatin structures obviated the requirement for an enzyme with an intrinsic ability to underwind DNA.

Future studies to investigate the actions of gyrase on overwound DNA could provide further insight into how the geometry of the substrate affects the enzyme. It is still unclear how much variation there is between gyrases of different species. To determine whether the fast, processive removal of (+) supercoils is a defining feature of gyrase, ensemble and single-molecule experiments need to be carried out with enzymes from other Gram-positive and Gram-negative species. Perhaps the first enzyme to examine is gyrase from *E. coli*, because other mechanistic aspects of this enzyme have already been well characterized.[177,181,193,194,224-228] Although one study reported relaxation of (+) supercoils by *E. coli* gyrase in a single-molecule system,[195] it would be useful to examine the *B. anthracis* enzyme and the *E. coli* enzyme side-by-side within the same experimental setup to facilitate more direct comparisons between their activities. Once the actions of these two example enzymes have been defined, it will be important to examine the recognition of DNA geometry by enzymes from other species. The vast majority of studies on both gyrase and topoisomerase IV have been carried out on the enzymes from *E. coli*, which has led the field to make many assumptions about the enzymology of all bacterial type II topoisomerases based on results with a single species. However, because species encoding only gyrase must, by definition, have a functionally distinct enzyme, and because both bacterial type II topoisomerases are valuable targets in the treatment of a number of

bacterial infections, it is crucial that the investigation of the mechanisms of gyrase and topoisomerase IV be expanded to enzymes from other species.

Recognition of supercoil geometry by bacterial type II topoisomerases during DNA cleavage

While gyrase and topoisomerase IV are both able to recognize supercoil geometry during strand passage, only gyrase is capable of distinguishing between overwound and underwound DNA during cleavage. The ability of gyrase to maintain low levels of cleavage complexes on (+)SC DNA makes it well suited to function on overwound DNA ahead of moving tracking systems. However, this recognition appears to occur through a different mechanism in gyrase than in topoisomerase IIα. In the human enzyme, the catalytic core is capable of distinguishing between (+) and (-) supercoils during cleavage. Conversely, in *M. tuberculosis* gyrase, the catalytic core does not distinguish supercoil handedness. Instead, the recognition of DNA geometry seems to be embedded within the N-terminal gate, indicating that the N-terminal region of bacterial type II topoisomerases may have important interactions with their DNA substrates that influence the levels of cleavage complexes maintained by the enzymes. This finding should be tested directly with a series of N-terminal deletion mutations of *M. tuberculosis* gyrase to pinpoint the region required for DNA geometry recognition, and should also be confirmed by examining similar mutations of gyrase from other species. Additionally, domain-swapping experiments to link the N-terminal gate of gyrase to the catalytic core of topoisomerase IV and vice versa could be used to confirm that the differences in the ability of these enzymes to recognize DNA geometry during cleavage arise from their N-terminal domains. These comparative

studies could provide valuable insight into how these enzymes recognize and function on the variety of DNA geometries they encounter within the cell.

Finally, the different abilities of gyrase and topoisomerase IV to recognize DNA geometry during cleavage along with their different cellular localizations may impact the relative efficacies of these enzymes as targets for quinolone antibacterials. Functioning ahead of a fork, gyrase is perfectly positioned to create cleavage complexes with the potential to be converted to permanent DNA damage. However, the diminished levels of cleavage complexes generated by the enzyme on (+)SC DNA may partially abrogate the cytotoxic effects of quinolones. Conversely, topoisomerase IV maintains high levels of cleavage complexes on overwound substrates, but typically acts behind the fork, where cleavage complexes are less likely to be disrupted by moving tracking systems. Ultimately, it is probable that the physiological locations and the recognition of DNA geometry by gyrase and topoisomerase IV both contribute to the complex relationship between quinolone targeting in purified systems and drug lethality in bacterial cells. Future studies to better define these relationships should examine cleavage complexes generated within cells treated with quinolones, where both enzymes can be affected while acting in their relevant cellular positions. This type of experiment has been carried out successfully in *E. coli*,[102] but has yet to be expanded to fully evaluate the cellular effects of quinolones relative to their *in vitro* activities.

Quinolone Mechanism and Resistance

The majority of studies on quinolone interactions with bacterial type II topoisomerases have utilized topoisomerase IV as the model enzyme. Results in Chapter VII describe the biochemical basis of quinolone interactions with a canonical gyrase and how the most

common resistance mutations alter drug affinity. Quinolones interact with *B. anthracis* gyrase through a water-metal ion bridge, similar to results reported for topoisomerase IV from *B. anthracis*[116,117] and *E. coli*[118] and gyrase from *M. tuberculosis*.[119] However, despite the fact that quinolone action against each of these four enzymes relies on a water-metal ion bridge, the anchors and/or function of the bridge differ in each case. Figure 52 summarizes the use of the water-metal ion bridge in each enzyme. In *B. anthracis* topoisomerase IV, both the serine and glutamic acid residues are important anchors for the bridge, and the primary function of the bridge is to facilitate binding of clinically relevant quinolones to the enzyme.[116,117] *E. coli* topoisomerase IV also uses both residues to anchor the bridge, but the bridge is not necessary for the binding of quinolones to the enzyme.[118] Instead, the bridge is required for appropriate positioning of the drug in the binding pocket. *M. tuberculosis* gyrase is unique in that it does not have the serine residue, so the bridge is anchored solely through the glutamic acid residue.[119] The bridge in *B. anthracis* gyrase is also anchored by only one residue, but in this case, the serine residue is the primary anchor. For both gyrases, the bridge is necessary for quinolone binding to the enzyme. Furthermore, although only one residue is used to anchor the bridge, mutations at the position of the second residue can still cause resistance, presumably due to the introduction of either extra bulk (*M. tuberculosis*) or a disruptive charge (*B. anthracis*).

These results highlight the importance of conducting thorough biochemical analyses of multiple bacterial type II topoisomerases to fully understand the water-metal ion bridge interaction. While it is clear that the general interactions are similar across the enzymes examined so far, we do not fully understand the nuances that determine the precise mechanism of action of quinolones with each individual topoisomerase. It is possible that

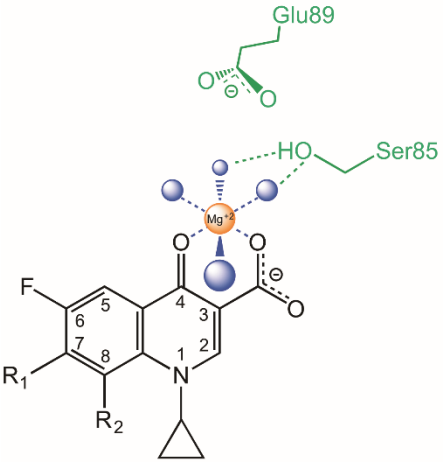

B. anthracis Gyrase
- One anchor (serine)
- Binding

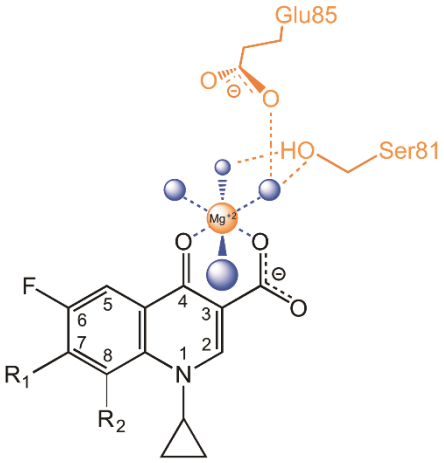

B. anthracis Topoisomerase IV
- Two anchors
- Binding

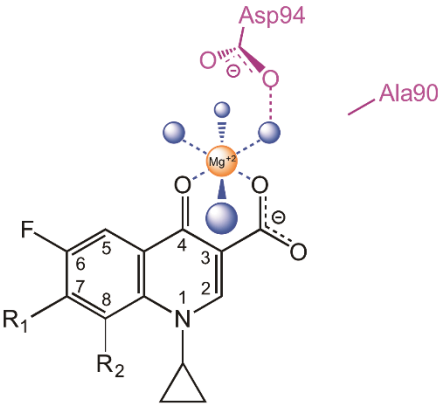

M. tuberculosis Gyrase
- One anchor (aspartate)
- Binding

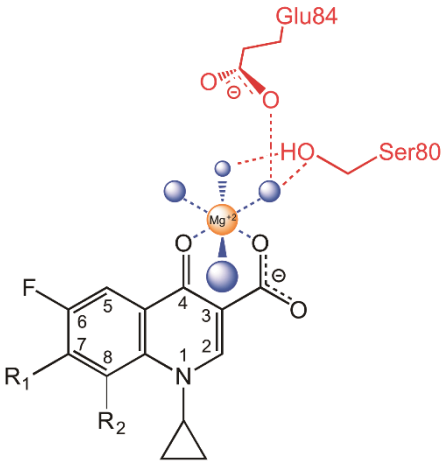

E. coli Topoisomerase IV
- Two anchors
- Positioning

Figure 52. Use and role of the water-metal ion bridge in bacterial type II topoisomerases examined to date. The Mg^{2+} ion is shown in orange, and coordinating water molecules are shown in blue. Blue dashed lines represent indicate the coordination sphere of the metal ion. Other dashed lines represent hydrogen bonding between water molecules and the serine and/or acidic residues. Although the water-metal ion bridge is only anchored by one residue in *B. anthracis* and *M. tuberculosis* gyrase, mutations at the non-anchoring position (Glu89 and Ala90, respectively) can still cause resistance. Figure adapted from Aldred *et al.*[117]

other residues within the quinolone binding pocket contribute to quinolone binding and orientation but have yet to be defined. Furthermore, it is likely that differences between various quinolones influence how well each drug interacts with each enzyme, which may account for the observation that the primary cellular target of quinolones in a given species can vary depending on the drug used.[73,101-106]

With all of the enzymes examined, it is possible to overcome resistance by introducing different substituents at the C7 and C8 positions.[118,119,142] As discussed in Chapter VII, replacing the existing C8 substituent of ciprofloxacin or moxifloxacin with a –methoxyl or –methyl group, respectively, increased the activity of the compound against *B. anthracis* gyrase carrying the most common quinolone resistance mutations. The effects were particularly striking for 8-methoxy-cipro, which was able to overcome resistance at ~20 μM drug. Studies with *B. anthracis* topoisomerase IV and *M. tuberculosis* gyrase showed that similar minor changes at the C8 position could overcome resistance without causing cross-reactivity with the human enzyme.[119,142] These results suggest that there are other contacts within the quinolone-binding pocket that are not being fully exploited by the quinolones in current clinical use. Therefore, it is possible to develop related but more effective drugs capable of forming multiple interactions with the enzyme. New quinolones with multiple contacts to the enzymes would have the potential to overcome existing resistance and would also be naturally more effective at preventing the emergence of resistance, as multiple mutations would be required to disrupt drug-enzyme interactions. Future studies should investigate quinolones with different C7/C8 combinations, particularly 8-methoxy-cipro in the case of *B. anthracis*, for their efficacy both *in vitro* and in bacterial culture.

REFERENCES

1. Wang, J. C. (2002) Cellular roles of DNA topoisomerases: a molecular perspective, *Nat. Rev. Mol. Cell Biol. 3*, 430-440.

2. Bates, A. D. and Maxwell, A. (2005) *DNA Topology*, Oxford University Press, New York, USA.

3. Liu, Z., Deibler, R. W., Chan, H. S., and Zechiedrich, L. (2009) The why and how of DNA unlinking, *Nucleic Acids Res. 37*, 661-671.

4. Koster, D. A., Crut, A., Shuman, S., Bjornsti, M. A., and Dekker, N. H. (2010) Cellular strategies for regulating DNA supercoiling: a single-molecule perspective, *Cell 142*, 519-530.

5. Vos, S. M., Tretter, E. M., Schmidt, B. H., and Berger, J. M. (2011) All tangled up: how cells direct, manage and exploit topoisomerase function, *Nat. Rev. Mol. Cell Biol. 12*, 827-841.

6. Bauer, W. R., Crick, F. H., and White, J. H. (1980) Supercoiled DNA, *Sci. Am. 243*, 100-113.

7. White, J. H. and Cozzarelli, N. R. (1984) A simple topological method for describing stereoisomers of DNA catenanes and knots, *Proc. Natl. Acad. Sci. U. S. A. 81*, 3322-3326.

8. Vologodskii, A. V. and Cozzarelli, N. R. (1994) Conformational and thermodynamic properties of supercoiled DNA, *Annu. Rev. Biophys. Biomol. Struct. 23*, 609-643.

9. Deweese, J. E., Osheroff, M. A., and Osheroff, N. (2008) DNA topology and topoisomerases: teaching a "knotty" subject, *Biochem. Mol. Biol. Educ. 37*, 2-10.

10. Ketron, A. C. and Osheroff, N. (2014) DNA topology and topoisomerases, In *Molecular Life Sciences: An Encyclopedic Reference* (Bell, E., Ed.), pp 1-19, Springer New York, New York, NY.

11. Espeli, O. and Marians, K. J. (2004) Untangling intracellular DNA topology, *Mol. Microbiol. 52*, 925-931.

12. Falaschi, A., Abdurashidova, G., Sandoval, O., Radulescu, S., Biamonti, G., and Riva, S. (2007) Molecular and structural transactions at human DNA replication origins, *Cell Cycle 6*, 1705-1712.

13. Travers, A. and Muskhelishvili, G. (2007) A common topology for bacterial and eukaryotic transcription initiation?, *EMBO Rep. 8*, 147-151.

14. McClendon, A. K. and Osheroff, N. (2007) DNA topoisomerase II, genotoxicity, and cancer, *Mutat. Res. 623*, 83-97.

15. Wang, J. C. (1996) DNA topoisomerases, *Annu. Rev. Biochem. 65*, 635-692.

16. Champoux, J. J. (2001) DNA topoisomerases: structure, function, and mechanism, *Annu. Rev. Biochem. 70*, 369-413.

17. Schoeffler, A. J. and Berger, J. M. (2005) Recent advances in understanding structure-function relationships in the type II topoisomerase mechanism, *Biochem. Soc. Trans. 33*, 1465-1470.

18. Leppard, J. B. and Champoux, J. J. (2005) Human DNA topoisomerase I: relaxation, roles, and damage control, *Chromosoma 114*, 75-85.

19. Pommier, Y. (2006) Topoisomerase I inhibitors: camptothecins and beyond, *Nat. Rev. Cancer 6*, 789-802.

20. Deweese, J. E. and Osheroff, N. (2009) The DNA cleavage reaction of topoisomerase II: wolf in sheep's clothing, *Nucleic Acids Res. 37*, 738-749.

21. Nitiss, J. L. (2009) DNA topoisomerase II and its growing repertoire of biological functions, *Nat. Rev. Cancer 9*, 327-337.

22. Pommier, Y., Leo, E., Zhang, H., and Marchand, C. (2010) DNA topoisomerases and their poisoning by anticancer and antibacterial drugs, *Chem. Biol. 17*, 421-433.

23. Berger, J. M., Gamblin, S. J., Harrison, S. C., and Wang, J. C. (1996) Structure and mechanism of DNA topoisomerase II, *Nature 379*, 225-232.

24. Wang, J. C. (1998) Moving one DNA double helix through another by a type II DNA topoisomerase: the story of a simple molecular machine, *Q. Rev. Biophys. 31*, 107-144.

25. Fortune, J. M. and Osheroff, N. (2000) Topoisomerase II as a target for anticancer drugs: when enzymes stop being nice, *Prog. Nucleic Acid Res. Mol. Biol. 64*, 221-253.

26. Velez-Cruz, R. and Osheroff, N. (2004) DNA topoisomerases: type II, In *Encyclopedia of Biological Chemistry*, pp 806-811, Elsevier Inc.

27. Osheroff, N. (1986) Eukaryotic topoisomerase II. Characterization of enzyme turnover, *J. Biol. Chem. 261*, 9944-9950.

28. Osheroff, N. (1987) Role of the divalent cation in topoisomerase II mediated reactions, *Biochemistry 26*, 6402-6406.

29. Roca, J. and Wang, J. C. (1992) The capture of a DNA double helix by an ATP-dependent protein clamp: a key step in DNA transport by type II DNA topoisomerases, *Cell 71*, 833-840.

30. Lindsley, J. E. and Wang, J. C. (1993) On the coupling between ATP usage and DNA transport by yeast DNA topoisomerase II, *J. Biol. Chem. 268*, 8096-8104.

31. Wilstermann, A. M. and Osheroff, N. (2001) Positioning the 3'-DNA terminus for topoisomerase II-mediated religation, *J. Biol. Chem. 276*, 17727-17731.

32. Drake, F. H., Zimmerman, J. P., McCabe, F. L., Bartus, H. F., Per, S. R., et al. (1987) Purification of topoisomerase II from amsacrine-resistant P388 leukemia cells. Evidence for two forms of the enzyme, *J. Biol. Chem. 262*, 16739-16747.

33. Drake, F. H., Hofmann, G. A., Bartus, H. F., Mattern, M. R., Crooke, S. T., and Mirabelli, C. K. (1989) Biochemical and pharmacological properties of p170 and p180 forms of topoisomerase II, *Biochemistry 28*, 8154-8160.

34. Tsai-Pflugfelder, M., Liu, L. F., Liu, A. A., Tewey, K. M., Whang-Peng, J., Knutsen, T., Huebner, K., Croce, C. M., and Wang, J. C. (1988) Cloning and sequencing of cDNA encoding human DNA topoisomerase II and localization of the gene to chromosome region 17q21-22, *Proc. Natl. Acad. Sci. U. S. A. 85*, 7177-7181.

35. Jenkins, J. R., Ayton, P., Jones, T., Davies, S. L., Simmons, D. L., Harris, A. L., Sheer, D., and Hickson, I. D. (1992) Isolation of cDNA clones encoding the beta isozyme of human DNA topoisomerase II and localisation of the gene to chromosome 3p24, *Nucleic Acids Res. 20*, 5587-5592.

36. Austin, C. A. and Marsh, K. L. (1998) Eukaryotic DNA topoisomerase IIβ, *Bioessays 20*, 215-226.

37. Tan, K. B., Dorman, T. E., Falls, K. M., Chung, T. D., Mirabelli, C. K., Crooke, S. T., and Mao, J. (1992) Topoisomerase II alpha and topoisomerase II beta genes: characterization and mapping to human chromosomes 17 and 3, respectively, *Cancer Res. 52*, 231-234.

38. Wilstermann, A. M. and Osheroff, N. (2003) Stabilization of eukaryotic topoisomerase II-DNA cleavage complexes, *Curr. Top. Med. Chem. 3*, 1349-1364.

39. Pendleton, M., Lindsey, R. H., Jr., Felix, C. A., Grimwade, D., and Osheroff, N. (2014) Topoisomerase II and leukemia, *Ann. N. Y. Acad. Sci. 1310*, 98-110.

40. Gentry, A. C. (2013) DNA Topoisomerases: Type II, In *The Encyclopedia of Biological Chemistry* (Lennarz W.J., a. L. M. D., Ed.), pp 163-168, Academic Press, Waltham, MA.

41. Heck, M. M., Hittelman, W. N., and Earnshaw, W. C. (1988) Differential expression of DNA topoisomerases I and II during the eukaryotic cell cycle, *Proc. Natl. Acad. Sci. U. S. A. 85*, 1086-1090.

42. Woessner, R. D., Mattern, M. R., Mirabelli, C. K., Johnson, R. K., and Drake, F. H. (1991) Proliferation- and cell cycle-dependent differences in expression of the 170 kilodalton and 180 kilodalton forms of topoisomerase II in NIH-3T3 cells, *Cell Growth Differ. 2*, 209-214.

43. Kimura, K., Saijo, M., Ui, M., and Enomoto, T. (1994) Growth state- and cell cycle-dependent fluctuation in the expression of two forms of DNA topoisomerase II and possible specific modification of the higher molecular weight form in the M phase, *J. Biol. Chem. 269*, 1173-1176.

44. Grue, P., Grasser, A., Sehested, M., Jensen, P. B., Uhse, A., Straub, T., Ness, W., and Boege, F. (1998) Essential mitotic functions of DNA topoisomerase IIα are not adopted by topoisomerase IIβ in human H69 cells, *J. Biol. Chem. 273*, 33660-33666.

45. Christensen, M. O., Larsen, M. K., Barthelmes, H. U., Hock, R., Andersen, C. L., et al. (2002) Dynamics of human DNA topoisomerases IIα and IIβ in living cells, *J. Cell Biol. 157*, 31-44.

46. Ju, B. G., Lunyak, V. V., Perissi, V., Garcia-Bassets, I., Rose, D. W., Glass, C. K., and Rosenfeld, M. G. (2006) A topoisomerase IIβ-mediated dsDNA break required for regulated transcription, *Science 312*, 1798-1802.

47. Cowell, I. G., Sondka, Z., Smith, K., Lee, K. C., Manville, C. M., et al. (2012) Model for MLL translocations in therapy-related leukemia involving topoisomerase IIβ-mediated DNA strand breaks and gene proximity, *Proc. Natl. Acad. Sci. U. S. A. 109*, 8989-8994.

48. Levine, C., Hiasa, H., and Marians, K. J. (1998) DNA gyrase and topoisomerase IV: biochemical activities, physiological roles during chromosome replication, and drug sensitivities, *Biochim. Biophys. Acta 1400*, 29-43.

49. Sissi, C. and Palumbo, M. (2010) In front of and behind the replication fork: bacterial type IIA topoisomerases, *Cell. Mol. Life Sci. 67*, 2001-2024.

50. Anderson, V. E. and Osheroff, N. (2001) Type II topoisomerases as targets for quinolone antibacterials: turning Dr. Jekyll into Mr. Hyde, *Curr. Pharm. Des. 7*, 337-353.

51. Gellert, M., Mizuuchi, K., O'Dea, M. H., and Nash, H. A. (1976) DNA gyrase: an enzyme that introduces superhelical turns into DNA, *Proc. Natl. Acad. Sci. U. S. A. 73*, 3872-3876.

52. Corbett, K. D. and Berger, J. M. (2004) Structure, molecular mechanisms, and evolutionary relationships in DNA topoisomerases, *Annu. Rev. Biophys. Biomol. Struct. 33*, 95-118.

53. Bates, A. D., Berger, J. M., and Maxwell, A. (2011) The ancestral role of ATP hydrolysis in type II topoisomerases: prevention of DNA double-strand breaks, *Nucleic Acids Res. 39*, 6327-6339.

54. Morrison, A. and Cozzarelli, N. R. (1981) Contacts between DNA gyrase and its binding site on DNA: features of symmetry and asymmetry revealed by protection from nucleases, *Proc. Natl. Acad. Sci. U. S. A. 78*, 1416-1420.

55. Kato, J., Nishimura, Y., Imamura, R., Niki, H., Hiraga, S., and Suzuki, H. (1990) New topoisomerase essential for chromosome segregation in *E. coli*, *Cell 63*, 393-404.

56. Hiasa, H. and Marians, K. J. (1994) Topoisomerase IV can support oriC DNA replication *in vitro*, *J. Biol. Chem. 269*, 16371-16375.

57. Zechiedrich, E. L., Khodursky, A. B., Bachellier, S., Schneider, R., Chen, D., Lilley, D. M., and Cozzarelli, N. R. (2000) Roles of topoisomerases in maintaining steady-state DNA supercoiling in *Escherichia coli*, *J. Biol. Chem. 275*, 8103-8113.

58. Crisona, N. J., Strick, T. R., Bensimon, D., Croquette, V., and Cozzarelli, N. R. (2000) Preferential relaxation of positively supercoiled DNA by *E. coli* topoisomerase IV in single-molecule and ensemble measurements, *Genes Dev. 14*, 2881-2892.

59. Wang, X., Reyes-Lamothe, R., and Sherratt, D. J. (2008) Modulation of *Escherichia coli* sister chromosome cohesion by topoisomerase IV, *Genes Dev. 22*, 2426-2433.

60. Joshi, M. C., Magnan, D., Montminy, T. P., Lies, M., Stepankiw, N., and Bates, D. (2013) Regulation of sister chromosome cohesion by the replication fork tracking protein SeqA, *PLoS Genet 9*, e1003673.

61. Zawadzki, P., Stracy, M., Ginda, K., Zawadzka, K., Lesterlin, C., Kapanidis, A. N., and Sherratt, D. J. (2015) The localization and action of topoisomerase IV in *Escherichia coli* chromosome segregation is coordinated by the SMC complex, MukBEF, *Cell Rep 13*, 2587-2596.

62. Nitiss, J. L. (2009) Targeting DNA topoisomerase II in cancer chemotherapy, *Nat. Rev. Cancer 9*, 338-350.

63. Austin, C. A., Patel, S., Ono, K., Nakane, H., and Fisher, L. M. (1992) Site-specific DNA cleavage by mammalian DNA topoisomerase II induced by novel flavone and catechin derivatives, *Biochem. J. 282*, 883-889.

64. Bandele, O. J. and Osheroff, N. (2007) Bioflavonoids as poisons of human topoisomerase IIα and IIβ, *Biochemistry 46,* 6097-6108.

65. Lopez-Lazaro, M., Willmore, E., Jobson, A., Gilroy, K. L., Curtis, H., Padget, K., and Austin, C. A. (2007) Curcumin induces high levels of topoisomerase I- and II-DNA complexes in K562 leukemia cells, *J. Nat. Prod. 70,* 1884-1888.

66. Bandele, O. J. and Osheroff, N. (2008) (-)-Epigallocatechin gallate, a major constituent of green tea, poisons human type II topoisomerases, *Chem. Res. Toxicol. 21,* 936-943.

67. Bandele, O. J., Clawson, S. J., and Osheroff, N. (2008) Dietary polyphenols as topoisomerase II poisons: B ring and C ring substituents determine the mechanism of enzyme-mediated DNA cleavage enhancement, *Chem. Res. Toxicol. 21,* 1253-1260.

68. Drlica, K., Hiasa, H., Kerns, R., Malik, M., Mustaev, A., and Zhao, X. (2009) Quinolones: action and resistance updated, *Curr. Top. Med. Chem. 9,* 981-998.

69. Lopez-Lazaro, M., Willmore, E., and Austin, C. A. (2010) The dietary flavonoids myricetin and fisetin act as dual inhibitors of DNA topoisomerases I and II in cells, *Mutat. Res. 696,* 41-47.

70. Lin, R. K., Zhou, N., Lyu, Y. L., Tsai, Y. C., Lu, C. H., et al. (2011) Dietary isothiocyanate-induced apoptosis via thiol modification of DNA topoisomerase IIα, *J. Biol. Chem. 286,* 33591-33600.

71. Ketron, A. C., Gordon, O. N., Schneider, C., and Osheroff, N. (2013) Oxidative metabolites of curcumin poison human type II topoisomerases, *Biochemistry 52,* 221-227.

72. Timmel, M. A., Byl, J. A., and Osheroff, N. (2013) Epimerization of green tea catechins during brewing does not affect the ability to poison human type II topoisomerases, *Chem. Res. Toxicol. 26,* 622-628.

73. Aldred, K. J., Kerns, R. J., and Osheroff, N. (2014) Mechanism of quinolone action and resistance, *Biochemistry 53,* 1565-1574.

74. Ketron, A. C. and Osheroff, N. (2014) Phytochemicals as anticancer and chemopreventive topoisomerase II poisons, *Phytochem. Rev. 13,* 19-35.

75. Vann, K. R., Sedgeman, C. A., Gopas, J., Golan-Goldhirsh, A., and Osheroff, N. (2015) Effects of olive metabolites on DNA cleavage mediated by human type II topoisomerases, *Biochemistry 54,* 4531-4541.

76. Hooper, D. C. and Jacoby, G. A. (2015) Mechanisms of drug resistance: quinolone resistance, *Ann. N. Y. Acad. Sci. 1354,* 12-31.

77. Bender, R. P. a. O., N. (2008) Treatment of cancer, In *Checkpoint Responses in Cancer Therapy*, pp 57-91, Humana Press, Totowa, NJ.

78. D'Arpa, P., Beardmore, C., and Liu, L. F. (1990) Involvement of nucleic acid synthesis in cell killing mechanisms of topoisomerase poisons, *Cancer Res. 50*, 6919-6924.

79. Baguley, B. C. and Ferguson, L. R. (1998) Mutagenic properties of topoisomerase-targeted drugs, *Biochim. Biophys. Acta 1400*, 213-222.

80. Felix, C. A., Kolaris, C. P., and Osheroff, N. (2006) Topoisomerase II and the etiology of chromosomal translocations, *DNA Repair (Amst.) 5*, 1093-1108.

81. Kaufmann, S. H. (1998) Cell death induced by topoisomerase-targeted drugs: more questions than answers, *Biochim. Biophys. Acta 1400*, 195-211.

82. Bender, R. P., Jablonksy, M. J., Shadid, M., Romaine, I., Dunlap, N., Anklin, C., Graves, D. E., and Osheroff, N. (2008) Substituents on etoposide that interact with human topoisomerase IIα in the binary enzyme-drug complex: contributions to etoposide binding and activity, *Biochemistry 47*, 4501-4509.

83. Pommier, Y. and Marchand, C. (2012) Interfacial inhibitors: targeting macromolecular complexes, *Nat. Rev. Drug Discov. 11*, 25-36.

84. Lindsey, R. H., Bender, R. P., and Osheroff, N. (2005) Stimulation of topoisomerase II-mediated DNA cleavage by benzene metabolites, *Chem. Biol. Interact. 153-154*, 197-205.

85. Bender, R. P., Ham, A. J., and Osheroff, N. (2007) Quinone-induced enhancement of DNA cleavage by human topoisomerase IIα: adduction of cysteine residues 392 and 405, *Biochemistry 46*, 2856-2864.

86. Bender, R. P. and Osheroff, N. (2007) Mutation of cysteine residue 455 to alanine in human topoisomerase IIα confers hypersensitivity to quinones: enhancing DNA scission by closing the N-terminal protein gate, *Chem. Res. Toxicol. 20*, 975-981.

87. Lindsey, R. H., Jr., Bromberg, K. D., Felix, C. A., and Osheroff, N. (2004) 1,4-Benzoquinone is a topoisomerase II poison, *Biochemistry 43*, 7563-7574.

88. Wang, H., Mao, Y., Chen, A. Y., Zhou, N., LaVoie, E. J., and Liu, L. F. (2001) Stimulation of topoisomerase II-mediated DNA damage *via* a mechanism involving protein thiolation, *Biochemistry 40*, 3316-3323.

89. Bender, R. P., Lehmler, H. J., Robertson, L. W., Ludewig, G., and Osheroff, N. (2006) Polychlorinated biphenyl quinone metabolites poison human topoisomerase IIα: altering enzyme function by blocking the N-terminal protein gate, *Biochemistry 45*, 10140-10152.

90. Mondrala, S. and Eastmond, D. A. (2010) Topoisomerase II inhibition by the bioactivated benzene metabolite hydroquinone involves multiple mechanisms, *Chem. Biol. Interact. 184*, 259-268.

91. Hooper, D. C. (1998) Clinical applications of quinolones, *Biochim. Biophys. Acta 1400*, 45-61.

92. Hooper, D. C. (2001) Mechanisms of action of antimicrobials: focus on fluoroquinolones, *Clin. Infect. Dis. 32 Suppl. 1*, S9-S15.

93. Linder, J. A., Huang, E. S., Steinman, M. A., Gonzales, R., and Stafford, R. S. (2005) Fluoroquinolone prescribing in the United States: 1995 to 2002, *Am. J. Med. 118*, 259-268.

94. Andriole, V. T. (2005) The quinolones: past, present, and future, *Clin. Infect. Dis. 41 Suppl. 2*, S113-119.

95. Hooper, D. C. (1999) Mode of action of fluoroquinolones, *Drugs 58 Suppl. 2*, 6-10.

96. Drlica, K., Malik, M., Kerns, R. J., and Zhao, X. (2008) Quinolone-mediated bacterial death, *Antimicrob. Agents Chemother. 52*, 385-392.

97. Laponogov, I., Sohi, M. K., Veselkov, D. A., Pan, X. S., Sawhney, R., Thompson, A. W., McAuley, K. E., Fisher, L. M., and Sanderson, M. R. (2009) Structural insight into the quinolone-DNA cleavage complex of type IIA topoisomerases, *Nat. Struct. Mol. Biol. 16*, 667-669.

98. Laponogov, I., Pan, X. S., Veselkov, D. A., McAuley, K. E., Fisher, L. M., and Sanderson, M. R. (2010) Structural basis of gate-DNA breakage and resealing by type II topoisomerases, *PLoS One 5*, e11338.

99. Bax, B. D., Chan, P. F., Eggleston, D. S., Fosberry, A., Gentry, D. R., et al. (2010) Type IIA topoisomerase inhibition by a new class of antibacterial agents, *Nature 466*, 935-940.

100. Wohlkonig, A., Chan, P. F., Fosberry, A. P., Homes, P., Huang, J., et al. (2010) Structural basis of quinolone inhibition of type IIA topoisomerases and target-mediated resistance, *Nat. Struct. Mol. Biol. 17*, 1152-1153.

101. Khodursky, A. B., Zechiedrich, E. L., and Cozzarelli, N. R. (1995) Topoisomerase IV is a target of quinolones in *Escherichia coli*, *Proc. Natl. Acad. Sci. U. S. A. 92*, 11801-11805.

102. Aedo, S. and Tse-Dinh, Y.-C. (2012) Isolation and quantitation of topoisomerase complexes accumulated on *Escherichia coli* chromosomal DNA, *Antimicrob. Agents Chemother. 56*, 5458-5464.

103. Pan, X.-S. and Fisher, L. M. (1997) Targeting of DNA gyrase in *Streptococcus pneumoniae* by sparfloxacin: selective targeting of gyrase or topoisomerase IV by quinolones, *Antimicrob. Agents Chemother. 41*, 471-474.

104. Pan, X.-S. and Fisher, L. M. (1999) *Streptococcus pneumoniae* DNA gyrase and topoisomerase IV: overexpression, purification, and differential inhibition by fluoroquinolones, *Antimicrob. Agents Chemother. 43*, 1129-1136.

105. Pan, X.-S., Ambler, J., Mehtar, S., and Fisher, L. M. (1996) Involvement of topoisomerase IV and DNA gyrase as ciprofloxacin targets in *Streptococcus pneumoniae, Antimicrob. Agents Chemother. 40*, 2321-2326.

106. Fournier, B., Zhao, X., Lu, T., Drlica, K., and Hooper, D. C. (2000) Selective targeting of topoisomerase IV and DNA gyrase in *Staphylococcus aureus*: different patterns of quinolone-induced inhibition of DNA synthesis, *Antimicrob. Agents Chemother. 44*, 2160-2165.

107. Brook, I., Elliott, T. B., Pryor, H. I., 2nd, Sautter, T. E., Gnade, B. T., Thakar, J. H., and Knudson, G. B. (2001) *In vitro* resistance of *Bacillus anthracis* Sterne to doxycycline, macrolides and quinolones, *Int. J. Antimicrob. Agents 18*, 559-562.

108. Price, L. B., Vogler, A., Pearson, T., Busch, J. D., Schupp, J. M., and Keim, P. (2003) *In vitro* selection and characterization of *Bacillus anthracis* mutants with high-level resistance to ciprofloxacin, *Antimicrob. Agents Chemother. 47*, 2362-2365.

109. Grohs, P., Podglajen, I., and Gutmann, L. (2004) Activities of different fluoroquinolones against *Bacillus anthracis* mutants selected *in vitro* and harboring topoisomerase mutations, *Antimicrob. Agents Chemother. 48*, 3024-3027.

110. Morgan-Linnell, S. K., Becnel Boyd, L., Steffen, D., and Zechiedrich, L. (2009) Mechanisms accounting for fluoroquinolone resistance in *Escherichia coli* clinical isolates, *Antimicrob. Agents Chemother. 53*, 235-241.

111. Bast, D. J., Athamna, A., Duncan, C. L., de Azavedo, J. C., Low, D. E., Rahav, G., Farrell, D., and Rubinstein, E. (2004) Type II topoisomerase mutations in *Bacillus anthracis* associated with high-level fluoroquinolone resistance, *J. Antimicrob. Chemother. 54*, 90-94.

112. Drlica, K. and Zhao, X. (1997) DNA gyrase, topoisomerase IV, and the 4-quinolones, *Microbiol. Mol. Biol. Rev. 61*, 377-392.

113. Yoshida, H., Kojima, T., Yamagishi, J., and Nakamura, S. (1988) Quinolone-resistant mutations of the gyrA gene of *Escherichia coli*, *Mol. Gen. Genet. 211*, 1-7.

114. Cullen, M. E., Wyke, A. W., Kuroda, R., and Fisher, L. M. (1989) Cloning and characterization of a DNA gyrase A gene from *Escherichia coli* that confers clinical resistance to 4-quinolones, *Antimicrob. Agents Chemother. 33*, 886-894.

115. Li, Z., Deguchi, T., Yasuda, M., Kawamura, T., Kanematsu, E., Nishino, Y., Ishihara, S., and Kawada, Y. (1998) Alteration in the GyrA subunit of DNA gyrase and the ParC subunit of DNA topoisomerase IV in quinolone-resistant clinical isolates of *Staphylococcus epidermidis*, *Antimicrob. Agents Chemother. 42*, 3293-3295.

116. Aldred, K. J., McPherson, S. A., Wang, P., Kerns, R. J., Graves, D. E., Turnbough, C. L., and Osheroff, N. (2012) Drug interactions with *Bacillus anthracis* topoisomerase IV: biochemical basis for quinolone action and resistance, *Biochemistry 51*, 370-381.

117. Aldred, K. J., McPherson, S. A., Turnbough, C. L., Kerns, R. J., and Osheroff, N. (2013) Topoisomerase IV-quinolone interactions are mediated through a water-metal ion bridge: mechanistic basis of quinolone resistance, *Nucleic Acids Res. 41*, 4628-4639.

118. Aldred, K. J., Breland, E. J., Vlckova, V., Strub, M. P., Neuman, K. C., Kerns, R. J., and Osheroff, N. (2014) Role of the water-metal ion bridge in mediating interactions between quinolones and *Escherichia coli* topoisomerase IV, *Biochemistry 53*, 5558-5567.

119. Aldred, K. J., Blower, T. R., Kerns, R. J., Berger, J. M., and Osheroff, N. (2016) Fluoroquinolone interactions with *Mycobacterium tuberculosis* gyrase: enhancing drug activity against wild-type and resistant gyrase, *Proc. Natl. Acad. Sci. U. S. A. 113*, E839-E846.

120. Blower, T. R., Williamson, B. H., Kerns, R. J., and Berger, J. M. (2016) Crystal structure and stability of gyrase-fluoroquinolone cleaved complexes from *Mycobacterium tuberculosis*, *Proc. Natl. Acad. Sci. U. S. A. 113*, 1706-1713.

121. Ashley, R. E. and Osheroff, N. (2014) Natural products as topoisomerase II poisons: effects of thymoquinone on DNA cleavage mediated by human topoisomerase IIα, *Chem. Res. Toxicol. 27*, 787-793.

122. Dunlap, N., Salyard, T. L., Pathiranage, A. L., Stubblefield, J., Pitts, S. L., Ashley, R. E., and Osheroff, N. (2014) Synthesis and evaluation of ether-linked demethylepipodophyllotoxin dimers, *Bioorg. Med. Chem. Lett. 24*, 5627-5629.

123. Gordon, O. N., Luis, P. B., Ashley, R. E., Osheroff, N., and Schneider, C. (2015) Oxidative transformation of demethoxy- and bisdemethoxycurcumin: products, mechanism of formation, and poisoning of human topoisomerase IIalpha, *Chem. Res. Toxicol. 28*, 989-996.

124. Lindsey, R. H., Jr., Pendleton, M., Ashley, R. E., Mercer, S. L., Deweese, J. E., and Osheroff, N. (2014) Catalytic core of human topoisomerase IIα: insights into enzyme-DNA interactions and drug mechanism, *Biochemistry 53*, 6595-65602.

125. McClendon, A. K., Rodriguez, A. C., and Osheroff, N. (2005) Human topoisomerase IIα rapidly relaxes positively supercoiled DNA: implications for enzyme action ahead of replication forks, *J. Biol. Chem. 280*, 39337-39345.

126. Rodriguez, A. C. (2002) Studies of a positive supercoiling machine: nucleotide hydrolysis and a multifunctional "latch" in the mechanism of reverse gyrase, *J. Biol. Chem. 277*, 29865-29873.

127. Kingma, P. S., Greider, C. A., and Osheroff, N. (1997) Spontaneous DNA lesions poison human topoisomerase IIα and stimulate cleavage proximal to leukemic 11q23 chromosomal breakpoints, *Biochemistry 36*, 5934-5939.

128. Worland, S. T. and Wang, J. C. (1989) Inducible overexpression, purification, and active site mapping of DNA topoisomerase II from the yeast *Saccharomyces cerevisiae*, *J. Biol. Chem. 264*, 4412-4416.

129. Dickey, J. S. and Osheroff, N. (2005) Impact of the C-terminal domain of topoisomerase IIα on the DNA cleavage activity of the human enzyme, *Biochemistry 44*, 11546-11554.

130. Wendorff, T. J., Schmidt, B. H., Heslop, P., Austin, C. A., and Berger, J. M. (2012) The structure of DNA-bound human topoisomerase IIα: conformational mechanisms for coordinating inter-subunit interactions with DNA cleavage, *J. Mol. Biol. 424*, 109-124.

131. Biersack, H., Jensen, S., Gromova, I., Nielsen, I., Westergaard, O., and Andersen, A. (1996) Active heterodimers are formed from human DNA topoisomerase IIα and IIβ isoforms, *Proc. Natl. Acad. Sci. U. S. A. 93*, 8288-8293.

132. Oestergaard, V. H., Bjergbaek, L., Skouboe, C., Giangiacomo, L., Knudsen, B. R., and Andersen, A. H. (2004) The transducer domain is important for clamp operation in human DNA topoisomerase IIα, *J. Biol. Chem. 279*, 1684-1691.

133. Nemec, J. (1986) Epipodophyllotoxinquinone glucoside derivatives, method of production and use, Google Patents.

134. Lovett, B. D., Strumberg, D., Blair, I. A., Pang, S., Burden, D. A., et al. (2001) Etoposide metabolites enhance DNA topoisomerase II cleavage near leukemia-associated MLL translocation breakpoints, *Biochemistry 40*, 1159-1170.

135. Jacob, D. A., Mercer, S. L., Osheroff, N., and Deweese, J. E. (2011) Etoposide quinone is a redox-dependent topoisomerase II poison, *Biochemistry 50*, 5660-5667.

136. Fortune, J. M. and Osheroff, N. (1998) Merbarone inhibits the catalytic activity of human topoisomerase IIα by blocking DNA cleavage, *J. Biol. Chem. 273*, 17643-17650.

137. Byl, J. A., Fortune, J. M., Burden, D. A., Nitiss, J. L., Utsugi, T., Yamada, Y., and Osheroff, N. (1999) DNA topoisomerases as targets for the anticancer drug TAS-103: primary cellular target and DNA cleavage enhancement, *Biochemistry 38*, 15573-15579.

138. Gentry, A. C., Pitts, S. L., Jablonsky, M. J., Bailly, C., Graves, D. E., and Osheroff, N. (2011) Interactions between the etoposide derivative F14512 and human type II topoisomerases: implications for the C4 spermine moiety in promoting enzyme-mediated DNA cleavage, *Biochemistry 50*, 3240-3249.

139. Dong, S., McPherson, S. A., Wang, Y., Li, M., Wang, P., Turnbough, C. L., Jr., and Pritchard, D. G. (2010) Characterization of the enzymes encoded by the anthrose biosynthetic operon of *Bacillus anthracis*, *J. Bacteriol. 192*, 5053-5062.

140. Hardin, A. H., Sarkar, S. K., Seol, Y., Liou, G. F., Osheroff, N., and Neuman, K. C. (2011) Direct measurement of DNA bending by type IIA topoisomerases: implications for non-equilibrium topology simplification, *Nucleic Acids Res. 39*, 5729-5743.

141. Corbett, K. D., Schoeffler, A. J., Thomsen, N. D., and Berger, J. M. (2005) The structural basis for substrate specificity in DNA topoisomerase IV, *J. Mol. Biol. 351*, 545-561.

142. Aldred, K. J., Schwanz, H. A., Li, G., McPherson, S. A., Turnbough, C. L., Kerns, R. J., and Osheroff, N. (2013) Overcoming target-mediated quinolone resistance in topoisomerase IV by introducing metal-ion-independent drug–enzyme interactions, *ACS Chem. Biol.*, 2660-2668.

143. Seol, Y. and Neuman, K. C. (2011) Single-molecule measurements of topoisomerase activity with magnetic tweezers, *Methods Mol. Biol. 778*, 229-241.

144. Ribeck, N. and Saleh, O. A. (2008) Multiplexed single-molecule measurements with magnetic tweezers, *Rev. Sci. Instrum. 79*, 094301.

145. Strick, T. R., Allemand, J. F., Bensimon, D., and Croquette, V. (1998) Behavior of supercoiled DNA, *Biophys. J. 74*, 2016-2028.

146. Gali-Muhtasib, H., Roessner, A., and Schneider-Stock, R. (2006) Thymoquinone: a promising anti-cancer drug from natural sources, *Int. J. Biochem. Cell Biol. 38*, 1249-1253.

147. Burits, M. and Bucar, F. (2000) Antioxidant activity of *Nigella sativa* essential oil, *Phytother. Res. 14*, 323-328.

148. Hajhashemi, V., Ghannadi, A., and Jafarabadi, H. (2004) Black cumin seed essential oil, as a potent analgesic and antiinflammatory drug, *Phytother. Res. 18*, 195-199.

149. Zohary, D. and Hopf, M. (2000) *Domestication of plants in the old world: the origin and spread of cultivated plants in West Asia, Europe, and the Nile Valley*, 3rd ed., Oxford University Press, Oxford New York.

150. Badary, O. A., Taha, R. A., Gamal el-Din, A. M., and Abdel-Wahab, M. H. (2003) Thymoquinone is a potent superoxide anion scavenger, *Drug Chem. Toxicol. 26*, 87-98.

151. Sayed, M. D. (1980) Traditional medicine in health care, *J. Ethnopharmacol. 2*, 19-22.

152. Khader, M., Bresgen, N., and Eckl, P. M. (2009) *In vitro* toxicological properties of thymoquinone, *Food Chem. Toxicol. 47*, 129-133.

153. Salomi, M. J., Nair, S. C., and Panikkar, K. R. (1991) Inhibitory effects of *Nigella sativa* and saffron (*Crocus sativus*) on chemical carcinogenesis in mice, *Nutr. Cancer 16*, 67-72.

154. Swamy, S. M. and Tan, B. K. (2000) Cytotoxic and immunopotentiating effects of ethanolic extract of *Nigella sativa* L. seeds, *J. Ethnopharmacol. 70*, 1-7.

155. Mabrouk, G. M., Moselhy, S. S., Zohny, S. F., Ali, E. M., Helal, T. E., Amin, A. A., and Khalifa, A. A. (2002) Inhibition of methylnitrosourea (MNU) induced oxidative stress and carcinogenesis by orally administered bee honey and *Nigella* grains in Sprague Dawely rats, *J. Exp. Clin. Cancer Res. 21*, 341-346.

156. Farah, I. O. (2005) Assessment of cellular responses to oxidative stress using MCF-7 breast cancer cells, black seed (*N. sativa* L.) extracts and H2O2, *Int. J. Environ. Res. Public Health 2*, 411-419.

157. Farah, I. O. and Begum, R. A. (2003) Effect of *Nigella sativa* (*N. sativa* L.) and oxidative stress on the survival pattern of MCF-7 breast cancer cells, *Biomed. Sci. Instrum. 39*, 359-364.

158. Hasan, T. N., Shafi, G., Syed, N. A., Alfawaz, M. A., Alsaif, M. A., Munshi, A., Lei, K. Y., and Alshatwi, A. A. (2013) Methanolic extract of *Nigella sativa* seed inhibits SiHa human cervical cancer cell proliferation through apoptosis, *Nat. Prod. Commun. 8*, 213-216.

159. Woo, C. C., Kumar, A. P., Sethi, G., and Tan, K. H. (2012) Thymoquinone: potential cure for inflammatory disorders and cancer, *Biochem. Pharmacol. 83*, 443-451.

160. Badary, O. A., Al-Shabanah, O. A., Nagi, M. N., Al-Rikabi, A. C., and Elmazar, M. M. (1999) Inhibition of benzo(a)pyrene-induced forestomach carcinogenesis in mice by thymoquinone, *Eur. J. Cancer Prev. 8*, 435-440.

161. Badary, O. A. and Gamal El-Din, A. M. (2001) Inhibitory effects of thymoquinone against 20-methylcholanthrene-induced fibrosarcoma tumorigenesis, *Cancer Detect. Prev. 25*, 362-368.

162. Banerjee, S., Padhye, S., Azmi, A., Wang, Z., Philip, P. A., Kucuk, O., Sarkar, F. H., and Mohammad, R. M. (2010) Review on molecular and therapeutic potential of thymoquinone in cancer, *Nutr. Cancer 62*, 938-946.

163. Osheroff, N., Shelton, E. R., and Brutlag, D. L. (1983) DNA topoisomerase II from *Drosophila melanogaster*. Relaxation of supercoiled DNA, *J. Biol. Chem. 258*, 9536-9543.

164. Bender, R. P., Lindsey, R. H., Jr., Burden, D. A., and Osheroff, N. (2004) N-acetyl-*p*-benzoquinone imine, the toxic metabolite of acetaminophen, is a topoisomerase II poison, *Biochemistry 43*, 3731-3739.

165. Schmidt, B. H., Osheroff, N., and Berger, J. M. (2012) Structure of a topoisomerase II-DNA-nucleotide complex reveals a new control mechanism for ATPase activity, *Nat. Struct. Mol. Biol. 19*, 1147-1154.

166. McClendon, A. K., Gentry, A. C., Dickey, J. S., Brinch, M., Bendsen, S., Andersen, A. H., and Osheroff, N. (2008) Bimodal recognition of DNA geometry by human topoisomerase IIα: preferential relaxation of positively supercoiled DNA requires elements in the C-terminal domain, *Biochemistry 47*, 13169-13178.

167. Wu, C. C., Li, T. K., Farh, L., Lin, L. Y., Lin, T. S., Yu, Y. J., Yen, T. J., Chiang, C. W., and Chan, N. L. (2011) Structural basis of type II topoisomerase inhibition by the anticancer drug etoposide, *Science 333*, 459-462.

168. Ezoe, S. (2012) Secondary leukemia associated with the anti-cancer agent, etoposide, a topoisomerase II inhibitor, *Int. J. Environ. Res. Public Health 9*, 2444-2453.

169. van Maanen, J. M. S., Retl, J., de Vries, J., and Pinedo, H. M. (1988) Mechanism of action of antitumor drug etoposide: a review, *J. Natl. Cancer Instit. 80*, 1526-1533.

170. Felix, C. A., Walker, A. H., Lange, B. J., Williams, T. M., Winick, N. J., et al. (1998) Association of CYP3A4 genotype with treatment-related leukemia, *Proc. Natl. Acad. Sci. U. S. A. 95*, 13176-13181.

171. Jacob, D. A., Gibson, E. G., Mercer, S. L., and Deweese, J. E. (2013) Etoposide catechol is an oxidizable topoisomerase II poison, *Chem. Res. Toxicol. 26*, 1156-1158.

172. Smith, N. A., Byl, J. A., Mercer, S. L., Deweese, J. E., and Osheroff, N. (2014) Etoposide quinone is a covalent poison of human topoisomerase IIβ, *Biochemistry 53*, 3229-3236.

173. Wilstermann, A. M., Bender, R. P., Godfrey, M., Choi, S., Anklin, C., Berkowitz, D. B., Osheroff, N., and Graves, D. E. (2007) Topoisomerase II - drug interaction domains: identification of substituents on etoposide that interact with the enzyme, *Biochemistry 46*, 8217-8225.

174. Long, B. H. (1987) Structure-activity relationships of podophyllin congeners that inhibit topoisomerase II, *NCI Monogr.*, 123-127.

175. Sinha, B. K., Politi, P. M., Eliot, H. M., Kerrigan, D., and Pommier, Y. (1990) Structure-activity relations, cytotoxicity and topoisomerase II dependent cleavage induced by pendulum ring analogues of etoposide, *Eur. J. Cancer 26*, 590-593.

176. Basu, A., Parente, A. C., and Bryant, Z. (2016) Structural dynamics and mechanochemical coupling in DNA gyrase, *J. Mol. Biol. 428*, 1833-1845.

177. Kampranis, S. C. and Maxwell, A. (1996) Conversion of DNA gyrase into a conventional type II topoisomerase, *Proc. Natl. Acad. Sci. U. S. A. 93*, 14416-144121.

178. Kramlinger, V. M. and Hiasa, H. (2006) The "GyrA-box" is required for the ability of DNA gyrase to wrap DNA and catalyze the supercoiling reaction, *J. Biol. Chem. 281*, 3738-3742.

179. Liu, L. F. and Wang, J. C. (1978) *Micrococcus luteus* DNA gyrase: active components and a model for its supercoiling of DNA, *Proc. Natl. Acad. Sci. U. S. A. 75*, 2098-2102.

180. Liu, L. F. and Wang, J. C. (1978) DNA-DNA gyrase complex: the wrapping of the DNA duplex outside the enzyme, *Cell 15*, 979-984.

181. Reece, R. J. and Maxwell, A. (1991) The C-terminal domain of the *Escherichia coli* DNA gyrase A subunit is a DNA-binding protein, *Nucleic Acids Res. 19*, 1399-1405.

182. Ullsperger, C. and Cozzarelli, N. R. (1996) Contrasting enzymatic acitivites of topoisomerase IV and DNA gyrase from *Escherichia coli*, *J. Biol. Chem. 271*, 31549-31555.

183. Marians, K. J. (1987) DNA gyrase-catalyzed decatenation of multiply linked DNA dimers, *J. Biol. Chem. 262*, 10362-10368.

184. Brown, P. O. and Cozzarelli, N. R. (1979) A sign inversion mechanism for enzymatic supercoiling of DNA, *Science 206*, 1081-1083.

185. Hsu, Y. H., Chung, M. W., and Li, T. K. (2006) Distribution of gyrase and topoisomerase IV on bacterial nucleoid: implications for nucleoid organization, *Nucleic Acids Res. 34*, 3128-3138.

186. Khodursky, A. B., Peter, B. J., Schmid, M. B., DeRisi, J., Botstein, D., Brown, P. O., and Cozzarelli, N. R. (2000) Analysis of topoisomerase function in bacterial replication fork movement: use of DNA microarrays, *Proc. Natl. Acad. Sci. U. S. A. 97*, 9419-9424.

187. Tadesse, S. and Graumann, P. L. (2006) Differential and dynamic localization of topoisomerases in *Bacillus subtilis*, *J. Bacteriol. 188*, 3002-3011.

188. McClendon, A. K. and Osheroff, N. (2006) The geometry of DNA supercoils modulates topoisomerase-mediated DNA cleavage and enzyme response to anticancer drugs, *Biochemistry 45*, 3040-3050.

189. Liu, L. F. and D'Arpa, P. (1992) Topoisomerase-targeting antitumor drugs: mechanisms of cytotoxicity and resistance, *Important Adv. Oncol.*, 79-89.

190. Li, T. K. and Liu, L. F. (2001) Tumor cell death induced by topoisomerase-targeting drugs, *Annu. Rev. Pharmacol. Toxicol. 41*, 53-77.

191. Higgins, N. P., Peebles, C. L., Sugino, A., and Cozzarelli, N. R. (1978) Purification of subunits of *Escherichia coli* DNA gyrase and reconstitution of enzymatic activity, *Proc. Natl. Acad. Sci. U. S. A. 75*, 1773-1777.

192. Mizuuchi, K., O'Dea, M. H., and Gellert, M. (1978) DNA gyrase: subunit structure and ATPase activity of the purified enzyme, *Proc. Natl. Acad. Sci. U. S. A. 75*, 5960-5963.

193. Kampranis, S. C., Bates, A. D., and Maxwell, A. (1999) A model for the mechanism of strand passage by DNA gyrase, *Proc. Natl. Acad. Sci. U. S. A. 96*, 8414-8419.

194. Gore, J., Bryant, Z., Stone, M. D., Nollmann, M., Cozzarelli, N. R., and Bustamante, C. (2006) Mechanochemical analysis of DNA gyrase using rotor bead tracking, *Nature 439*, 100-104.

195. Nollmann, M., Stone, M. D., Bryant, Z., Gore, J., Crisona, N. J., et al. (2007) Multiple modes of *Escherichia coli* DNA gyrase activity revealed by force and torque, *Nat. Struct. Mol. Biol. 14*, 264-271.

196. Papillon, J., Menetret, J. F., Batisse, C., Helye, R., Schultz, P., Potier, N., and Lamour, V. (2013) Structural insight into negative DNA supercoiling by DNA gyrase, a bacterial type 2A DNA topoisomerase, *Nucleic Acids Res. 41*, 7815-7827.

197. Gubaev, A. and Klostermeier, D. (2014) The mechanism of negative DNA supercoiling: a cascade of DNA-induced conformational changes prepares gyrase for strand passage, *DNA Repair (Amst) 16*, 23-34.

198. Liu, B., Baskin, R. J., and Kowalczykowski, S. C. (2013) DNA unwinding heterogeneity by RecBCD results from static molecules able to equilibrate, *Nature 500*, 482-485.

199. McCarthy, D., Minner, C., Bernstein, H., and Bernstein, C. (1976) DNA elongation rates and growing point distributions of wild-type phage T4 and a DNA-delay amber mutant, *J. Mol. Biol. 106*, 963-981.

200. Seol, Y., Gentry, A. C., Osheroff, N., and Neuman, K. C. (2013) Chiral discrimination and writhe-dependent relaxation mechanism of human topoisomerase IIα, *J. Biol. Chem. 288*, 13695-13703.

201. Neuman, K. C., Charvin, G., Bensimon, D., and Croquette, V. (2009) Mechanisms of chiral discrimination by topoisomerase IV, *Proc. Natl. Acad. Sci. U. S. A. 106*, 6986-6991.

202. McClendon, A. K., Dickey, J. S., and Osheroff, N. (2006) Ability of viral topoisomerase II to discern the handedness of supercoiled DNA: bimodal recognition of DNA geometry by type II enzymes, *Biochemistry 45*, 11674-11680.

203. Stone, M. D., Bryant, Z., Crisona, N. J., Smith, S. B., Vologodskii, A., Bustamante, C., and Cozzarelli, N. R. (2003) Chirality sensing by *Escherichia coli* topoisomerase IV and the mechanism of type II topoisomerases, *Proc. Natl. Acad. Sci. U. S. A. 100*, 8654-8659.

204. Schvartzman, J. B. and Stasiak, A. (2004) A topological view of the replicon, *EMBO Rep. 5*, 256-261.

205. Liu, L. F. and Wang, J. C. (1987) Supercoiling of the DNA template during transcription, *Proc. Natl. Acad. Sci. U. S. A. 84*, 7024-7027.

206. Wu, H. Y., Shyy, S. H., Wang, J. C., and Liu, L. F. (1988) Transcription generates positively and negatively supercoiled domains in the template, *Cell 53*, 433-440.

207. Peter, B. J., Ullsperger, C., Hiasa, H., Marians, K. J., and Cozzarelli, N. R. (1998) The structure of supercoiled intermediates in DNA replication, *Cell 94*, 819-827.

208. Fraser, C. M., Norris, S. J., Weinstock, G. M., White, O., Sutton, G. G., et al. (1998) Complete genome sequence of *Treponema pallidum*, the syphilis spirochete, *Science 281*, 375-388.

209. Tomb, J. F., White, O., Kerlavage, A. R., Clayton, R. A., Sutton, G. G., et al. (1997) The complete genome sequence of the gastric pathogen *Helicobacter pylori*, *Nature 388*, 539-547.

210. Parkhill, J., Wren, B. W., Mungall, K., Ketley, J. M., Churcher, C., et al. (2000) The genome sequence of the food-borne pathogen *Campylobacter jejuni* reveals hypervariable sequences, *Nature 403*, 665-668.

211. Cole, S. T., Eiglmeier, K., Parkhill, J., James, K. D., Thomson, N. R., et al. (2001) Massive gene decay in the leprosy bacillus, *Nature 409*, 1007-1011.

212. Cole, S. T., Brosch, R., Parkhill, J., Garnier, T., Churcher, C., et al. (1998) Deciphering the biology of *Mycobacterium tuberculosis* from the complete genome sequence, *Nature 393*, 537-544.

213. WHO. (2016) Global tuberculosis report 2016.

214. Aubry, A., Fisher, L. M., Jarlier, V., and Cambau, E. (2006) First functional characterization of a singly expressed bacterial type II topoisomerase: the enzyme from *Mycobacterium tuberculosis*, *Biochem. Biophys. Res. Commun. 348*, 158-165.

215. Tretter, E. M. and Berger, J. M. (2012) Mechanisms for defining supercoiling set point of DNA gyrase orthologs: II. The shape of the GyrA subunit C-terminal domain (CTD) is not a sole determinant for controlling supercoiling efficiency, *J. Biol. Chem. 287*, 18645-18654.

216. Bouige, A., Darmon, A., Piton, J., Roue, M., Petrella, S., Capton, E., Forterre, P., Aubry, A., and Mayer, C. (2013) *Mycobacterium tuberculosis* DNA gyrase possesses two functional GyrA-boxes, *Biochem. J. 455*, 285-294.

217. Drlica, K., Mustaev, A., Towle, T. R., Luan, G., Kerns, R. J., and Berger, J. M. (2014) Bypassing fluoroquinolone resistance with quinazolinediones: studies of drug-gyrase-DNA complexes having implications for drug design, *ACS Chem. Biol. 9*, 2895-2904.

218. Bossi, P., Tegnell, A., Baka, A., Van Loock, F., Hendriks, J., Werner, A., Maidhof, H., and Gouvras, G. (2004) Bichat guidelines for the clinical management of anthrax and bioterrorism-related anthrax, *Eurosurveillance 9*, 1-7.

219. Waterer, G. W. and Robertson, H. (2009) Bioterrorism for the respiratory physician, *Respirology 14*, 5-11.

220. Harvey, A. L. (2008) Natural products in drug discovery, *Drug Discov. Today 13*, 894-901.

221. Newman, D. J. and Cragg, G. M. (2012) Natural products as sources of new drugs over the 30 years from 1981 to 2010, *J. Nat. Prod. 75*, 311-335.

222. Cragg, G. M. and Newman, D. J. (2013) Natural products: a continuing source of novel drug leads, *Biochim. Biophys. Acta 1830*, 3670-3695.

223. Fangman, W. L. and Brewer, B. J. (1992) A question of time: replication origins of eukaryotic chromosomes, *Cell 71*, 363-366.

224. Maxwell, A. and Gellert, M. (1984) The DNA dependence of the ATPase activity of DNA gyrase, *J. Biol. Chem. 259*, 14472-14480.

225. Westerhoff, H. V., O'Dea, M. H., Maxwell, A., and Gellert, M. (1988) DNA supercoiling by DNA gyrase, *Cell Biophys. 12*, 157-181.

226. Reece, R. J. and Maxwell, A. (1991) Probing the limits of the DNA breakage-reunion domain of the *Escherichia coli* DNA gyrase A protein, *J. Biol. Chem. 266*, 3540-3546.

227. Reece, R. J. and Maxwell, A. (1991) DNA gyrase: structure and function, *Crit. Rev. Biochem. Mol. Biol. 26*, 335-375.

228. Noble, C. G. and Maxwell, A. (2002) The role of GyrB in the DNA cleavage-religation reaction of DNA gyrase: a proposed two metal-ion mechanism, *J. Mol. Biol. 318*, 361-371.